universität wien

MASTERARBEIT / MASTER'S THESIS

Titel der Masterarbeit / Title of the Master's Thesis

„Structural analysis of Andersen Tawil syndrome mutations in the Kir2.1 channel“

verfasst von / submitted by

Philipp Wicho, BSc

angestrebter akademischer Grad / in partial fulfilment of the requirements for the degree of

Magister pharmaciae (Mag.pharm.)

Wien, 2023 / Vienna, 2023

Studienkennzahl lt. Studienblatt / degree programme code as it appears on the student record sheet:	UA 066 605
Studienrichtung lt. Studienblatt / degree programme as it appears on the student record sheet:	Masterstudium Pharmazie
Betreut von / Supervisor:	Assoc. Prof. Priv. Doz. Dr. Anna Weinzinger

Acknowledgements

First, I want to thank my supervisor, Assoc. Prof. Priv. Doz. Dr. Anna Weinzinger, for her continuous support and encouragement while working in her team during the process of writing my master thesis. Additionally, to my colleague Karen Pfeiler, with whom I worked closely in the beginning of the thesis process, thank you for the great teamwork.

Thank you to my family and friends for their patience and support throughout my studies. Especially my parents, who, as pharmacists themselves, created the perfect environment for me to pursue my academic career.

I am grateful that I have such a good support system that never turned their back on me, no matter the obstacles life presented.

Table of contents

1. Abstract /Zusammenfassung

1.1 Abstract

The Kir2.1 channel plays an important role in depolarization, repolarization and resting membrane potential[1] [2]. It cannot only be found in skeletal and heart muscle cells but also blood cells, epithelial cells, neuron or glia cells[3].
The channel has a multimeric structure built out of four protein chains and is located in the cell membrane. It has a cytoplasmatic domain and a transmembrane domain creating a pore only K^+ ions can pass. Crucial regions for normal channel function are the selectivity filter, PIP_2 binding site and the G-loop.[4]
Several locations for mutations in Kir2.1 are known to alter the function and cause diseases like Andersen Tawil syndrome, atrial fibrillation, short QT-syndrome or catecholaminergic polymorphic ventricular tachycardia[5].
There are two types of mutations, gain of function mutations and loss of function mutations[1]. Most mutations are missense mutations exchanging an amino acid with a different one, thereby changing the polarity, the charge or the size of the side chain resulting in different problems with the surrounding residues[6]. We analyzed the mutations based on a model structure created by AlphaFold2[7] [8], as the available cryo-EM structure[4] we started with, turned out not to be of sufficient quality.

1.2 Zusammenfassung

Der Kir2.1-Kanal spielt eine wichtige Rolle bei der Depolarisierung, Repolarisierung und dem Erhalt des Ruhemembranpotenzials[1] [2]. Er kommt nicht nur in Skelett- und Herzmuskelzellen, sondern auch in Blutzellen, Epithelzellen, Neuronen oder Gliazellen vor[3].

Der Kanal hat eine multimere Struktur, die aus vier Proteinketten aufgebaut ist, und befindet sich in der Zellmembran. Er hat eine zytoplasmatische Domäne und eine Transmembrandomäne, die eine Pore bildet, die nur K^+-Ionen passieren können. Entscheidende Bereiche für eine normale Kanalfunktion sind der Selektivitätsfilter, die PIP2-Bindungsstelle und die G-Schleife.[4]

Es ist bekannt, dass verschiedene Mutationen in Kir2.1 die Funktion verändern und Krankheiten wie das Andersen-Tawil-Syndrom, Vorhofflimmern, das „short QT-

syndrom“ oder die katecholaminerge polymorphe ventrikuläre Tachykardie verursachen[5].

Es gibt zwei Arten von Mutationen: gain-of-function Mutationen und loss-of-function Mutationen[1]. Bei den meisten Mutationen handelt es sich um Missense-Mutationen, bei denen eine Aminosäure gegen eine andere ausgetauscht wird, wodurch sich die Polarität, die Ladung oder die Größe der Seitenkette ändert, was zu unterschiedlichen Problemen mit den umgebenden Aminosäuren führt[6]. Wir analysierten die Mutationen auf der Grundlage einer von AlphaFold2[7] [8] erstellten Modellstruktur, da sich die verfügbare Kryo-EM-Struktur[4], mit der wir begannen, als nicht ausreichend hochwertig erwies.

2. Introduction

2.1 Overview of potassium inward rectifier channel family

The Potassium inward rectifier family is a group of proteins integrated into the cell membrane. It regulates the inward and outward current of Potassium ions (K^+)[3]. Many different physiological processes require an influx or efflux of K^+ -Ions, therefore K^+-channels are found in various types of cells like skeletal and heart muscle cells, blood cells, epithelial cells as well as neuron or glia cells[3]. Kir2.1 belongs to a subfamily of potassium channels including Kir1-7[1]. The Kir family is divided into 4 different groups: Kir2.x is categorized as classical Kir channels, Kir3.x as G-protein gated channels, Kir6.x as ATP-sensitive K^+-channels. Kir1.x, Kir4.x, Kir5.x and Kir7.x form the last group of K^+-transport channels[3]. Kir2, Kir3 and Kir6 subfamilies play an important role in cardiac electrophysiology[1]. The Kir6 family are ligand activated and in combination with SUR subunits make up the K_{ATP} channel[9] and is responsible for cellular response. Strong inward rectification is known for Kir2 and Kir3 subfamily. Kir3 is G-protein dependent[10] whereas Kir2 family is activated by phosphatidylinositol-4,5-bisphosphate (PIP_2)[11] [4].

In 1949 B. Katz first identified K^+ inward currents in skeletal muscle fibers of frogs. He was working with a solution of high K^+ concentrations and other then expected and predicted by Nernst equation, he found greater flow into rather than out of the cells. He called it “anomalous rectification”.[12] In later years this name was changed into “inward rectification”, which is still commonly used for the Kir family. Until the discovery of B. Katz voltage gated K^+-channels currents were measured in squid giant axons by Cole and Curtis[13]. Kir2 channels are more dependent on the electrochemical gradient of potassium ions and show greater flow at negative membrane potential (mV)[3]. Also, Kir2.x channels are primarily gated by intracellular substances, like Mg^{2+} or polyamines. Polyamines, like spermidine, show a stronger block of the efflux of K^+ ions. Both types of blockers enter the pore from the cytosolic side of the pore.[14] [15]

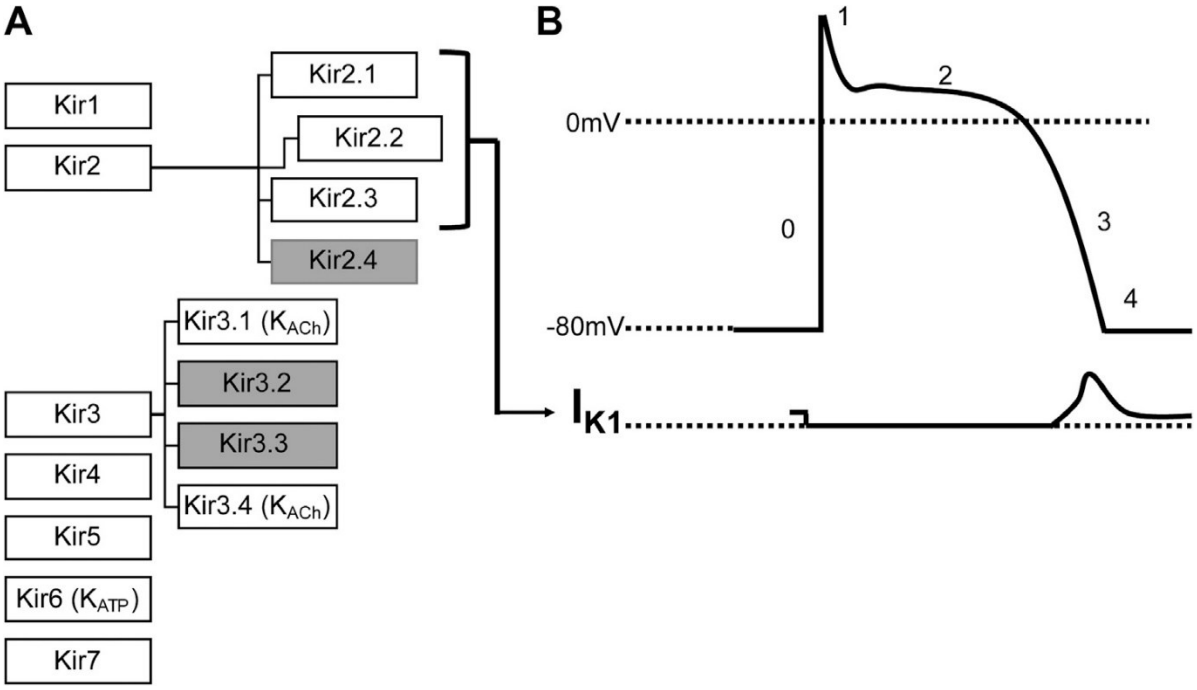

Figure 1: Kir superfamily and role in cardiac action potential. A: Hierarchy plot showing different Kir family members. B: Ventricular cardiac action potential with I_{k1} current activity highlighted below.[1] (reprinted with permission)

Kir2.1 plays a crucial role in phase 3 repolarization and maintaining resting membrane potential (E_{res}) after every heartbeat, as shown in Figure 1 B[1].

Originally the channel was named because of the inward current of K^+ ions, but in fact the direction of K^+ ions flow can change. At physiological voltages Kir 2.1 conducts outward K^+ currents, which peak at -60 to -40mV. The more positive the membrane potential gets, the lower the K+ flow out of the cell. The strong inward current of the Kir family appears, when the membrane potential reaches the equilibrium potential of potassium (E_K), close to -80mV and the K^+ current reverses. This phase is reached during hyperpolarization in neuron cells for example, but not in cardiac cells.[1] Besides Kir-channel gating mechanism is controlled by a variety of intracellular messengers like phosyphatidylinositol-4,5-bisphosphate (PIP_2), G-protein, adenosine 5'-triphosphat (ATP) or pH-changes. Furthermore, the pore can be blocked during depolarized status from the cytosolic side by Mg^{2+} or polyamines, which results in a reduction of outward K^+ flow[14]. This block can be reversed during hyperpolarization due to the strong inward current.[4] Phosphatidylinositol-4,5-bisphosphate (PIP_2) is known to be a signaling lipid, with a wide range of effects on ion channels. All eucaryotic Kir channels are activated by PIP_2, whereas in bacterial Kir channels, like KirBac1.1 for example, it acts as an inactivator.[16]

2.2 Kir2.1 structure

A cryo-electron microscopy structure has been published in September 2022 with an average resolution of 4.3Å[4], [17]. Kir2.1 is composed of 4 identical subunits in a tetrameric complex. Each subunit has a transmembrane domain (TMD) and a large cytoplasmatic domain (CTD)[4].

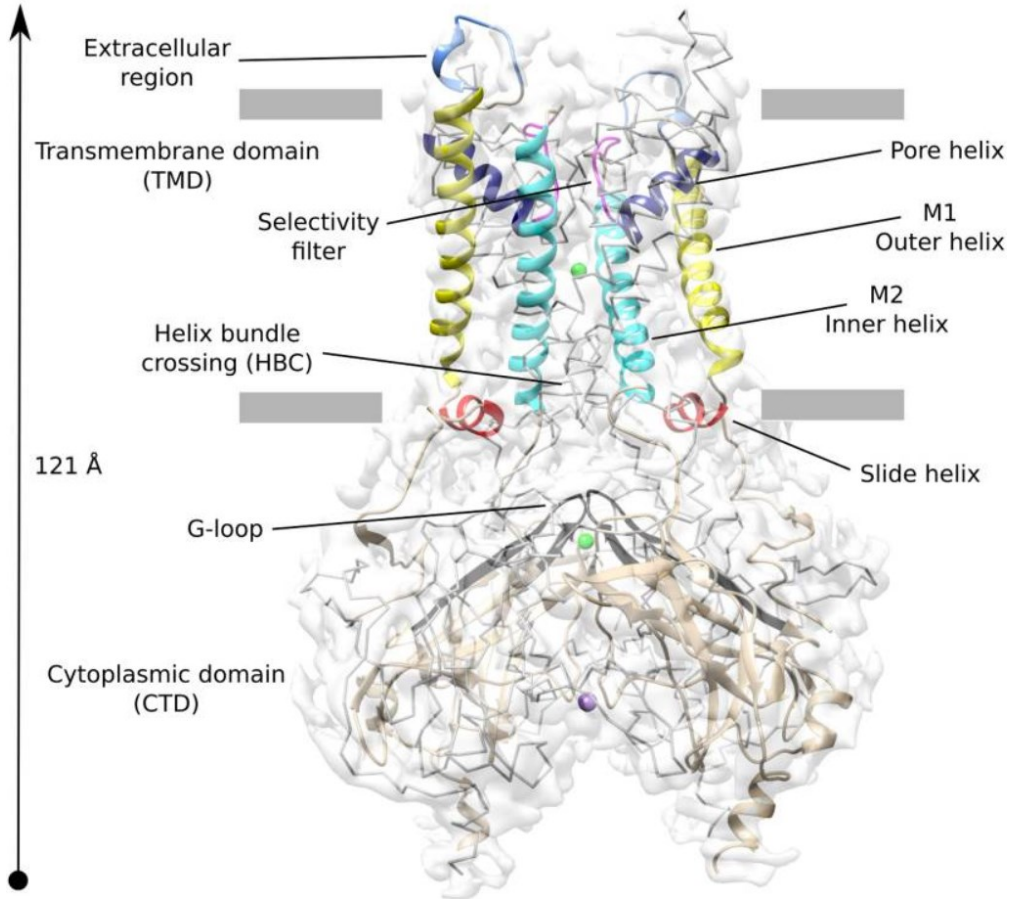

Figure 2: Side view of human Kir2.1 atomic structure fitted in the cryo-EM map (white surface). The chains A and C are in cartoon and highlight the typical structural features of Kir channels: outer helix (M1, yellow), inner helix (M2, cyan), pore helix (dark blue), slide helix (red), selectivity filter (magenta), extracellular region (light blue), G-loop (black), and helix bundle crossing (HBC) region. The Sr2+ (green) and K+ (purple) ions inside the pore channel are represented as spheres. Chains B and D are in gray ribbons for clarity. Gray horizontal bars indicate the plasma membrane. The TMD and CTD are indicated.[4] (reprinted with permission)

The transmembrane domain (TMD) includes a smaller pore helix, the selectivity filter (amino acids 140-148), an outer helix, an inner helix and a slide helix. A small extracellular part of the channel is formed by a short loop region connecting the outer helix and the pore helix. C-terminus and N-terminus are both located in the

cytoplasmatic domain (CTD). The cytoplasmatic domain (CTD) mainly consists of beta-strands and beta-sheets. Characteristic for the Kir-channel family is the so called cytoplasmatic pore, which extends the ion pathway by about 30 Å[3]. The pore of human Kir2.1 has 4 constriction point, one being the selectivity filter, the 3 others at residues I176, M180 and A306. Only residue A306 is in the cytoplasmatic domain, at the apex of the G-loop (amino acids 300-312[10]) and is unique to Kir2.1.[4]

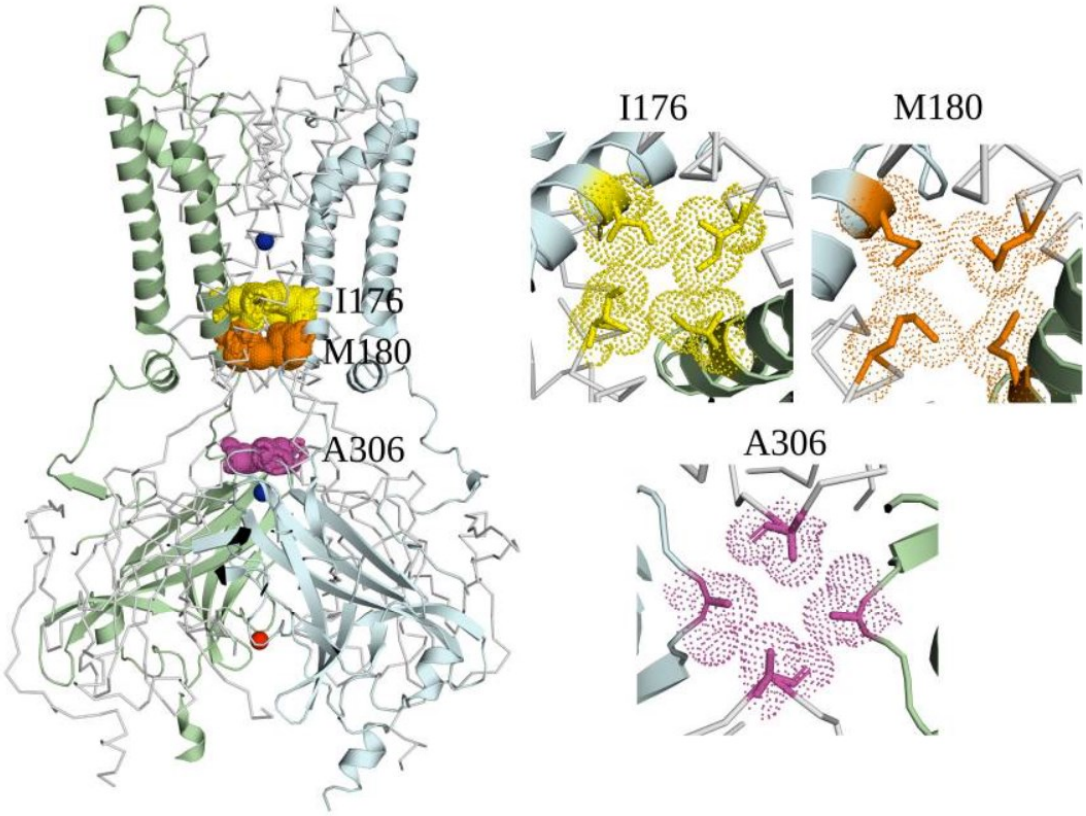

Figure 3: Three constriction points below the selectivity filter: I176 (yellow sphere), M180 (orange sphere), and A306 (purple sphere). Chains A and C are in light blue and green cartoons, respectively. Chains B and D are in gray ribbons for clarity. Sr2+ (blue) and K+ (red) ions are represented as spheres. The insets show the zoom of the three constriction points, where the spheres represent the van der Waals surfaces.[4] (reprinted with permission)

The whole structure is 121 Å long and 78 Å wide, but it can change size when switching between open and closed state and PIP_2 binding. Furthermore, the channel performs a swing motion, which enables a better accessibility at residue K187. K187 is directly involved in PIP_2 binding and is located between the transmembrane domain (TMD) and the cytoplasmatic domain (CTD) in the central region of the inner loop.[4] The binding site for PIP_2 involves residues R80, W81, R82, K182, K185,

K187, K188, R189, R218 and K219 of each chain resulting in 4 possible locations. Mutations in these locations effect PIP_2 binding with reduced binding energies.[18]

2.3 Kir2.1 mutations and diseases

Kir2.1 is a product of the KCNJ2 gene. Various mutations are known for Kir2.1[5]. Some are silent, others cause diseases like Andersen Tawil syndrome (ATS), atrial fibrillation (AF), short QT-syndrome (SQT) or catecholaminergic polymorphic ventricular tachycardia (CPVT). In general, there are two types of mutations: loss of function mutations, leading to Andersen Tawil syndrome and catecholaminergic polymorphic ventricular tachycardia and gain of function mutations, leading to atrial fibrillation and short QT-syndrome.[4]

2.3.1 Andersen Tawil syndrome

Andersen Tawil syndrome, also known as Andersen Syndrome or Long QT-syndrome Type 7, is a genetic disorder caused by different mutations of the KCNJ2 gene coding for Kir2.1. It is therefore classified as a channelopathy, a group of diseases cause by the dysfunction of ion channels and not to be confused with Andersen's Syndrome, a type IV glycogen storage disease. Several mutations were found in KCNJ2, which disrupt normal channel function. Many of them in crucial regions, like the selectivity filter, pore helix or PIP_2 binding sites. ATS is inherited in an autosomal dominant pattern and characterized by three major traits: a periodic paralysis of skeletal muscles, cardiac arrythmia and developmental dysmorphism.[19] However there is a great variability within the disease, because not every individual concerned shows all three characteristics. Furthermore, the severity for each phenotypic expression is different, ranging from negligible deformities to prominent face dysmorphism or asymptotic long QT to cardiac arrest. Episodes of paralysis occur due to muscle hyperexcitability in exchange with hypo excitability and are unrelated to K^+ serum levels.[20] [21]

Table1: ATS mutations in Kir2.1[19] (reprinted with permission)

Mutation	Location	Reports
R67 W*	N-terminus	3
D71N	N-terminus	1
D71V	N-terminus	1
T75R	N-terminus	1
Δ95–98	Transmembrane 1	1
S136F	Pore helix	1
G144S	Pore selectivity filter	1
G146D	Pore selectivity filter	1
P186L*	C-terminus	1
R189I*	C-terminus	1
T192A	C-terminus	1
G215D	C-terminus	1
N216H	C-terminus	1
R218 W*	C-terminus	7
R218Q*	C-terminus	1
G300V*	C-terminus	2
G300D*	C-terminus	1
V302M	C-terminus	1
E303K*	C-terminus	1
R312 C*	C-terminus	1
Δ314–315	C-terminus	1

*When mutated, residues decrease PIP2 binding.
Reports = number of independent mutations in different families.

Additionally to ATS Type I, which is caused by KCJN2 mutations, which are responsible for ~50-60% of all cases, Type II ATS is caused by mutations in KCNJ5. KCNJ5 is encoding for G-protein activated inwardly rectifying K^+ channel Kir3.4 and concerns ~15% of patients. Another 30% of cases are as-yet for unknown reasons and suggest involvement of other gene mutations.[22]

3. Materials and methods

3.1 Charmm gui

As a first step to compare the wild type channel with a mutated one, we needed to set up a molecular dynamic simulation with the Kir2.1 cryo-electron microscopy structure we wanted to use[4] [17]. Charmm gui has different input generators, like Membrane Builder, Solvator or PDB Reader. We used the Membrane Builder[23] [24] [25] function to build a bilayer lipid membrane for the channel. Furthermore, we added water molecules inside the pore and surrounding the cytoplasmatic domain. Some water molecules needed to be deleted manually, because they were generated outside the pore and inside the membrane. We also needed to add 120 K^+ ions to determine if the structure is in open or closed state and 106 Cl^- ions to neutralize the solution (KCL = 150mM). We chose the lipids of the membrane to be phosphatidylcholine (POPC) as standard lipid, because the exact information of the percentual composition of lipids in the sarcolemma, the cell membrane surrounding skeletal muscle fibers and cardiomyocytes, is not known. POPC is the standard lipid used in MD simulations of various ion channels. 233 lipids were generated in total. For protonation of amino acids, we used PDB2PQR[26] to calculate.

Table2: Protonation of amino acids in Kir2.1 calculated by PDB2PQR[26]

Chain	Amino acid	Position	Type
A	GLU	138	GLUP
A	GLU	224	GLUP
A	GLU	293	GLUP
A	GLU	299	GLUP
B	GLU	138	GLUP
B	GLU	293	GLUP
C	LYS	185	LSN
C	GLU	138	GLUP
C	GLU	293	GLUP
C	GLU	299	GLUP
D	GLU	138	GLUP

We work with Amber forcefield FF14SB and with a temperature of 310K which equals 36°C (body temperature).[27] [28]

3.2 Gromacs

Molecular dynamic simulation were performed using Gromacs Version 2023.02 [29] [30]. We simulated the wildtype protein of Kir2.1, which we embedded in a bilayer membrane of POPC surrounded by water molecules, K^+ and Cl^- ions, using Charmm gui. First, we performed energy minimization steps and therefore we restrained the protein atoms by a force of 1000 kJ/mol/nm^2 to ensure that the membrane lipids, small molecules and ions get packed to our channel without changing the protein structure itself. Each step of equilibration was performed for 5ns at constant pressure (1bar) and temperature (310K). The final 100 ns MD simulation was calculated using the Vienna Scientific Cluster[31].

3.3 Root mean square fluctuation

With our trajectory file resulting from the MD simulation, we calculated the root mean square fluctuation (RMSF) to confirm the stability and flexibility of the protein. RMSF is a numerical measurement of how much a specific residue moves during the simulation. Lower values indicate a stable position, without much flexibility in the side chain, whereas higher numbers show flexible side chains. RMSF is calculated for every amino acid and only shows one score for the hole simulation per residue.[32]

3.4 AlphaFold2 and pLDDT

The prediction of the structure of Kir2.1 was performed with AlphaFold2[7] [8] developed by google deepmind using neurosnap.ai[8] [33] [34] [35]. The FASTA sequence of Kir2.1, amino acid S45 to E387, was used as a tetramer. C- and N-termini were not modeled due to high mobility of the chains and the resulting unreliability of the structure. To generate the model, we used alphafold2_multimere_v3 and as template we used pdb70. The outcome structures were ranked using predicted local distance difference test (pLDDT)[36] to show the confidence in accuracy of the model. pLDDT values compare the predicted structure with multiple alignment data and ranks it from 0 to 100. Scores >70 are considered confident[37].

3.5 Pymol

The figures of each mutation and all measurements were performed with Pymol version 2.5.5[38].

4. Results

4.1 Molecular dynamics simulation and RMSF

The MD simulation revealed that the available cryo-EM structure (average resolution of 4.3Å[4]) is very unstable, which is not uncommon for structures of very low resolution, as is the case for Kir2.1. The channel did not collapse completely, but it showed crucial changes in important regions like the selectivity filter, G-loop or PIP_2 binding site. In chain D we can see the outer helix in the TMD is starting to uncoil. When we compare the view through the channel from the CTD, we can see that the pore is no longer clearly visible.

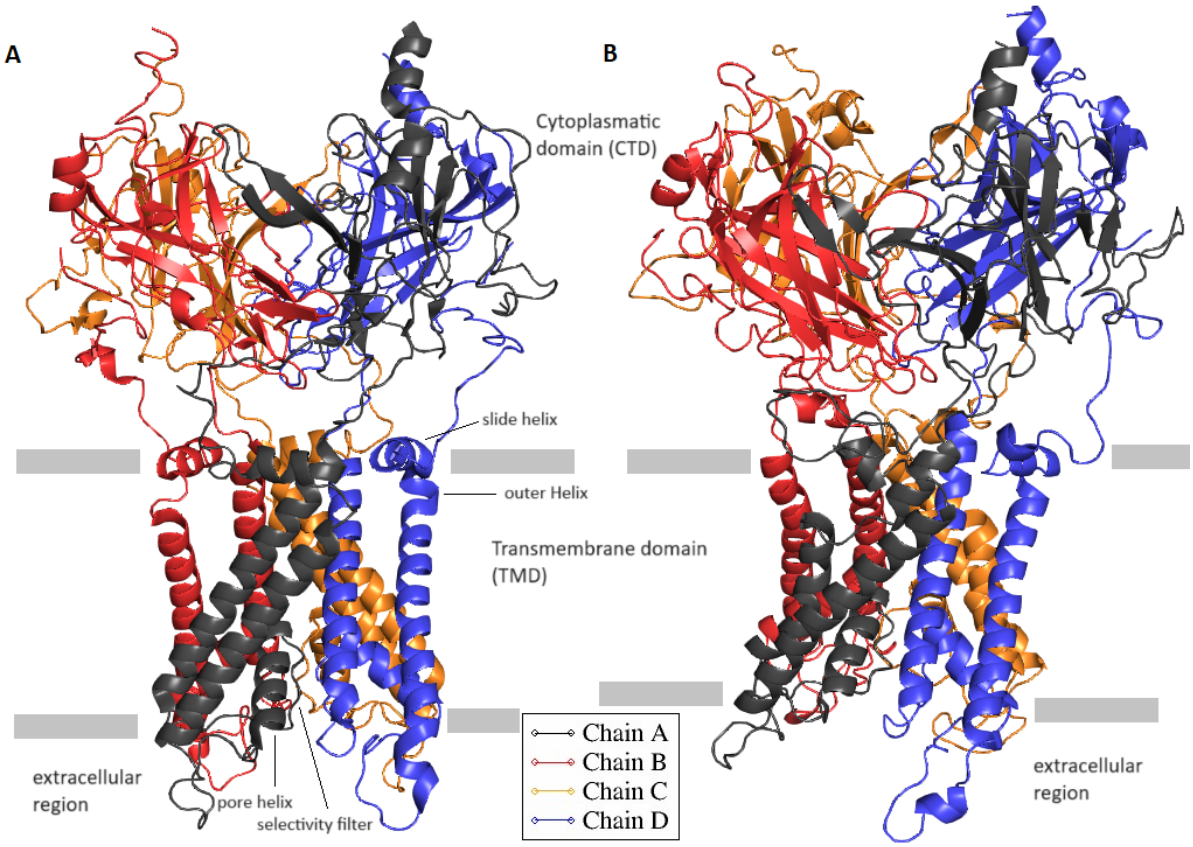

Figure 4: A) Kir2.1 before the MD simulation. B) Kir2.1 after the MD simulation. TMD and CTD are closer together and not as clearly separated as before. The outer helix in chain D (blue) is starting to uncoil.

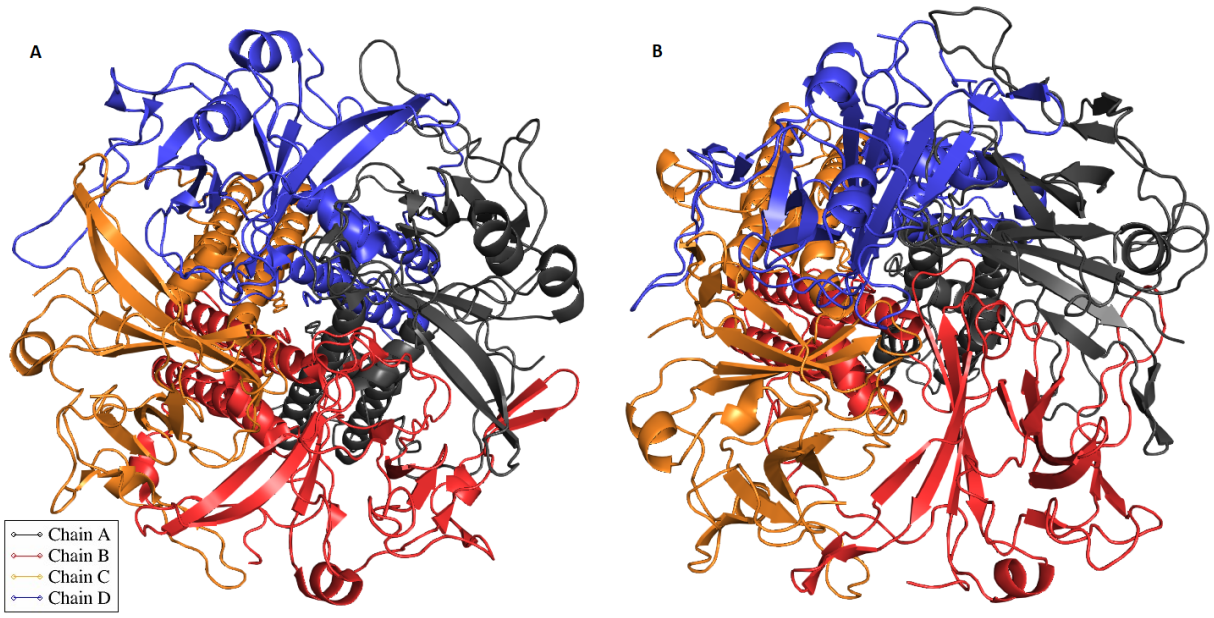

Figure 5: A) View through the pore form CTD of Kir2.1 channel before MD simulation. B) View through the pore form CTD of Kir2.1 after MD simulation. The pore is no longer clearly visible, because the TDM is no longer centered compared to the CTD. TDM has bent towards chain C (orange) and chain D (blue).

We performed RMSF calculations to receive information on the amino acid flexibility. In important regions like the selectivity filter (amino acids 140-148) or the pore region we expected to get scores <0,1nm, but some of the values are above 0,3nm, which means that our protein is not stable. Exacts scores for the important regions are listed in the table below.

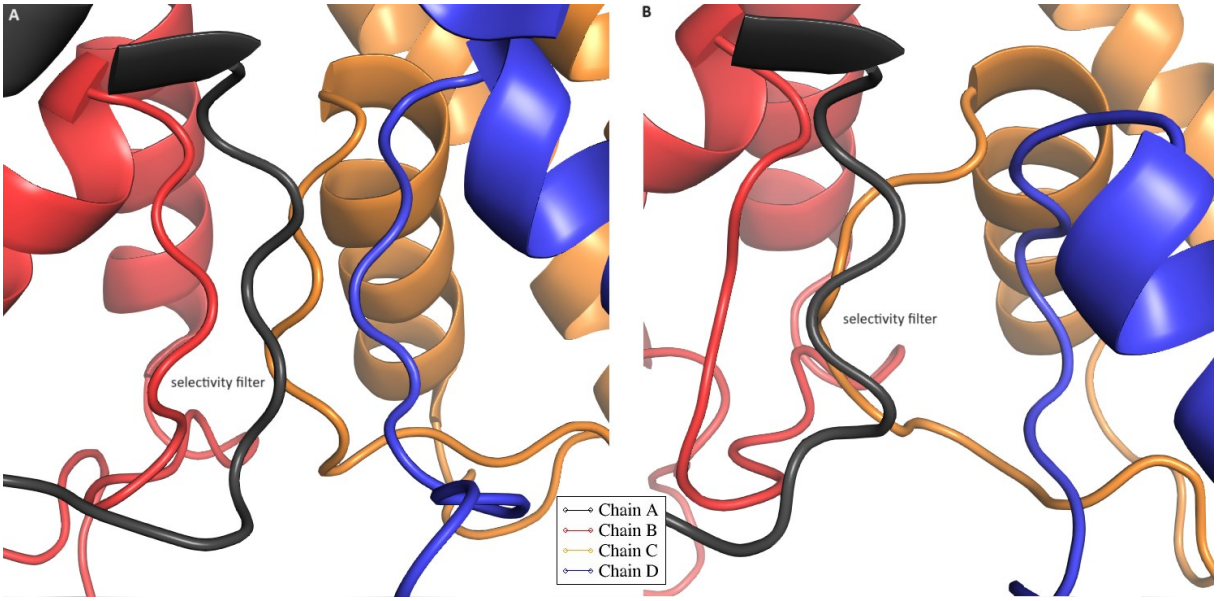

Figure 6: A) Selectivity filter before the MD simulation. B) Selectivity filter after the MD simulation. In both figures the pore helix of chain A is removed up to T139 to get a clear view.

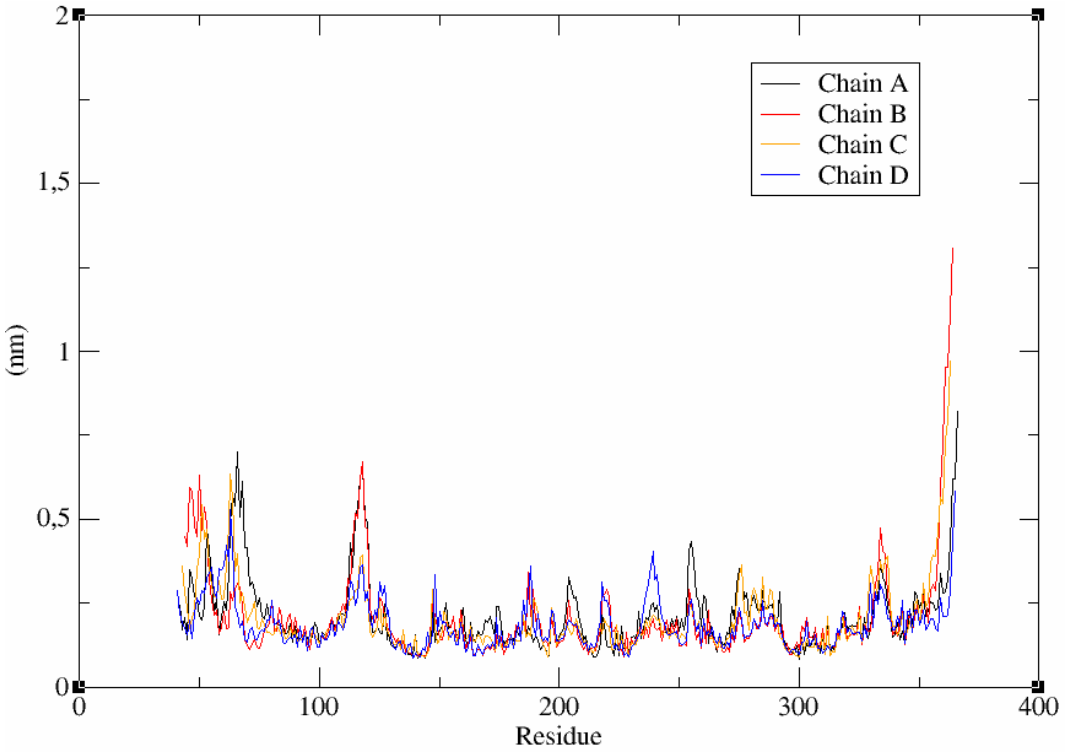

Figure 7: RMSF after 100ns MD simulation of Kir2.1 for all residues.

Table3: RMSF scores for important amino acids and their possible mutations. Marked in yellow are scores for the selectivity filter, grey for G-loop and green for PIP_2 binding site >0,1nm.

Position	RMSF score in nm				Mutation
	Chain A	Chain B	Chain C	Chain D	
C54	0.4083	0.3170	0.3570	0.3418	C54F
R67	0.5078	0.2982	0.2501	0.1789	R67Q, R67W
D71	0.3035	0.1105	0.2137	0.1696	D71H, D71N, D71V
T75	0.2639	0.1153	0.1729	0.1626	T75A, T75M, T75R
D78	0.2458	0.1780	0.1642	0.1985	D78G, D78H, D78Y
R80	0.2514	0.2574	0.1568	0.2597	
W81	0.1888	0.1683	0.1579	0.1838	
R82	0.1872	0.1680	0.1798	0.1939	R82Q, R82W
V93	0.1399	0.1527	0.1449	0.1335	V93I
SWLF95-98	0.1421	0.1282	0.1381	0.1095	SWLF95-98>missing
	0.1142	0.1134	0.1331	0.1666	
	0.1606	0.1670	0.1708	0.1775	
	0.1923	0.1563	0.1596	0.1540	
S136	0.1117	0.1058	0.1164	0.0979	S136F
Q140	0.1558	0.0991	0.1511	0.1020	
T141	0.0855	0.0895	0.0885	0.0929	
T142	0.1029	0.0999	0.0933	0.0899	
I143	0.0950	0.0948	0.0944	0.1169	
G144	0.0882	0.0955	0.0910	0.1070	G144A, G144D, G144S
Y145	0.1138	0.1098	0.1021	0.1638	
G146	0.1188	0.1594	0.1257	0.1193	G146A, G146D, G146S

F147	0.2369	0.2481	0.2894	0.1633	
R148	0.1343	0.2122	0.1812	0.3354	
C154	0.1761	0.1847	0.1422	0.1544	C154F, C154Y
D172	0.1771	0.1276	0.1299	0.1350	D172N
I176	0.1827	0.1500	0.1206	0.1684	
M180	0.1399	0.1538	0.1541	0.1546	
K182	0.1731	0.1864	0.1431	0.1570	
K185	0.2054	0.1961	0.2147	0.2598	
P186	0.1474	0.1684	0.1472	0.2001	P186L, P186Q
K187	0.1802	0.3413	0.1638	0.2809	
K188	0.1649	0.2116	0.1535	0.3598	
R189	0.1352	0.2922	0.2621	0.1851	R189G, R189I, R189K, R189T
T192	0.1119	0.1854	0.1619	0.1572	
G215	0.0886	0.1090	0.1194	0.1246	G215D
N216	0.1052	0.1462	0.1642	0.1678	N21H
R218	0.2127	0.2654	0.1580	0.3130	R218L, R218P, R218Q, R218W
K219	0.1907	0.2770	0.2042	0.2586	
R228	0.1209	0.1618	0.1192	0.1029	R228Q
R260	0.2745	0.1824	0.1943	0.2032	R260P
G300	0.0831	0.1108	0.0914	0.0972	G300A, G300D, G300V
M301	0.1495	0.1816	0.1407	0.1332	M301L, M301R, M301V
V302	0.0993	0.1670	0.1107	0.1395	V302M
E303	0.1287	0.2076	0.1455	0.1975	E303K
A304	0.1197	0.1472	0.1183	0.1225	
T305	0.1276	0.1474	0.1199	0.1365	T305A, T305P
A306	0.1618	0.1461	0.1213	0.1400	
M307	0.1251	0.1795	0.1454	0.1568	M307V
T308	0.1291	0.1157	0.1072	0.1158	
T309	0.1013	0.1248	0.1155	0.1156	T309I
Q310	0.1472	0.1743	0.1581	0.1016	
C311	0.0970	0.1199	0.0983	0.1084	
R312	0.1969	0.1670	0.2114	0.1242	R312C, R312H
SY314-315	0.1183	0.1236	0.1074	0.1234	SY314-315>missing
	0.1060	0.1171	0.1061	0.1221	
W322	0.1848	0.1598	0.1830	0.1599	W322C

PIP_2 binding site containing the residues R80, W81, R82, K182, K185, K187, K188, R189, R218 and K219[39] all having scores between R189 0.13nm and K188 0.35nm indicating a great flexibility in this important region.

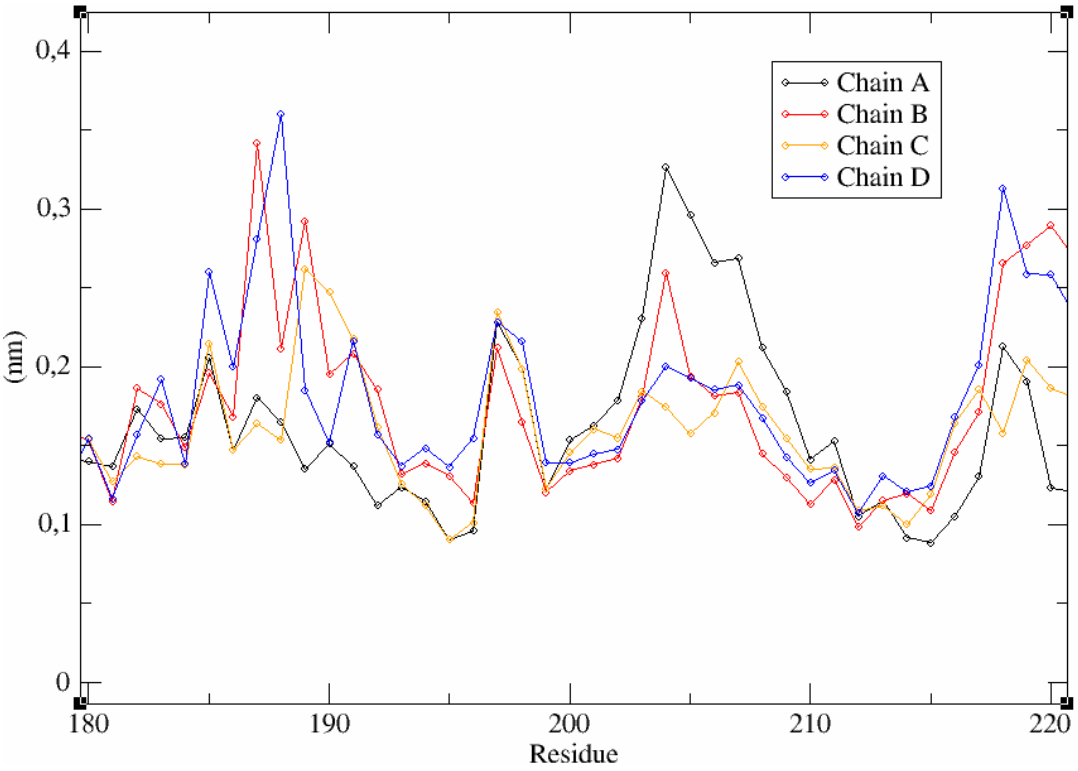

Figure 8: RMSF scores for PIP_2 binding site residues in nm for all 4 chains. (chain A black, chain B red, chain C orange and chain D blue)

Another crucial region is the selectivity filter, located at residues Q140-R148. These amino acids especially need a very low RMSF score, preferably <0.1nm. This is important because every little bit of extra space may allow other ions than K^+ or water molecules to slip through the channel uncontrolled like it was shown in the work of T. Friesacher et al [40] and as reported in K^+ channel of streptomyces A[41]. RMSF scores for this region ranging from T141 in chain A 0.08nm to R148 0.33nm in chain D. A change in the structure of ~3.3 Å (0.33nm) in this crucial region suggests that the selectivity filter would not work as intended any longer in this conformational state. Therefore, we cannot perform any mutation studies with this structure, because no significant changes could be proven, since the wildtype structure is already unstable.

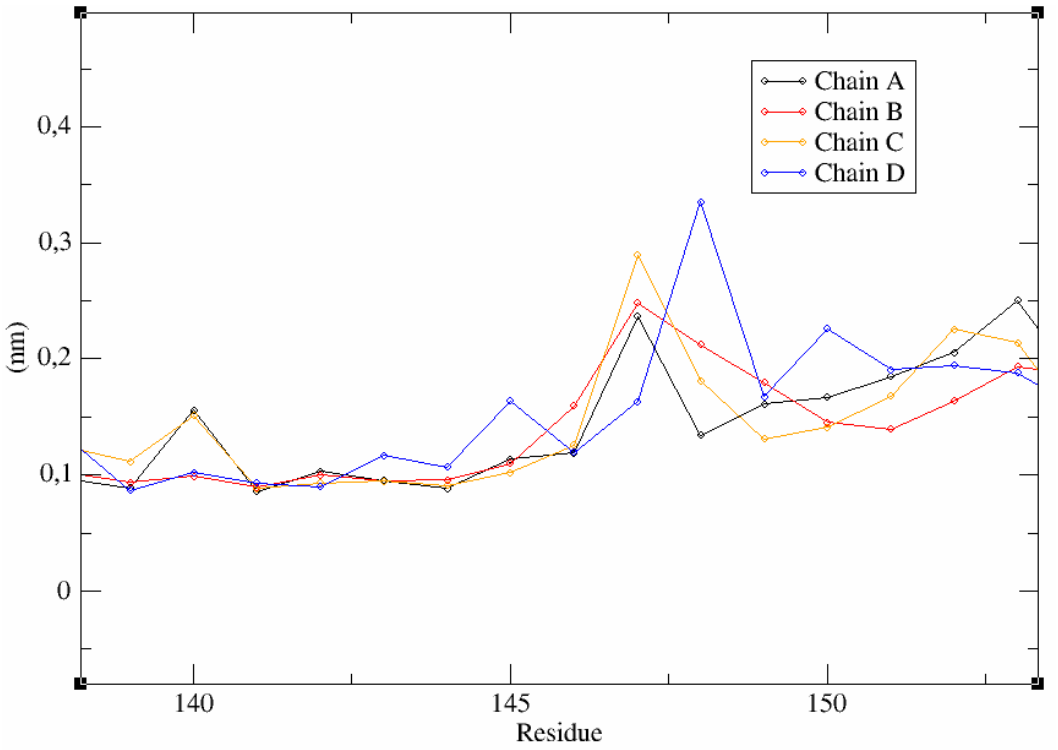

Figure 9: RMSF scores of the selectivity filter (residues Q140-R148) in all 4 chains (chain A black, chain B red, chain C orange and chain D blue)

If we take a look at the G-loop, involving residues G300 to Y315[4], the RMSF scores vary from G300 0.08nm to R312 0.21nm with most of them being <0.1nm. This shows us that in many important positions throughout the protein the structure is unstable and therefore it is not possible to make any comparing simulations between wild type and mutated channels to obtain structural information.

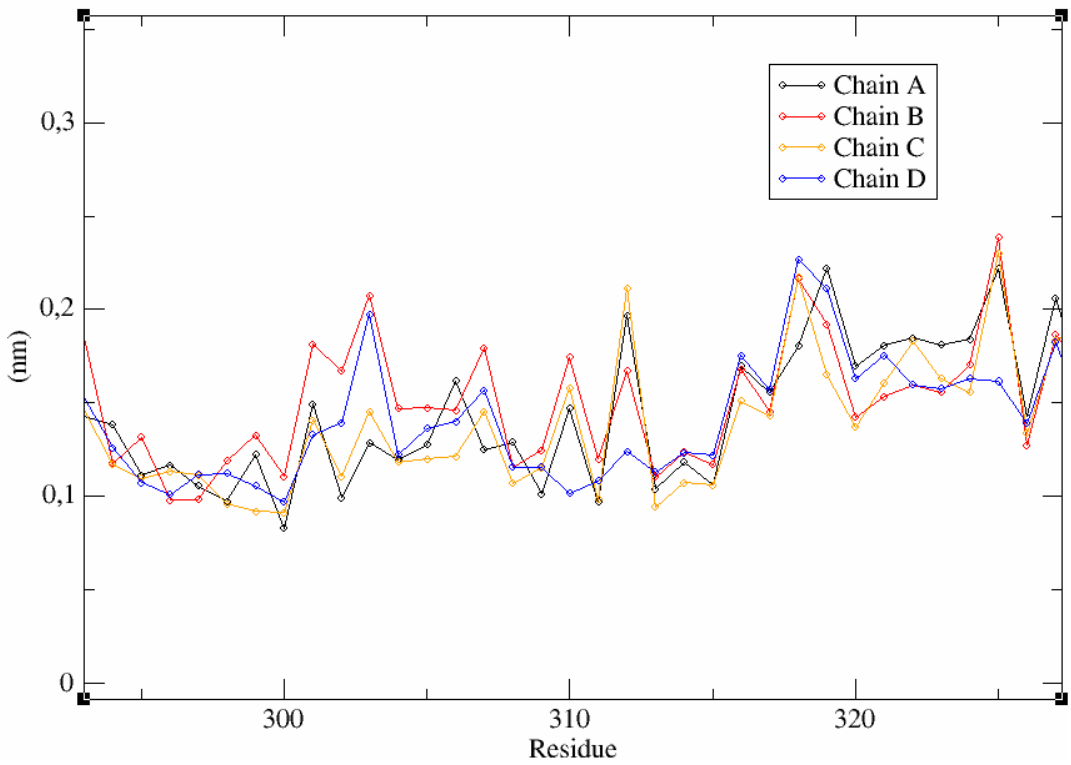

Figure 10: RMSF scores of the G-loop (residues G300-Y315[4]) in all 4 chains (chain A black, chain B red, chain C orange and chain D blue)

4.2 AlphaFold2

To obtain a possibly higher quality structure of Kir2.1 we used AlphaFold2[7] [8]. We started to model with residue S42 and ended with E387, because the first predictions with the whole protein showed, that the N- and C-termini contain disordered loop regions, which are too flexible to get a confident structure.

The resulting predictions are ranked by pLDDT, which assigns a score from 0-100 to every amino acid. The score represents the confidence the program has in the structure of the model. >90 means very high confidence, 70-90 confident, 50-70 low confidence and <50 very low confidence. The best structures all have values >90 pLDDT and the differences are only in the loop region close to the N- and C-termini of each chain and in the loop connecting the outer helix and the pore helix.[36]

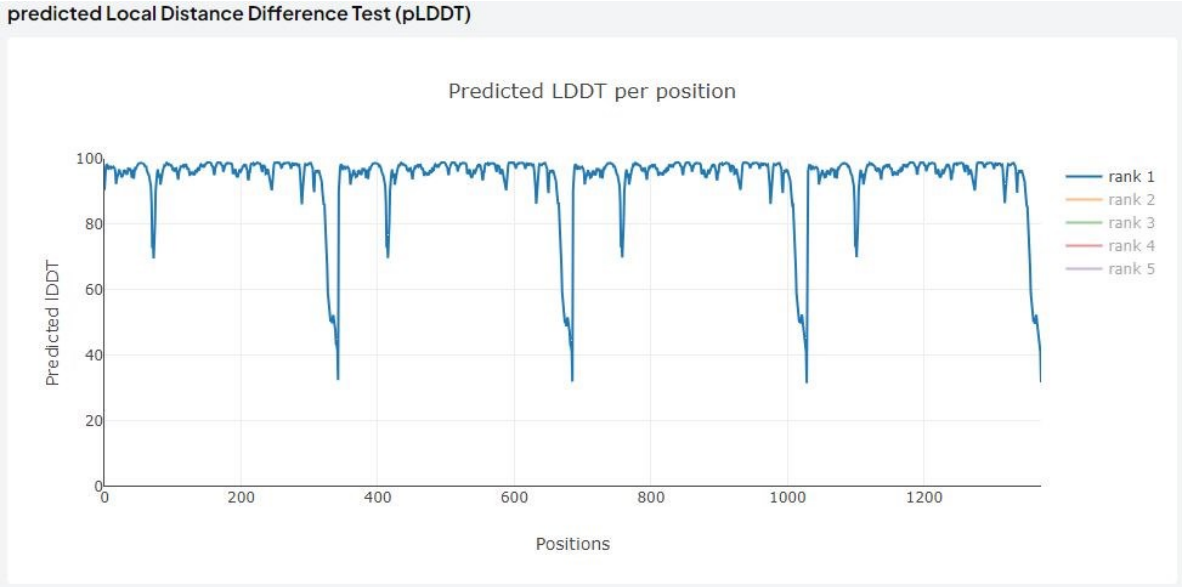

Figure 11: pLDDT[36] of Kir2.1 modeled with AlphaFold2_v3 and pd70 template as a homotetramer by neurosnap.ai[8] [33] [34] [35].

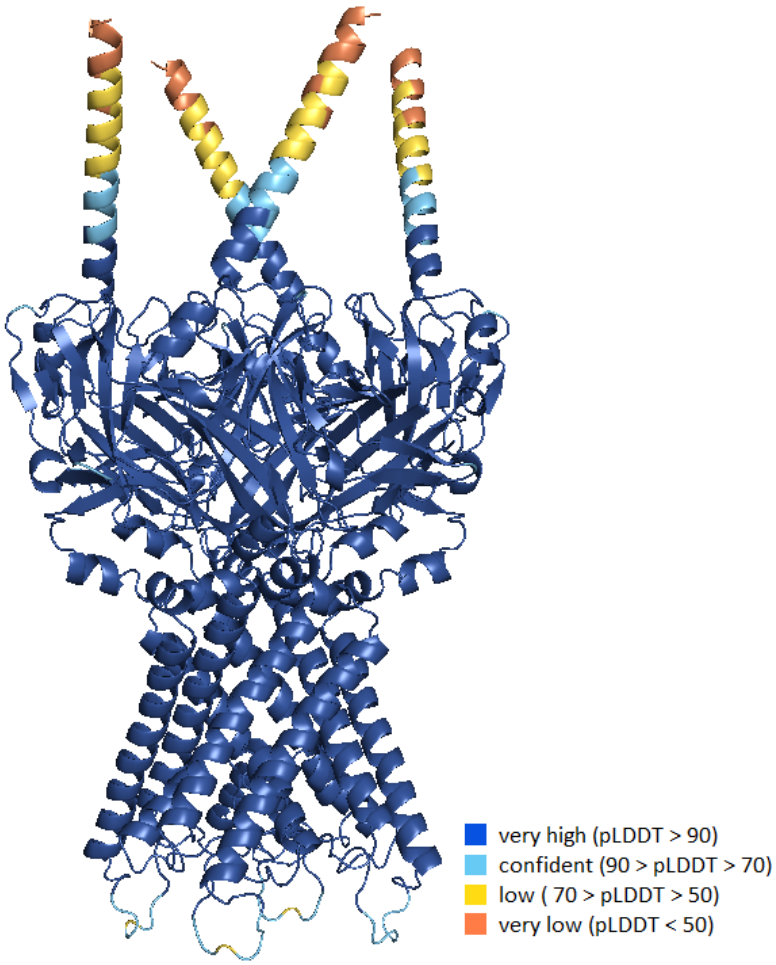

Figure 12: Kir2.1 model predicted by AlphaFold2[7] [8] using neurosnap.ai[8] [33] [34] [35], colored to pLDDT[36] values.

4.3 Structural interpretation of disease causing variants

4.3.1 C54F

In the AlphaFold2[7] [8] structure cysteine 54 is located in a well conserved region of the N-terminus of the chain. It is able to form hydrogen bonds or disulfide bonds with other cysteines, which are often used to connect different subunits and stabilize the quaternary structure. In this case it is involved in pH-dependent gating after PIP_2 binding.[42] In our model it does not look as if C54 is involved in hydrogen bonds or disulfide bridges, but if the channel changes conformation, this might be required.

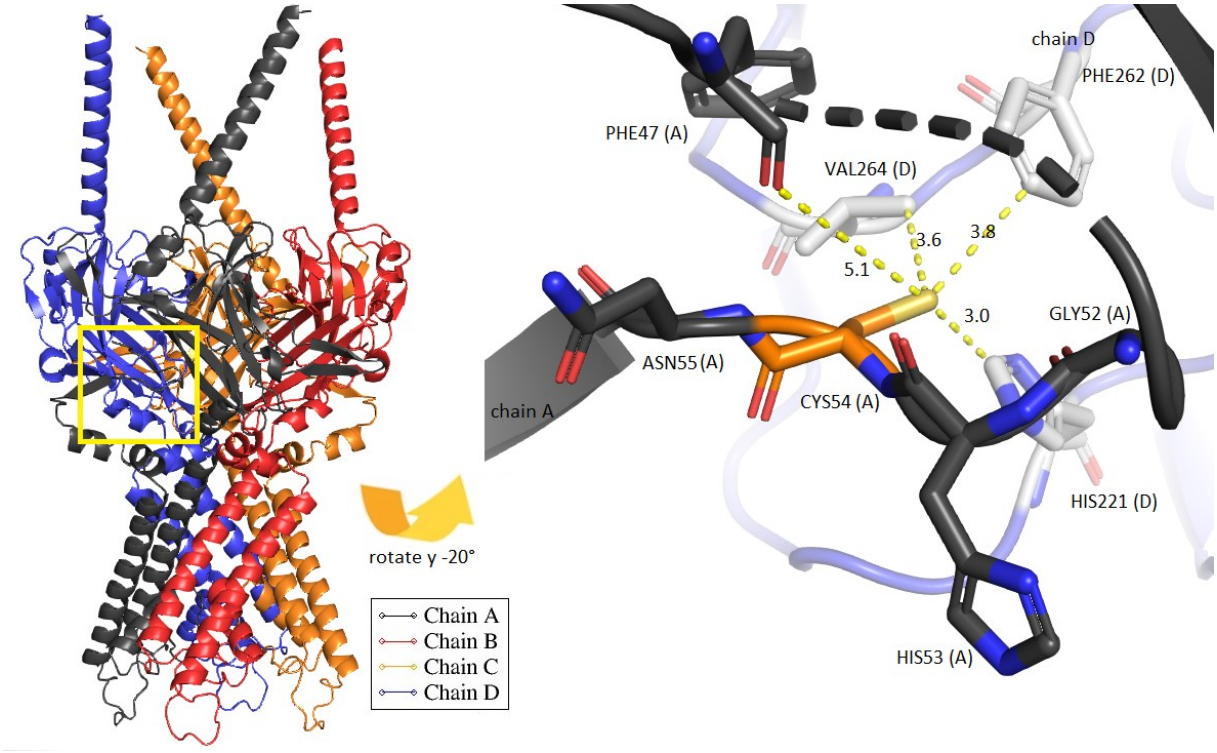

Figure 13: left: Overview of Kir2.1 with 4 subunits. Right: Cysteine 54 (orange) in chain A (black) and the surrounding residues within a radius of ~5Å. Chain D in blue/white and yellow lines indicate measurements in Å.

The mutation of cysteine to phenylalanine causes several changes in the structure. For once phenylalanine is bigger than cysteine and therefore requires more space. As shown in figure 13 there are clashes with H221, V264 and F262 all in chain D, if the backbone does not adapt. C54 is not embedded in helix or a beta sheet, so there might be enough room for the backbone to shift, but the loss of a the -SH group is another crucial change. The polarity of the residue changes thereby from a hydrophilic side chain to a hydrophobic side chain and loses the ability to form

disulfide bridges or hydrogen bonds. On the other hand, the new aromatic ring of the side chain an interact with its surroundings via π-stacking.

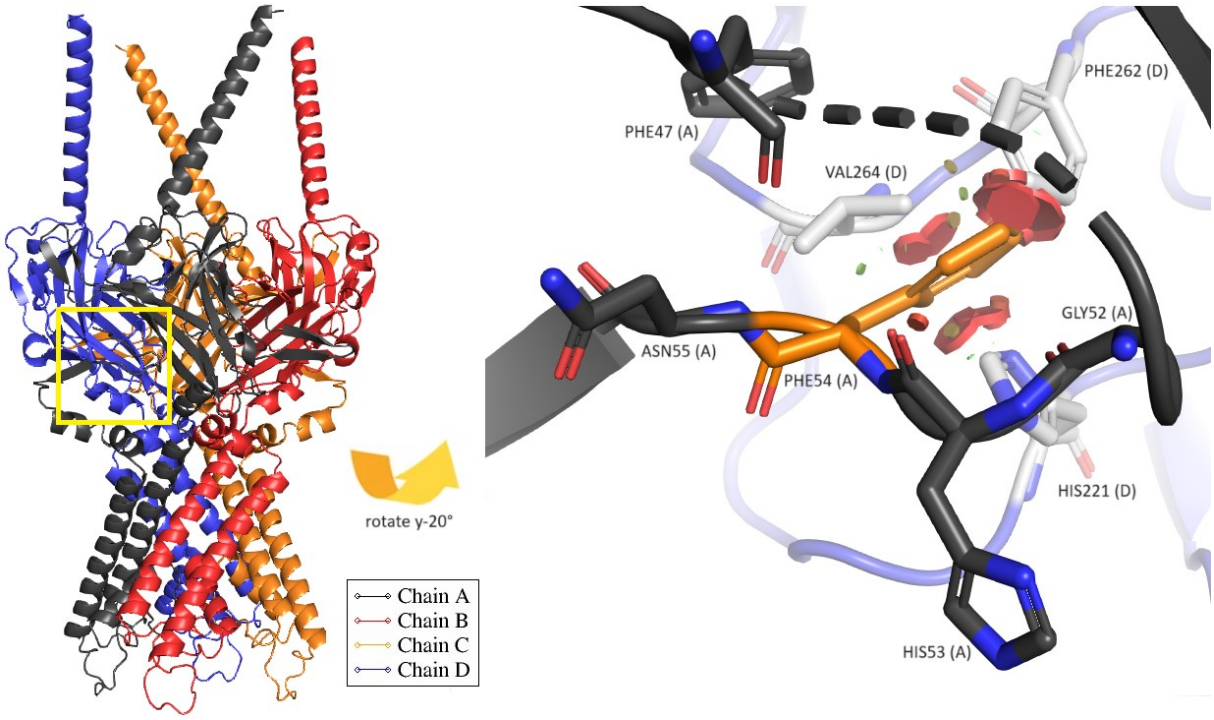

Figure 14: Left: Overview of Kir2.1 with 4 subunits. Right: C54F (orange) in chain A (black) and the surrounding residues within a radius of ~5Å. Chain D in blue/white. Circles show clashes caused by the mutation: Size and color changes from green to red indicate the severity of the clash.

4.3.2 R67Q and R67W

Arginine is a large amino acid and carries a guanidino group. This guanidino group can be protonated and therefore is positively charged[43]. R67 is close to the secondary binding pocket of PIP_2 and performs a similar motion to K64, when the pocket opens and closes. It can penetrate the membrane and gets closer to the phosphate groups of the inner membrane. This suggests that R67 and K64 may have coupled movements and play an important role in conformational change, when PIP_2 is bound and released.[4] Furthermore, in our model it has the possibility to form hydrogen bonds or salt bridges with glutamic acid 191 of chain D linking 2 subunits.

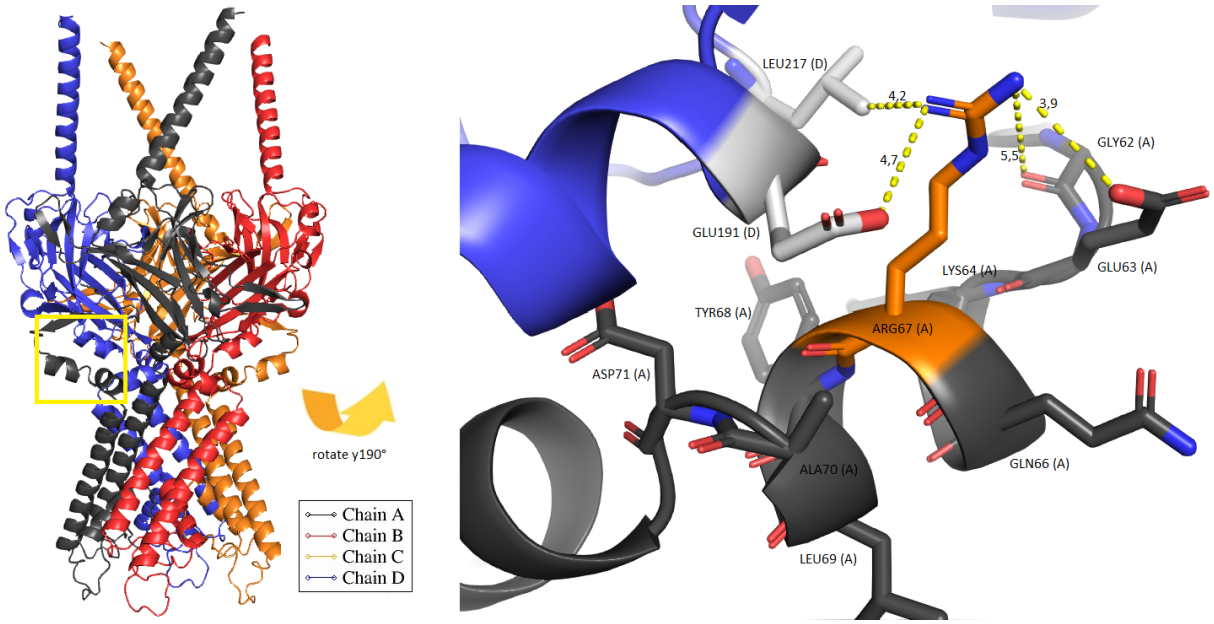

Figure 15: Left: Overview of Kir2.1 with 4 subunits. Right: Arginine 67 (orange) and the surrounding residues in a radius of ~5 Å in chain A (black) and chain D (blue/white). Yellow lines indicate measurement in Å.

The $-NH_2$ and -NH group of Arginine is surrounded by -OH groups of the nearby glutamic acid 191 of chain D and glutamic acid 63 of chain A, giving it the possibility to form a hydrogen bond or ionic interactions, given that arginine is a cationic and glutamic acid an anionic amino acid.

The R67Q mutation causes the exchange of a cationic arginine with a neutral glutamine and prevents all ionic interactions. The removal of the positive charge will also affect the interaction with the phosphate groups of the membrane during conformational changes. Studies showed, that R67Q mutation causes catecholaminergic polymorphic ventricular tachycardia[44].

In case of R67W not only the positive charge is removed, but there is also a big change in the size of the sidechain. Tryptophan is a non-polar, aromatic amino acid and due to its two rings very bulky compared to arginine. There is a structural problem with L217 of chain D, but otherwise it fits surprisingly well. There is a possible hydrogen bond between W67 (A) and E63 (A) or E191 (D) but no longer an ionic interaction suggesting that the positive charge is crucial. R67W is known to cause symptoms of ATS with the full clinical triad[45].

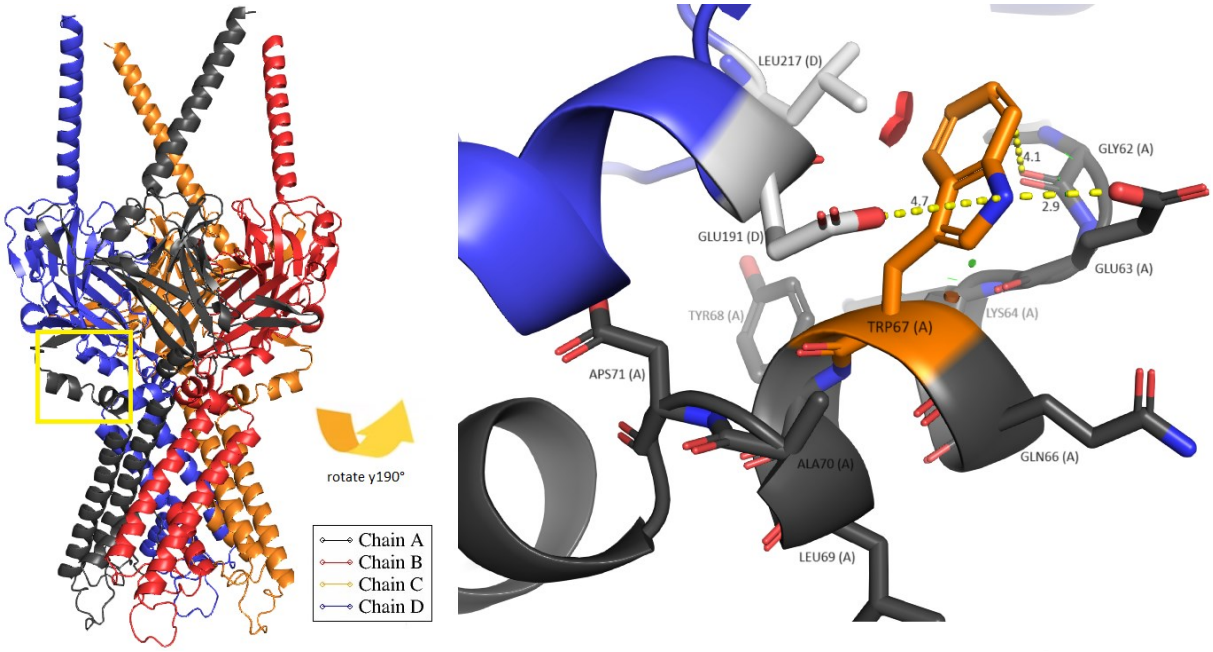

Figure 16: Left: Overview of Kir2.1 with 4 subunits. Right: R67W (orange) and the surrounding residues in a radius of ~5 Å in chain A (black) and chain D (blue/white). Yellow lines indicate measurement in Å. Circles show clashes caused by the mutation: Size and color changes from green to red indicate the severity of the clash.

4.3.3 D71H, D71N and D71V

Aspartic acid 71 is a hydrophilic amino acid, that is negatively charged[43]. It can form hydrogen bonds or ionic interactions with close by residues, like threonine 74 (chain A) arginine 218 (chain D), arginine 189 (chain D) or threonine 192 (chain D), thereby linking two subunits. It is located near the N-terminus of the protein and separates two helices from each other.

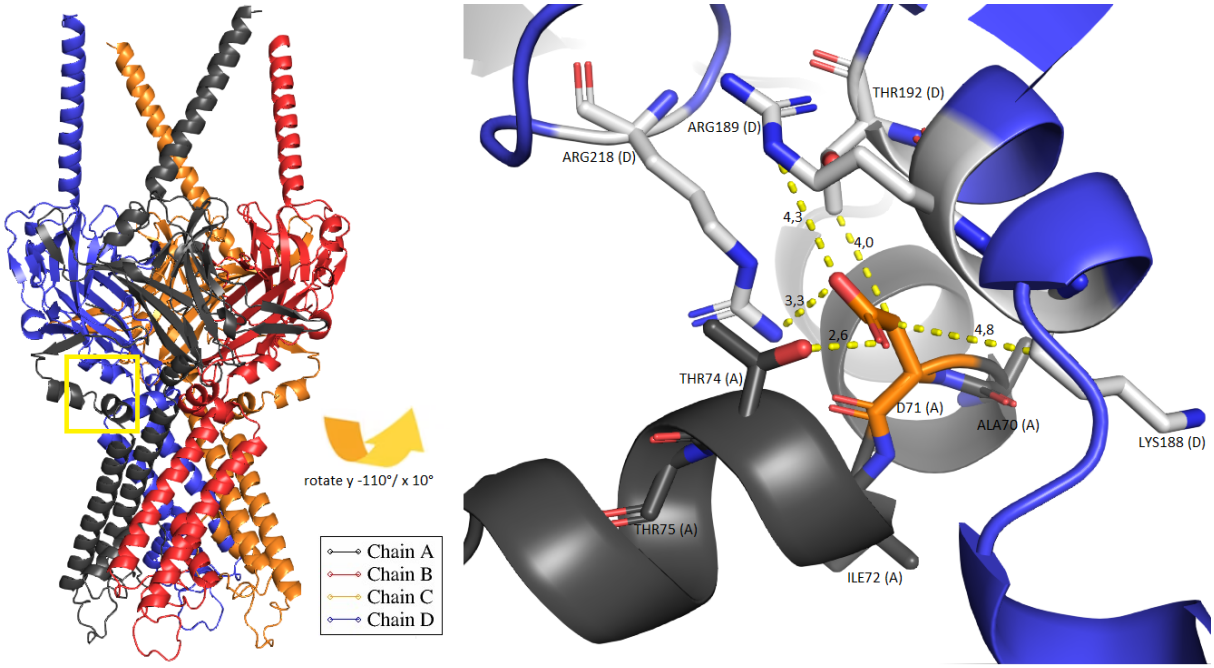

Figure 17: Left: Overview of Kir2.1 with 4 subunits. Right: Aspartic acid 71 (orange) in chain A (black) and surrounding residues in a radius of ~5Å. Backbone of chain D (blue) and interacting residues of chain D (white). Yellow lines indicate measurement in Å.

Mutations of D71 are known to cause ATS, although the exact function of the region it is located in is not completely clear at the moment[46] [47].

D71N is only a slight change in the structure, but the residue changes from a negatively charged to a neutral amino acid. The resulting amide group is less acidic and hydrogen bonds, even though still possible, are weaker.

D71V is not only a change in size, but a change from a negative carboxy group to a non-polar, aliphatic side chain and therefore the loss of hydrogen bonds, ionic or hydrophilic interactions. This mutation causes a loss of function and a dominant negative effect.[46] It does not alter channel assembly or trafficking suggesting that the slide helix has a role in channel gating[48].

4.3.4 T75A, T75M and T75R

Threonine 75 is located in a short helix near the cytoplasmatic N-terminus, a highly conserved region[47]. It is a hydrophilic, neutral amino acid[43] and its -OH group in the side chain can act as a hydrogen bond donor. This hydrogen bond can play a crucial role for the protein as it links chain A and chain D with each other.

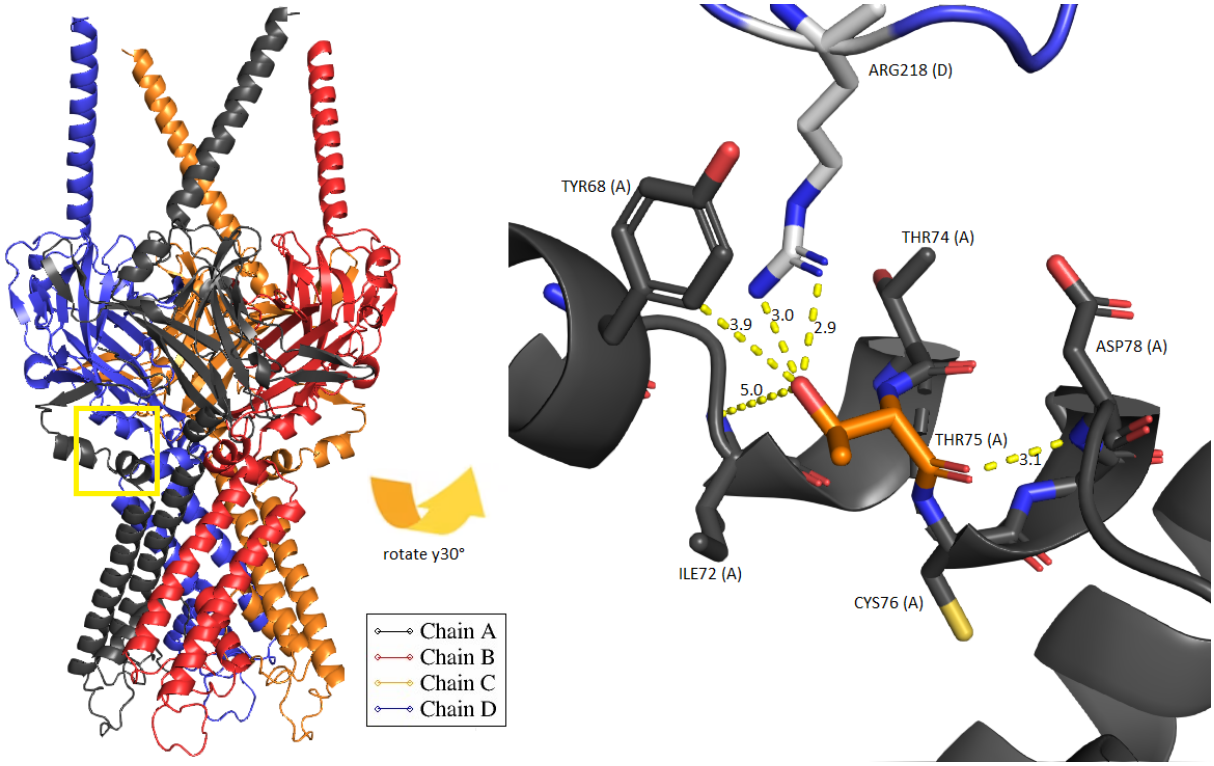

Figure 18: Left: Overview of Kir2.1 with 4 subunits. Right: Threonine 71 (orange) in chain A (black) and surrounding residues in a radius of ~5Å. Backbone of chain D (blue) and interacting residues of chain D (white). Yellow lines indicate measurement in Å.

T75A is a missense mutation form threonine to alanine leading to a loss of function[47]. T75A mutation changes a hydrophilic, neutral amino acid with an aliphatic, hydrophobic one[43]. Due to the loss of the -OH group in the side chain there is no longer the ability to create hydrogen bonds with arginine 218 (chain D) for example, which is within 2.9Å in wild type.

T75M mutation exchanges the hydrophilic threonine with hydrophobic methionine. The -OH functional group of threonine is changed to a longer side chain containing a $-SCH_3$ group. This mutation is a loss of function mutation by impaired trafficking and causes ATS. Mg^{+2}-block is also affected by T75M mutation.[49]

In case of T75R the small, polar, neutral threonine is exchanged with a large arginine, introducing a positive charge in the side chain[43]. The newly introduced positive charge of T75R leads to a repulsive effect with the arginine 218 of chain D and results in structural changes in this area. The T75R mutant is still able to co-assemble and traffic to cell membrane, but is non-functional and has a strong negative dominant effect[50].

4.3.5 D78G, D78H and D78Y

Aspartic acid 78 is a negatively charged amino acid[43] located in the cytoplasmatic N-terminus close to the membrane. The exact role of the slide helix is still unknown, but it is suggested that it is connected to the gating mechanism and its mutations cause ATS[51].

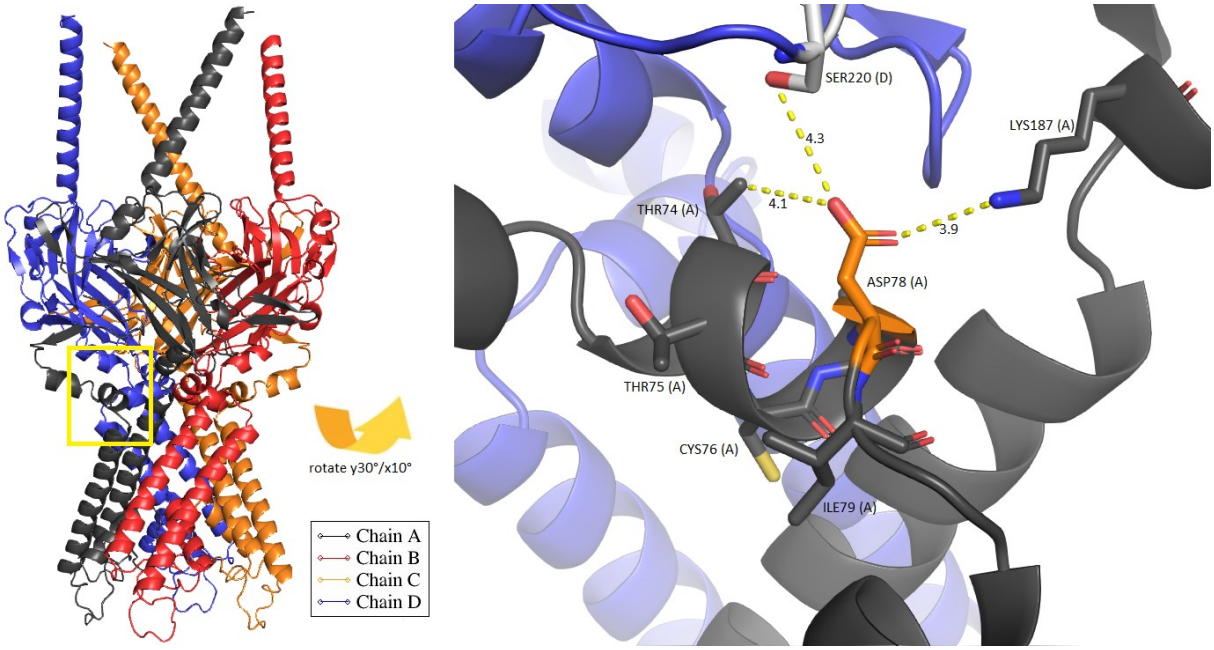

Figure 19: Left: Overview of Kir2.1 with 4 subunits. Right: Aspartic acid 78 (orange) in chain A (black) and surrounding residues in a radius of ~5Å. Backbone of chain D (blue) and interacting residues of chain D (white). Yellow lines indicate measurement in Å.

D78G is a missense mutation causing ATS[52]. As in other mutations in this area the hydrophilia seems to be important. Different hydrophilic residues are facing the same side of the helix and when mutated change their hydrophilia, like R67, D71 or T74. The same is true for D78G, where aspartic acid, which is carrying a negative charge is exchanged with glycine, a non-polar amino acid.[43]

The exchange of aspartic acid 78 with histidine results in a change of an acidic with a weak basic residue. Histidine has an aromatic ring in its side chain and can be positively charged resulting in a repulsive effect with the positive lysine 187 (A).

In case of D78Y the exchange includes an aromatic ring and changes the residue from negative charge to neutral and increases its size. Even though the trafficking is not impaired, it causes a loss of function, due to a disturbed interaction between the slide helix and the C-terminus.[51]

4.3.6 R82Q and R82W

Arginine 82 is located in the transmembrane helix and is part of the PIP_2 binding site and therefore in a crucial region of the Kir2.1 channel[39]. It contains a guanidino group and therefore is a positively charged amino acid[43].

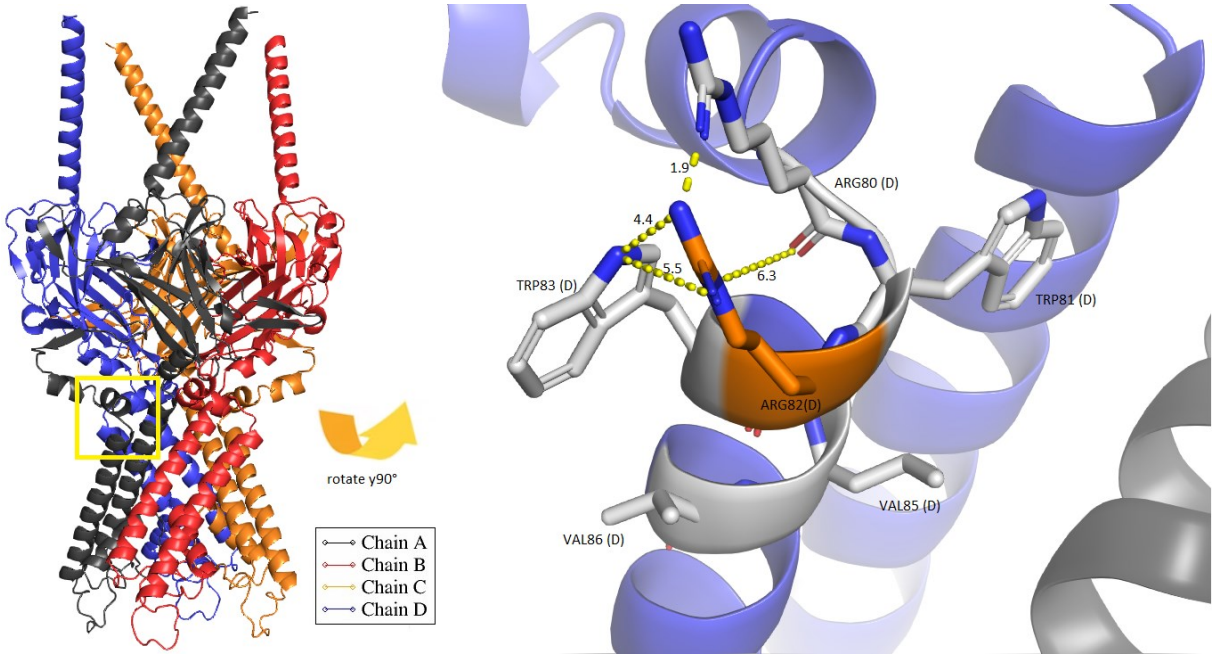

Figure 20: Left: Overview of Kir2.1 with 4 subunits. Right: Arginine 82 (orange) in chain D (blue) and surrounding residues of chain D (white). Yellow lines indicate measurement in Å.

R82Q changes the positively charged to a neutral but still polar side chain[43]. There are no steric problems, because the side chain faces to the outside. The channel is still able to form tetramers und traffics to the cell membrane, but shows very low currents[52]. The mutation shows no effect on PIP_2 interaction, but still has an impact on channel activation[53].

The missense mutation R82W is showing no measurable currents but has a dominant negative effect on wild type channel[54]. The positively charged arginine 82 is replaced by an aromatic, non-polar, neutral tryptophan[43]. Facing to the outside of the channel the change in size does not matter that much, which suggests that the positive charge of arginine is essential for channel function.

4.3.7 V93I

Valine 93 is a highly conserved amino acid in Kir2.1 channels in different species. It is located in the outer helix (M1) of the TMD. A mutation in this position leads to a gain of function and causes atrial fibrillation.[55] Valine is an aliphatic, neutral, non-polar amino acid[43].

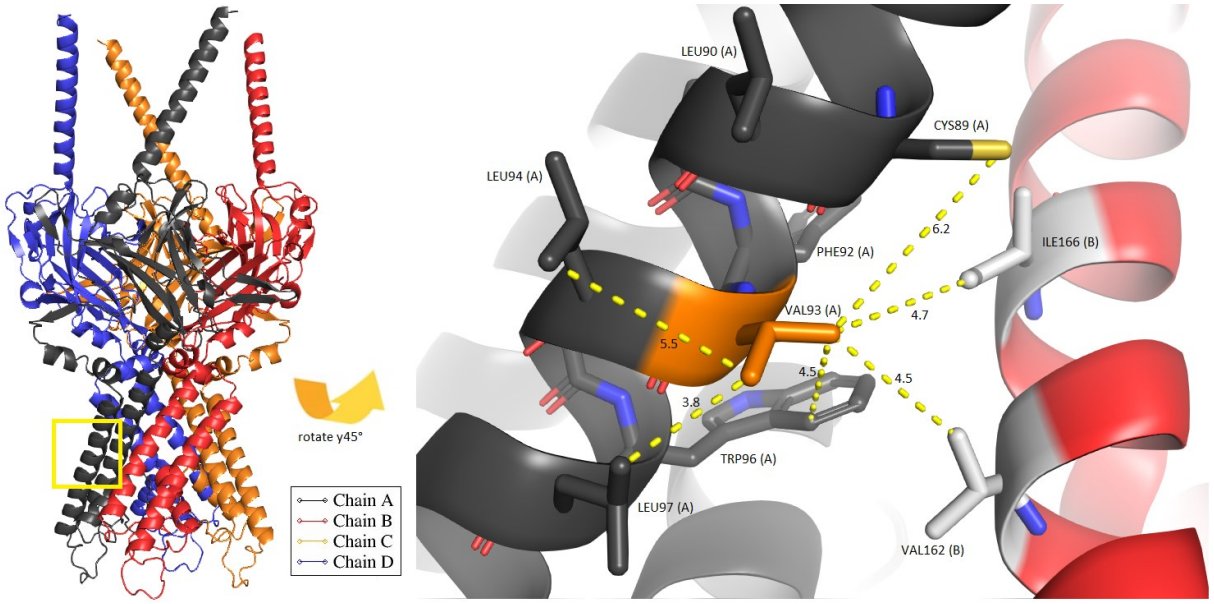

Figure 21: Left: Overview of Kir2.1 with 4 subunits. Right: Valine 93 (orange) in chain A (black) and surrounding residues in a radius of ~6Å. Backbone of chain B (red) and interacting residues of chain B (white). Yellow lines indicate measurement in Å.

In this case there is no change in polarity or charge. Valine and Isoleucine are both aliphatic, neutral, non-polar amino acids[43]. The only difference is an additional -CH_3 group in isoleucine. The V93I mutation is a gain of function mutation, which leads to increased activity of the channel. This causes short QT syndrome type 3, atrial fibrillation, due to increased currents, both inside and out the cell, which lead to a shortened action potential duration. The change in conduction is most likely due to the close proximity of V93 to the pore. [55] [56] [57]

4.3.8 SWLF95-98

Amino acids serine 95, tryptophane 96, leucine 97 and phenylalanine 98 are located inside the M1 helix near the pore helix and the selectivity filter. In this case there is no exchange of residues, but a deletion, resulting in a structural change. This effects the trafficking of the channel and causes a loss of function.[54] This might be caused by a misfolding of the protein and may cause degradation[48].

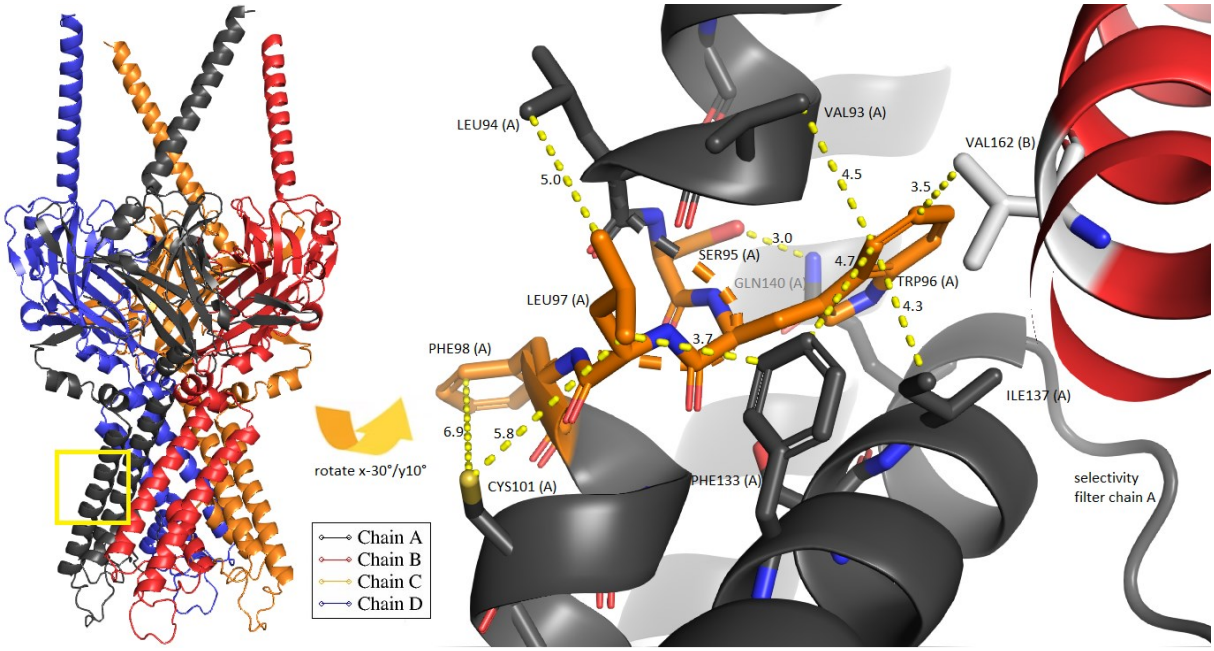

Figure 22: Left: Overview of Kir2.1 with 4 subunits. Right: Serine 95, tryptophane 96, leucine 97 and phenylalanine 98 (orange) in chain A (black) and surrounding residues in a radius of ~7Å. Backbone of chain B (red) and interacting residues of chain B (white). Yellow lines indicate measurement in Å. In the bottom right corner is a part of the selectivity filter of chain A near SWLF95-98 (A).

4.3.9 S136F

Serine is a polar, neutral[43] amino acid and has a -OH group in its side chain. This hydroxy group is able to form a hydrogen bond with nearby residues like glutamine 164. The pore helix, in which S136 is located in, is directly connected to the selectivity filter and is crucial for channel function[48].

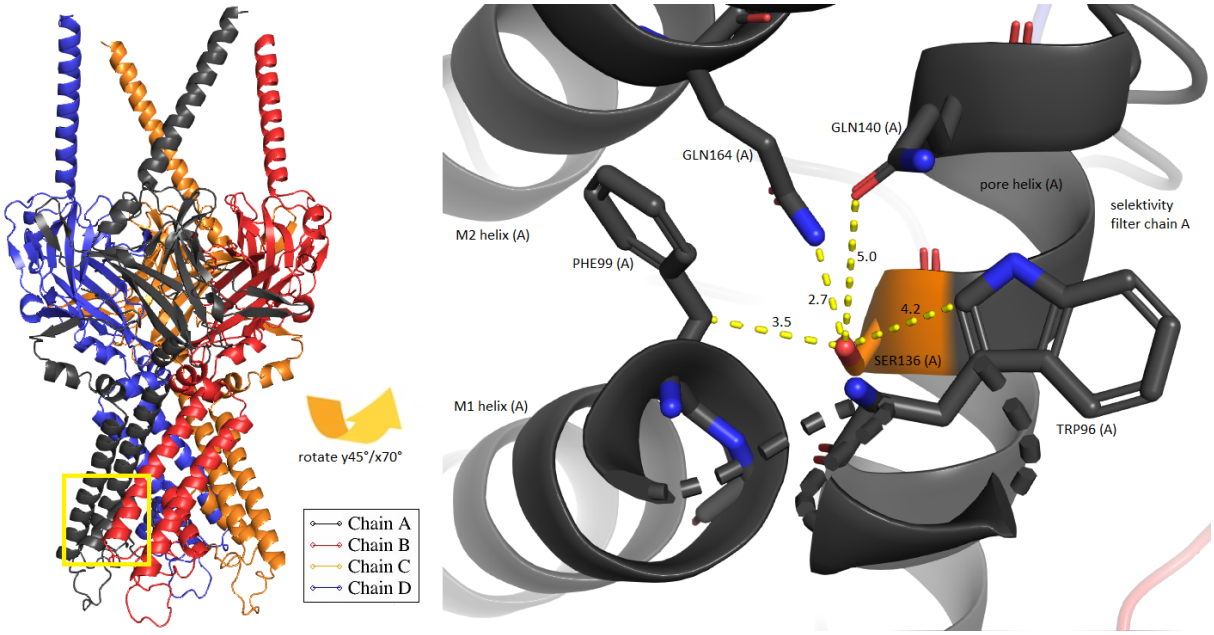

Figure 23: Left: Overview of Kir2.1 with 4 subunits. Right: Serine 136 (orange) in the pore helix of chain A (black) and surrounding residues in a radius of ~5Å. Yellow lines indicate measurement in Å. In the top right corner is the selectivity filter.

S136F is a missense mutation, which exchanges the polar serine with an aromatic, non-polar phenylalanine[43]. Apart from the loss of ability to create hydrogen bonds the ring structure of phenylalanine requires a lot more space. As shown in figure24 there are a lot of clashes with the neighboring side chains. The presence of F99 and W96 may result in π-stacking with the newly added aromatic ring of phenylalanine 136. This mutation leads to a loss of function and a dominant negative effect on wild type channels[46] [58].

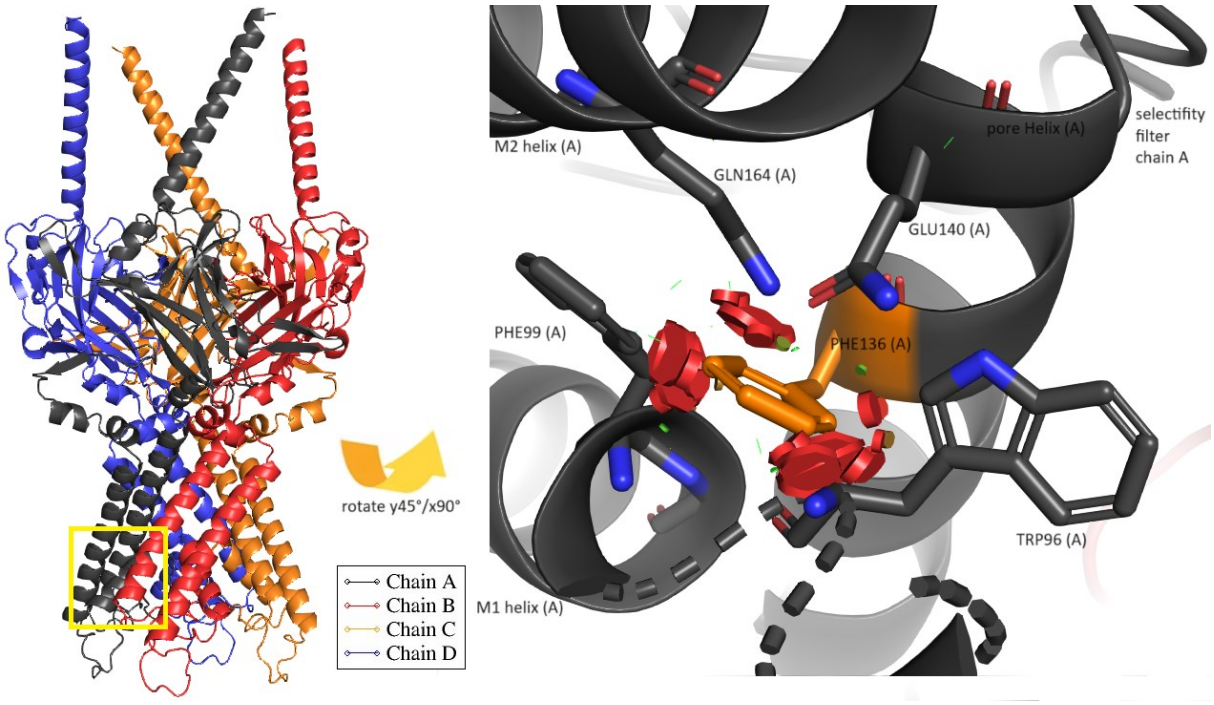

Figure 24: Left: Overview of Kir2.1 with 4 subunits. Right: S136F (orange) in the pore helix of chain A (black) and surrounding residues in a radius of ~5Å. Circles show clashes caused by the mutation: Size and color changes from green to red indicate the severity of the clash.

4.3.10 G144A, G144D and G144S

Glycine 144 is located directly inside the K^+ ion selectivity filter which is a highly conserved region as part of the typical GYG sequence[46]. Every change in the structure causes a difference in the distance between the oxygen atoms of the backbone facing into the pore. These distances are crucial for the selectivity for K^+ ions and is one of 4 constriction point in Kir2.1[4]. Changes in this region effect the gating mechanism of the channel[59].

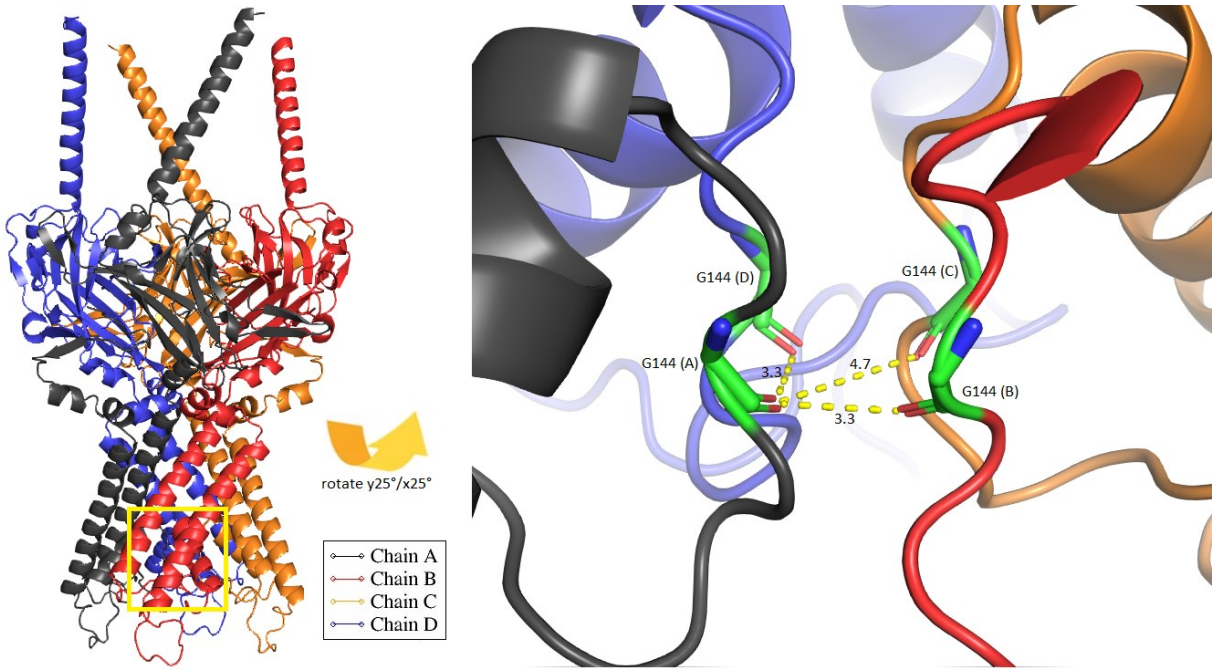

Figure 25: Left: Overview of Kir2.1 with 4 subunits. Right: Glycine 144 (green) in the selectivity filter of all chains (A black, B red, C orange, D blue). Yellow lines indicate measurement in Å between the backbone of the 4 subunits.

G144A, exchanging glycine with alanine, is a loss of function mutation, which traffics normally to the membrane but shows no inward rectifying currents and is known to cause ATS[60]. The structural change only effects the size of the residue, which may affect the diameter of the pore. Both amino acids are neutral and hydrophobic[43].

G144D switches the glycine for an aspartic acid. This results not only in a change of size, but also a change of polarity, because aspartic acid has a -COOH group that can be negatively charged[43]. As this region is very important to the correct function of the channel, a change in size of the side chain as big as G144D produces multiple clashes with the surrounding residues, as shown in figure 26. This mutation causes

an atypical phenotype of ATS and shows dominant negative suppression effects on outward currents[61].

The missense mutation G144S not only changes the size of the side chain, but also introduces a polar group[43]. This leads to a loss of function, causing ATS[46]. Like in G144A the G144S mutation shows no measurable K^+ currents[58].

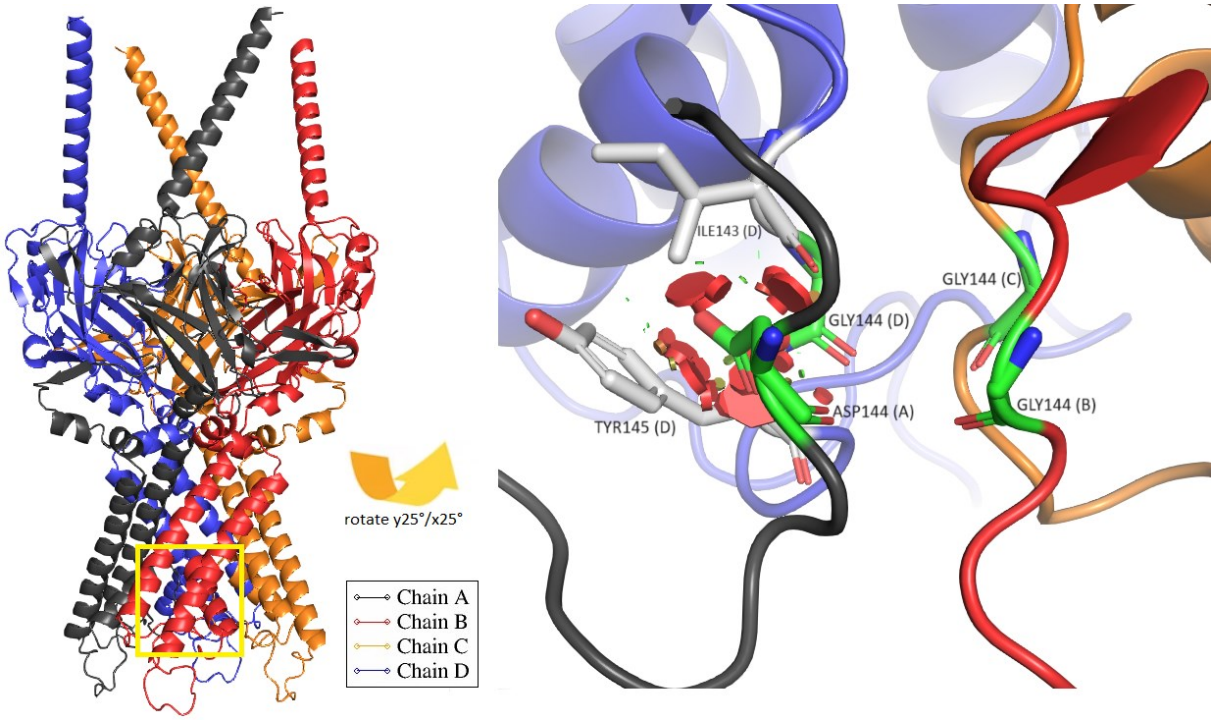

Figure 26: Left: Overview of Kir2.1 with 4 subunits. Right: Glycine 144 (green of chains B red, C orange, D blue) and G144D (green) in the selectivity filter of chain A (black). Circles show clashes caused by the mutation: Size and color changes from green to red indicate the severity of the clash.

4.3.11 G146A, G146D and G146S

G146 is part of the selectivity filter for K^+ ions, a highly conserved region of the channel and the third residue of the typical GYG sequence[46] [62].

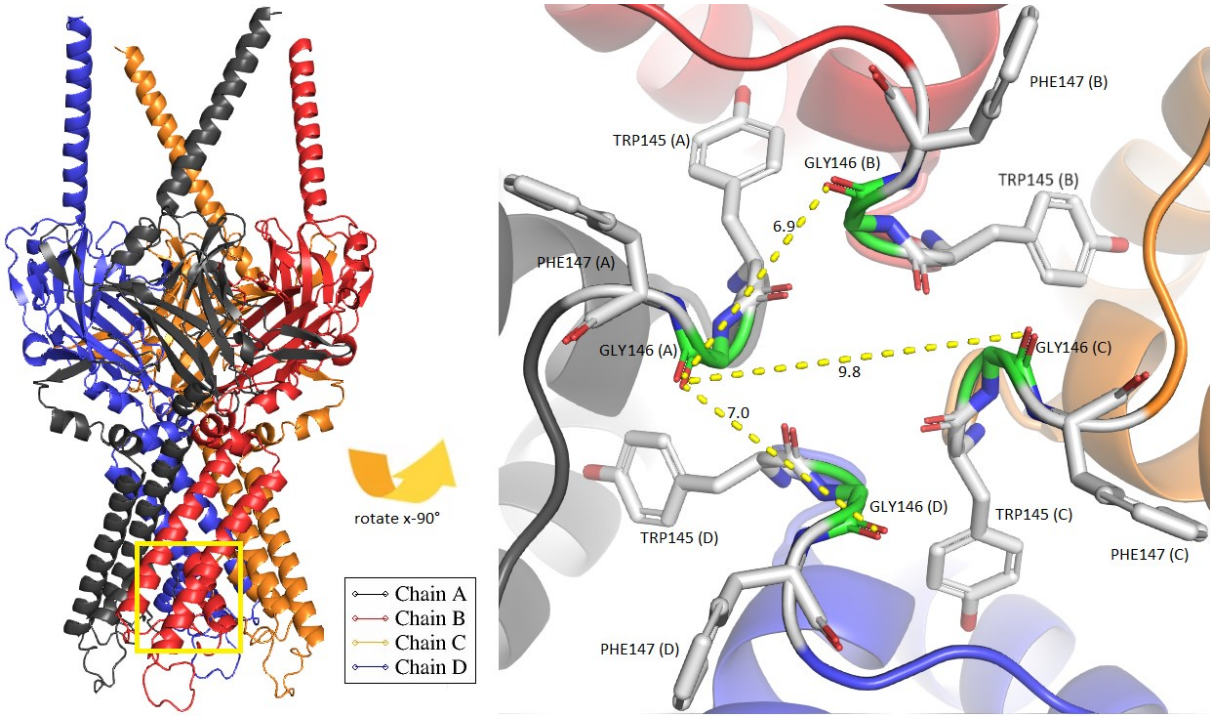

Figure 27: Left: Overview of Kir2.1 with 4 subunits. Right: Glycine 146 (green) in the selectivity filter of all chains (A black, B red, C orange, D blue). Tryptophane 145 and phenylalanine 147 of all 4 subunits in white. Yellow lines indicate measurement in Å between the backbone of the 4 subunits. View through the pore from the TMD.

The missense mutation G146A swaps the Glycine for an alanine resulting in a loss of function and causes ATS[63]. As shown in figure 28 the mutation changes the diameter of the channel, due to the side chain facing inside the pore. This either means the backbone has to change its position or the selectivity filter is constricted by the side chain. For the G146D and G146S mutation this problem will be even worse, due to the bigger side chains.

If glycine 146 is exchanged for aspartic acid 146 this changes the electrochemical characteristics of the residue. Aspartic acid has a -COOH group in the side chain, which can be negatively charged[43] and requires more space than the single proton of glycine. This results in an alteration in PIP_2 binding and therefore causes ATS[45].

G146S introduces a polar -OH group into the side chain, changing the polarity of the residue. This results in a loss of function and causes ATS. G146S shows no inward

rectifying currents and has a strong dominant negative effect, when co-expressed with wild type channel[64].

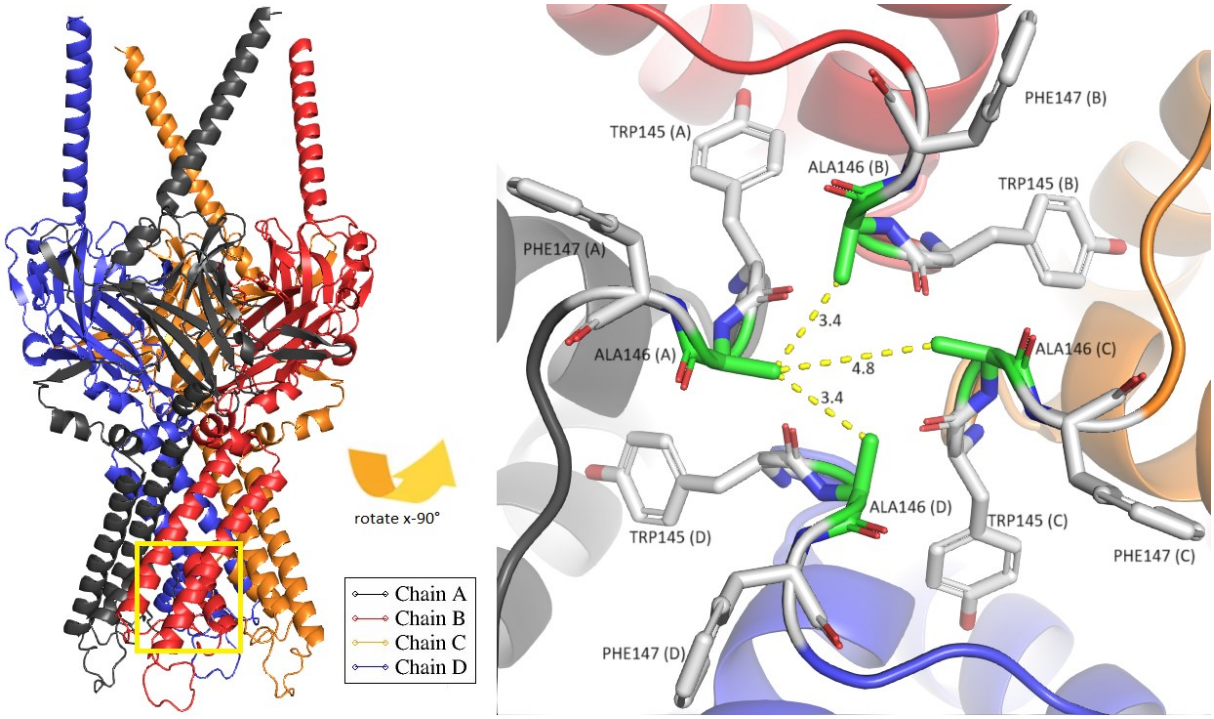

Figure 28: Left: Overview of Kir2.1 with 4 subunits. Right: G146A (green) in the selectivity filter of all chains (A black, B red, C orange, D blue). Tryptophane 145 and phenylalanine 147 of all 4 subunits in white. Yellow lines indicate measurement in Å between the -CH_3 groups of the 4 mutated side chains. View through the pore from the TMD.

4.3.12 C154F and C154Y

Cysteine 154 carries a -SH group in the sidechain, which is important for the structure of the channel, because, in our model, it forms a disulfide bridge with cysteine 122 of the same chain. It is located at end of the TMD, close to the extracellular loop region.[4]

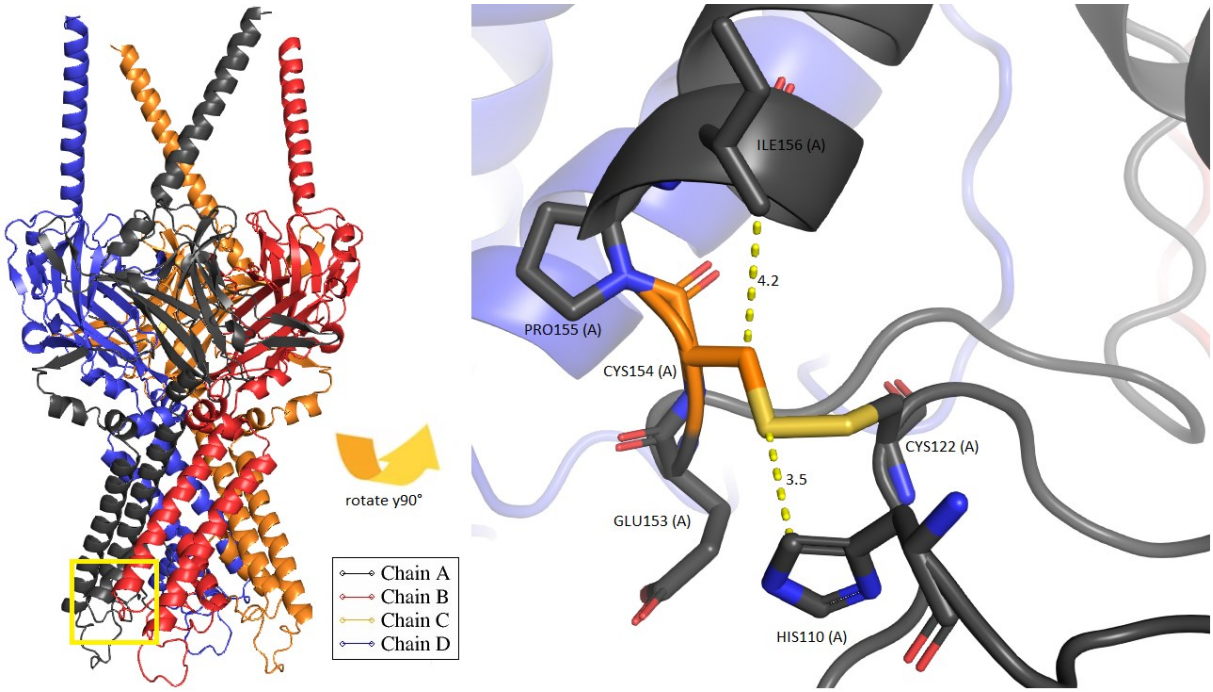

Figure 29: Left: Overview of Kir2.1 with 4 subunits. Right: Cysteine 154 (orange) in chain A (black) forming a disulfide bridge with cysteine 122 (chain A). Yellow lines indicate measurements in Å.

C154F is a missense mutation, which results in a loss of function and causes ATS and shows a dominant negative effect on wildtype channel[64]. The exchanged residue has no -SH group and cannot form a disulfide bridge to stabilize this region. No clashes are caused, because there is enough room for the bulky side chain of phenylalanine.

Like with C154F, C154Y is a missense mutation and is associated with ATS[65]. The exchange of cysteine with tyrosine causes the same issue with the disulfide bridge like in the C154F mutation. Tyrosine has no -SH group in the side chain to create the disulfide bridge, linking position 154 with C122 of the same chain. As it is located on the outside of the channel, there are no steric clashes.

4.3.13 D172N

Aspartic acid 172 is located inside the M2 helix of the TMD just outside the selectivity filter. It creates a negative ring inside the channel pore which is crucial for channel block via Mg^{2+} and polyamines.[4]

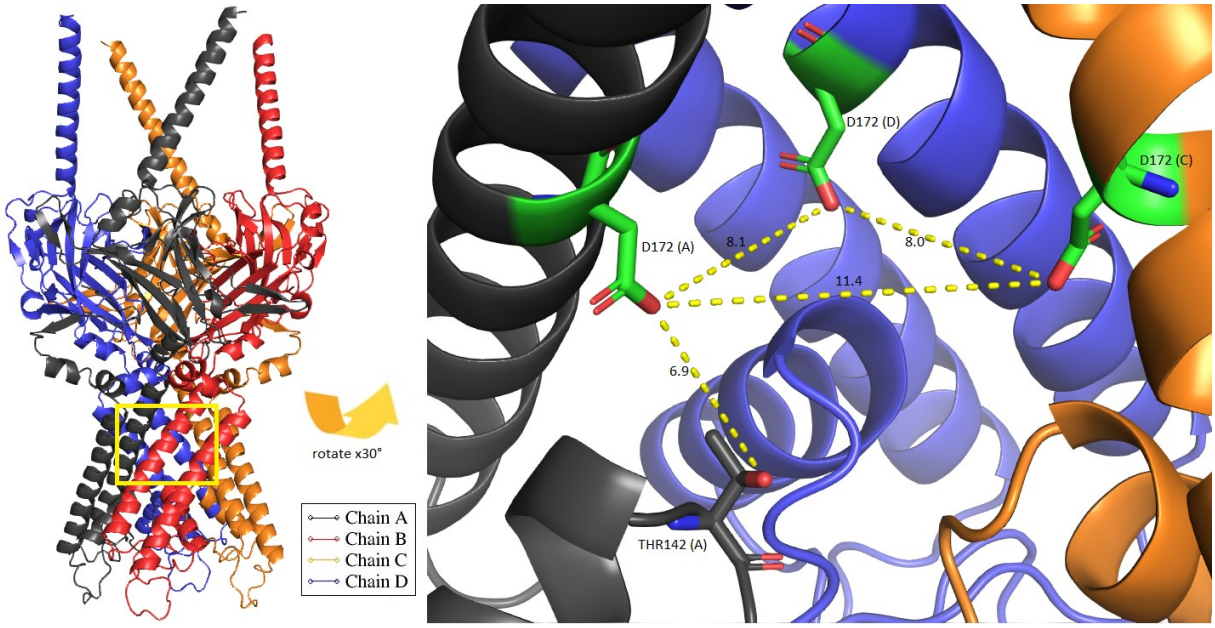

Figure 30: Left: Overview of Kir2.1 with 4 subunits. Right: Aspartic acid (green) in chain A (black), C (orange) and D (blue) forming a negatively charged ring inside the pore channel. Threonine 142 (chain A) marking the start of the selectivity filter. Yellow lines indicate measurements in Å. Chain B is removed for clarity.

In this mutation the aspartic acid 172 is exchanged with asparagine 172. This changes the carboxyl group, which can be negatively charged, for a neutral amide group[43] but does not influence the size very much. The negatively charged ring is necessary for interaction with Mg^{2+} and polyamines, which results in an increased K^+ current leading to a gain of function. D172N is associated with short QT syndrome type 3 and atrial fibrillation.[57] [66]

4.3.14 P186L and P186Q

Proline is a special amino acid, due to its structure. The backbone is linked with the side chain a second time forming a ring with the amine group, making it very rigid. Because of this inflexibility it is also known as a helix breaker[67]. Position 186 is part of the PKKR motive, which is crucial for PIP_2 binding[68].

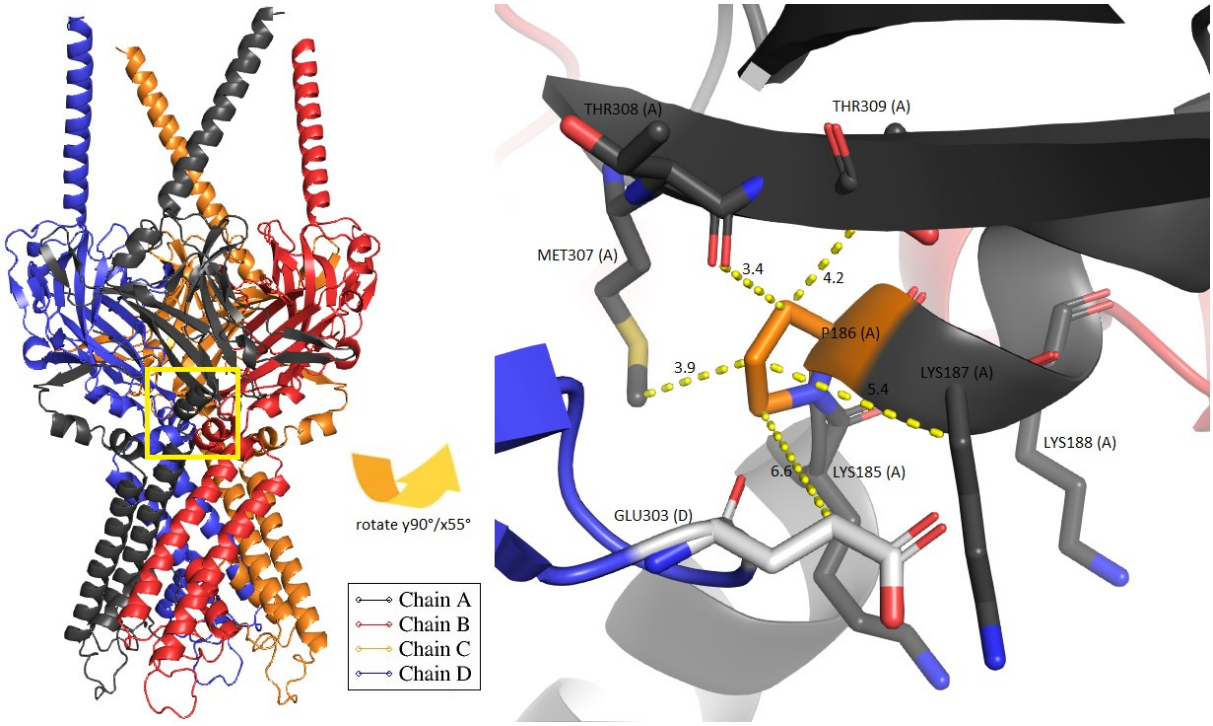

Figure 31: Left: Overview of Kir2.1 with 4 subunits. Right: Proline 186 (orange) in chain A (black) and surrounding residues of chain A (black) and chain D (blue/white). Yellow lines indicate measurements in Å.

The ability of proline to break a helix may be of great importance in this position, as it separates 2 helices within 3 residues[67].

The missense mutations P186L and P186Q alter the crucial PKKR sequence and lower the sensibility for PIP_2[69]. P186Q even shows almost no currents through the channel and may even effect the correct trafficking to the membrane[70]. This is a result of the steric clashes due to the change in size of the sidechain that force the backbone to shift it position. See figure 32. P186Q changes the neutral, cyclic proline with glutamine, a polar residue[43], that can engage in hydrogen bonds.

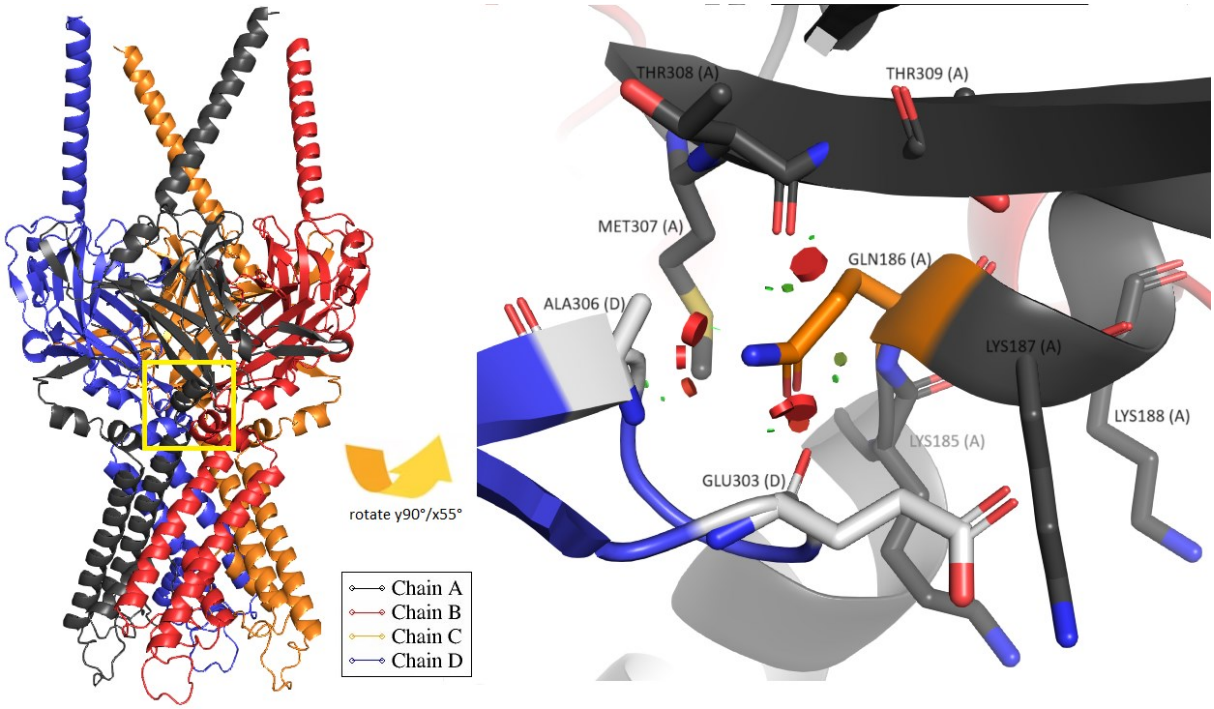

Figure 32: Left: Overview of Kir2.1 with 4 subunits. Right: P186Q (orange) in chain A (black) and surrounding residues of chain A (black) and chain D (blue/white). Circles show clashes caused by the mutation: Size and color changes from green to red indicate the severity of the clash.

4.3.15 R189G, R189I, R189K and R189T

Like proline 186, arginine 189 is part of the PIP_2 binding site and has therefore a crucial role in channel activation. The unique guanidino group gives this residue a basic characteristic and the possibility to carry a positive charge[43] to interact with ligands or other amino acids like H221[4]. The weak interaction between H221-R189, both in chain A, is involved in g-loop gating mechanism[71]. In our structure H221 is facing away from R189, but the interaction with H221 may be seen, if there is a PIP_2-ligand docked to the channel or in a different state. The interactions between R189 (A) and T192 (A) or D71 (B) are more likely in this state of the channel.

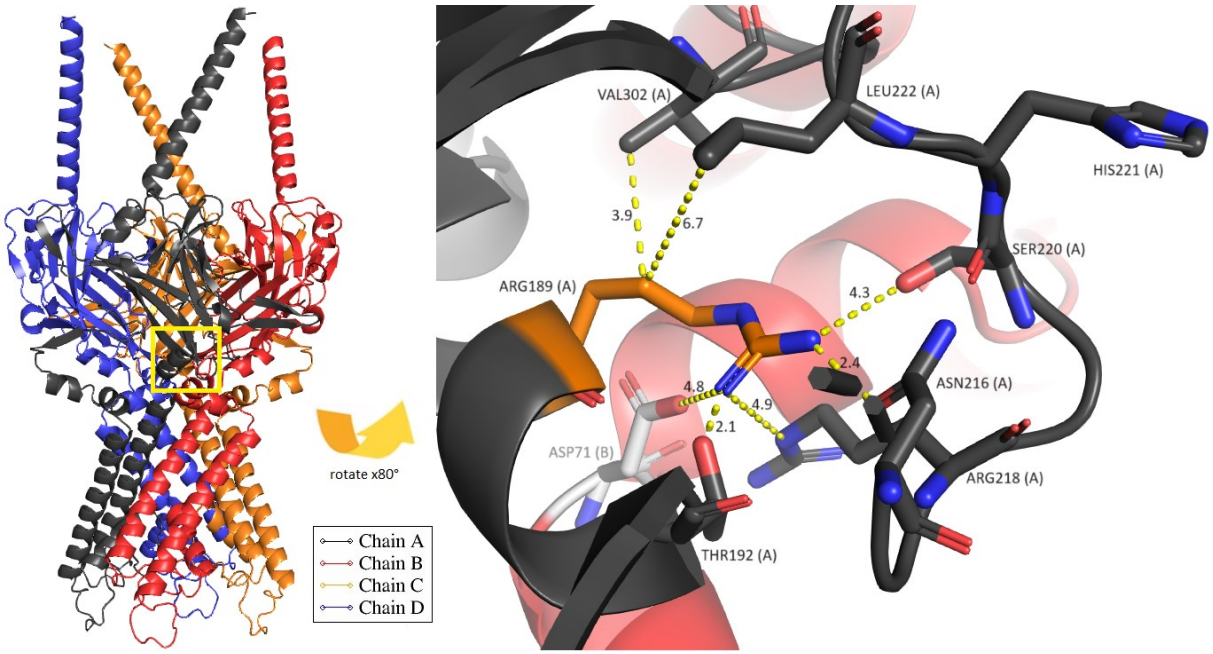

Figure 33: Left: Overview of Kir2.1 with 4 subunits. Right: Arginine 189 (orange) in chain A (black) and surrounding residues. Backbone of chain B (red) and interacting residues of chain B (white). Yellow lines indicate measurement in Å.

Mutations R189G and R189I both change the polar characteristics of arginine to a neutral side chain, removing the possibility of hydrogen bonds or ionic interactions with ligands or H221[4]. This will impact the sensitivity for PIP_2 and alter the activation of Kir2.1[53] [71]. For glycine there are no steric problems, but isoleucine causes some minor clashes especially with valine 302 (A).

In case of R189K the positive charge is preserved, but the ability to engage in hydrogen bonds is reduced. There are no major steric clashes as the side chain is similar to arginine.

The R189T mutation still has the ability to create hydrogen bonds but is no longer charged. Steric clashes are neglectable as the side chain is much smaller, which leads to the conclusion that the most important feature of this position is its positive charge and the ability to create hydrogen bonds.

4.3.16 T192A and T192I

Threonine 192 is located in the highly conserved PIP_2 binding site after the M2 helix and is important for channel activation and multimerization. Missense mutations are known to cause ATS[72]. Due to its -OH group in the side chain it can interact with ligands or other residue via hydrogen bonds stabilizing the area or linking subunit A and B.

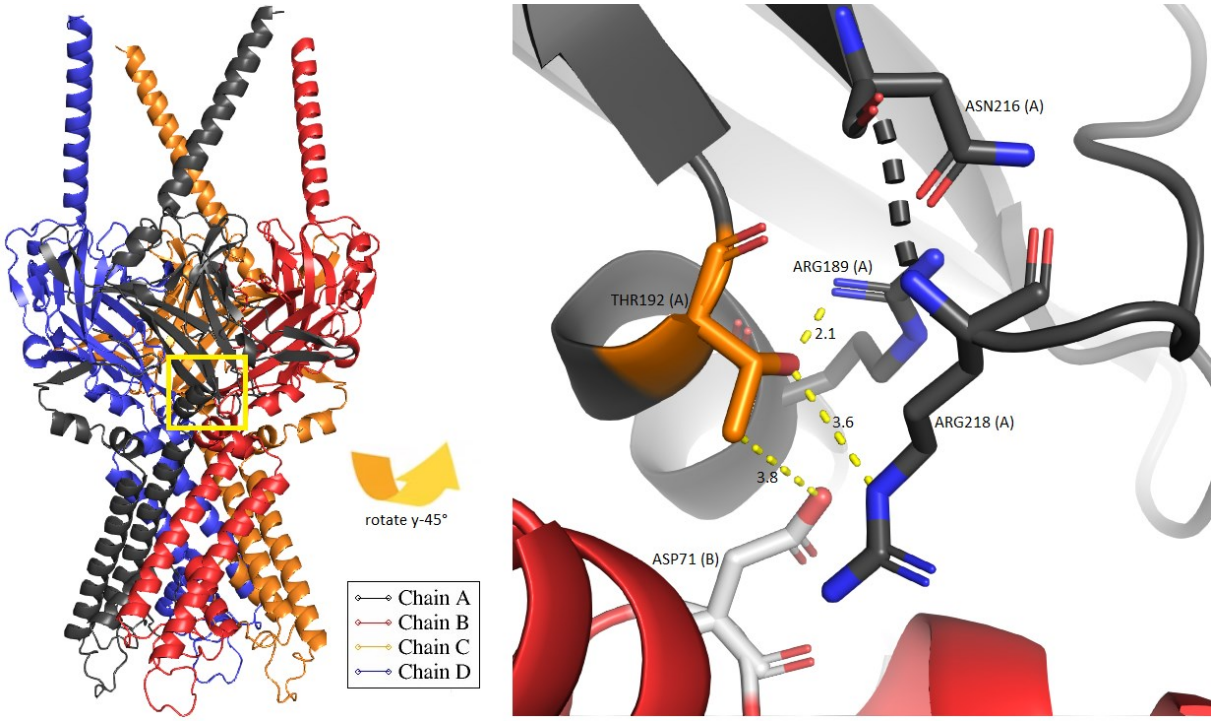

Figure 34: Left: Overview of Kir2.1 with 4 subunits. Right: Threonine 192 (orange) in chain A (black) and surrounding residues in a radius of ~5Å. Backbone of chain B (red) and interacting residues of chain B (white). Yellow lines indicate measurement in Å.

T192A changes the polar side chain with the -OH group for a neutral, non-polar, shorter side chain of alanine[43], removing the ability to form hydrogen bonds. Under homomeric conditions this mutation prevents all K^+ ion currents and leaves the channel non-functional. In co-expression with wild type subunits, currents are lowered but not completely missing[66] [72]. This suggests that the binding of PIP_2, which stabilizes the open state of the channel, is affected and that the ability to engage in hydrogen bonds is crucial for this residue.

If threonine 192 is swapped with isoleucine, the side chain loses its polar function. This will disrupt the stability due to the lack of hydrogen bonds to other residues und will affect PIP_2 binding. The change in size also effects the surroundings and causes

several clashes with R218 and R189 both in chain A. As a missense mutation T192I is known to cause ATS.[73]

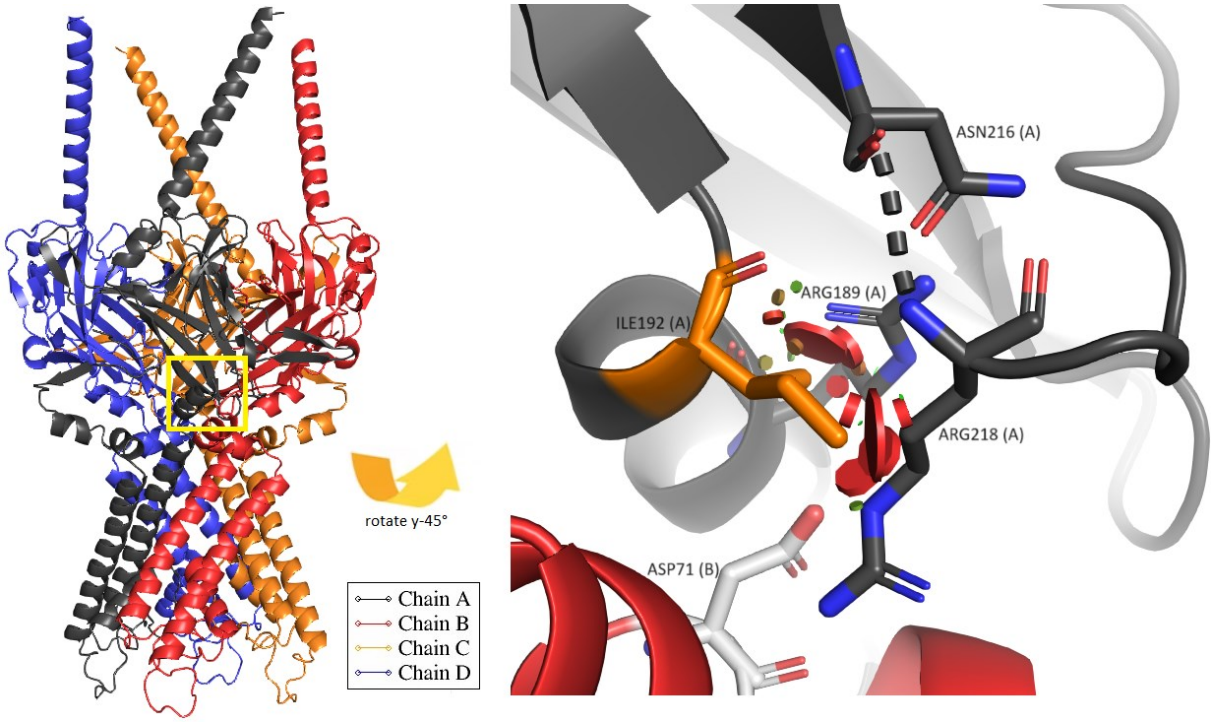

Figure 35: Left: Overview of Kir2.1 with 4 subunits. Right: T192I (orange) in chain A (black) and surrounding residues of chain A (black) and chain B (red/white). Circles show clashes caused by the mutation: size and color changes from green to red indicate the severity of the clash.

4.3.17 G215D

Glycine 215 is buried in the protein interface in the CTD, a highly conserved region. It is involved in Kir2.1 assembly.[74] G215 is near arginine 218, which is involved in PIP_2 binding[4].

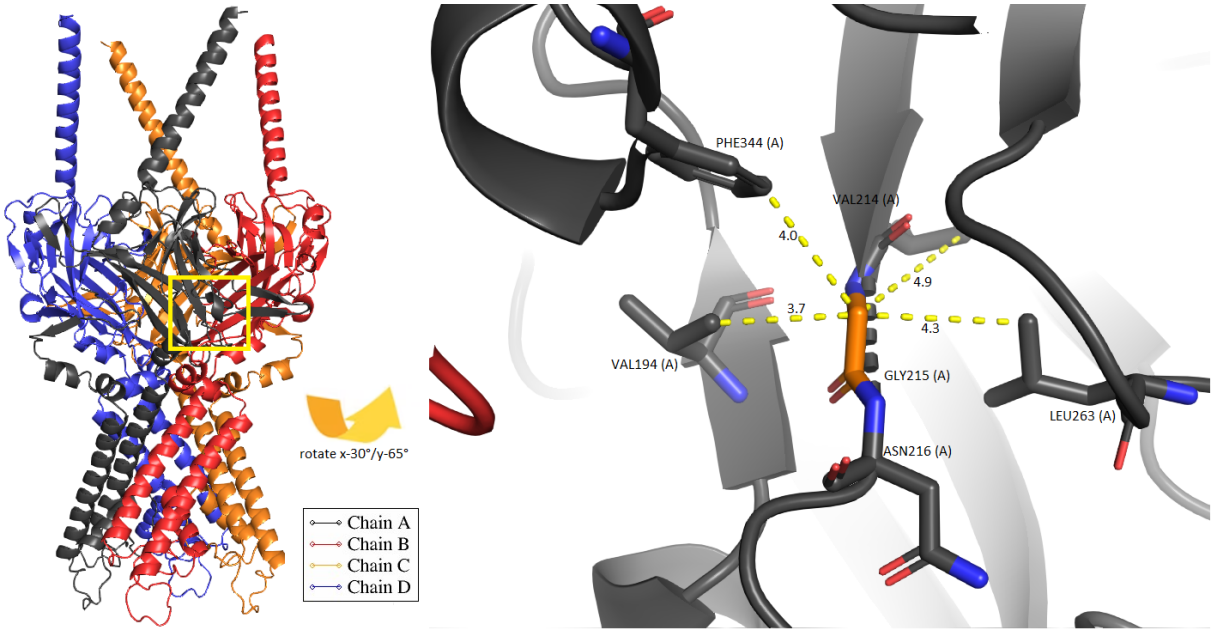

Figure 36: Left: Overview of Kir2.1 with 4 subunits. Right: Glycine 215 (orange) in chain A (black) and surrounding residues in a radius of ~5Å. Yellow lines indicate measurement in Å.

G215D is a mutation causing ATS, with cardiac arrhythmia, periodic paralysis and dysmorphic features. Trafficking is only influenced by this mutation when expressed homomeric, but the K^+ ion currents are reduced even in combination with wild type subunits leading to a malfunctioning channel. When co-expressed with wild type channel it shows a dominant negative effect.[74] Due to structural changes, there are many clashes with surrounding residues forcing the backbone to shift. Furthermore, introducing a positive charge in the PIP_2 binding pocket close to arginine 218 can affect the PIP_2 sensitivity due to ionic interactions.

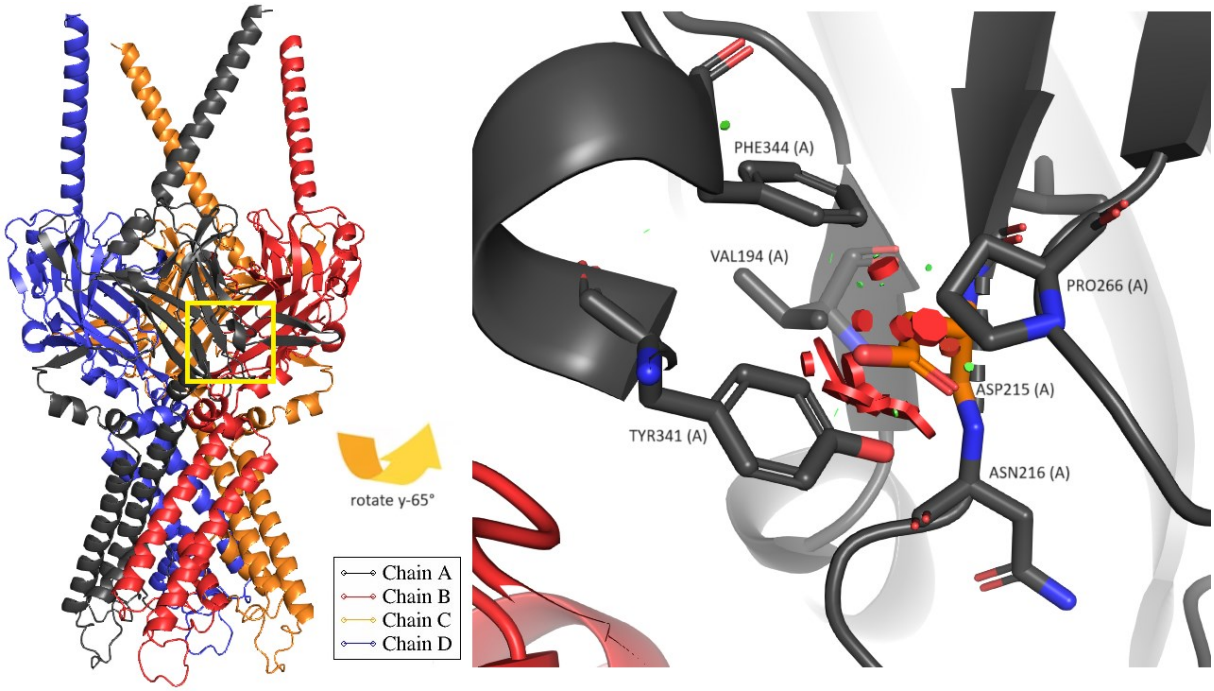

Figure 37: Left: Overview of Kir2.1 with 4 subunits. Right: G215D (orange) in chain A (black) and surrounding residues in a radius of ~5Å. Circles show clashes caused by the mutation: Size and color changes from green to red indicate the severity of the clash.

4.3.18 N216H

Asparagine 216 is part of a region in the C-terminus and is involved in PIP_2 interaction and therefore may influence the gating mechanism. Mutations of this residue are known to cause ATS.[48]

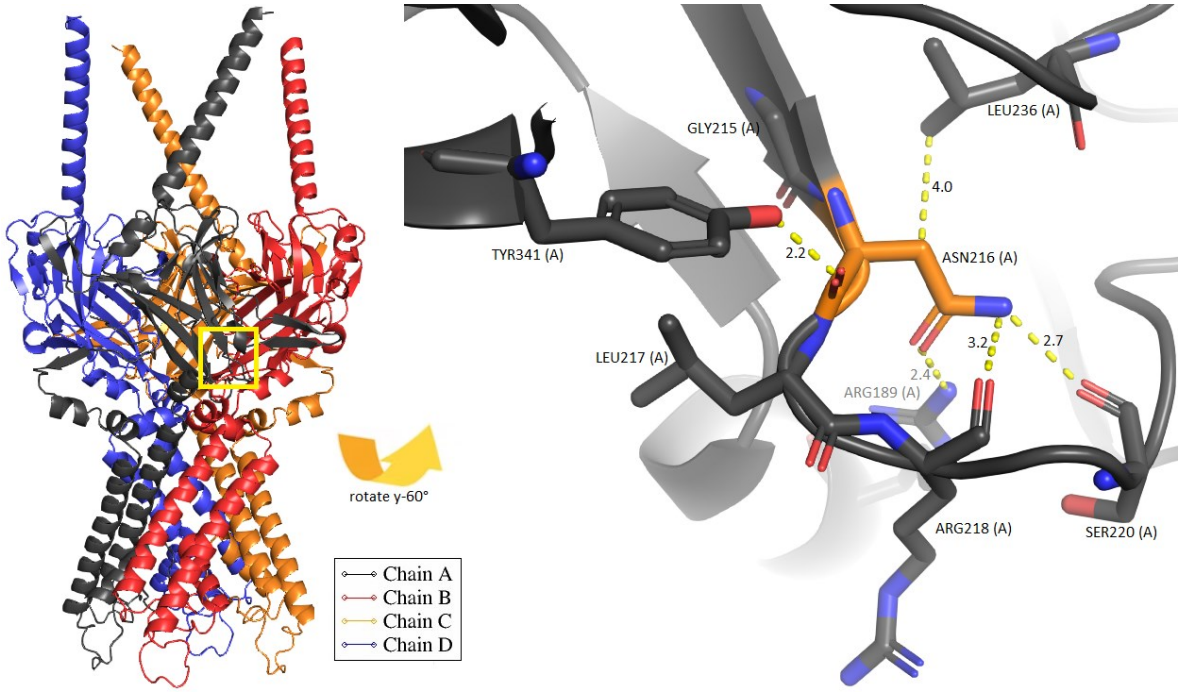

Figure 38: Left: Overview of Kir2.1 with 4 subunits. Right: Asparagine 216 (orange) in chain A (black) and surrounding residues in a radius of ~5Å. Yellow lines indicate measurement in Å.

N216H mutation changes the polar, neutral side chain to an aromatic one that can be positively charged[43]. This mutation affects trafficking of the channel when expressed alone and leads to a loss of function. It can form channels in combination with wild type subunits, trafficking normally to the membrane, but leads to reduced currents.[48] In our model the positive charge of histidine causes a repulsive effect with arginine 189 of chain A and the bulky aromatic side chain causes several steric clashes with arginine 218 and arginine 189 both in chain A, forcing the backbone to alter its structure.

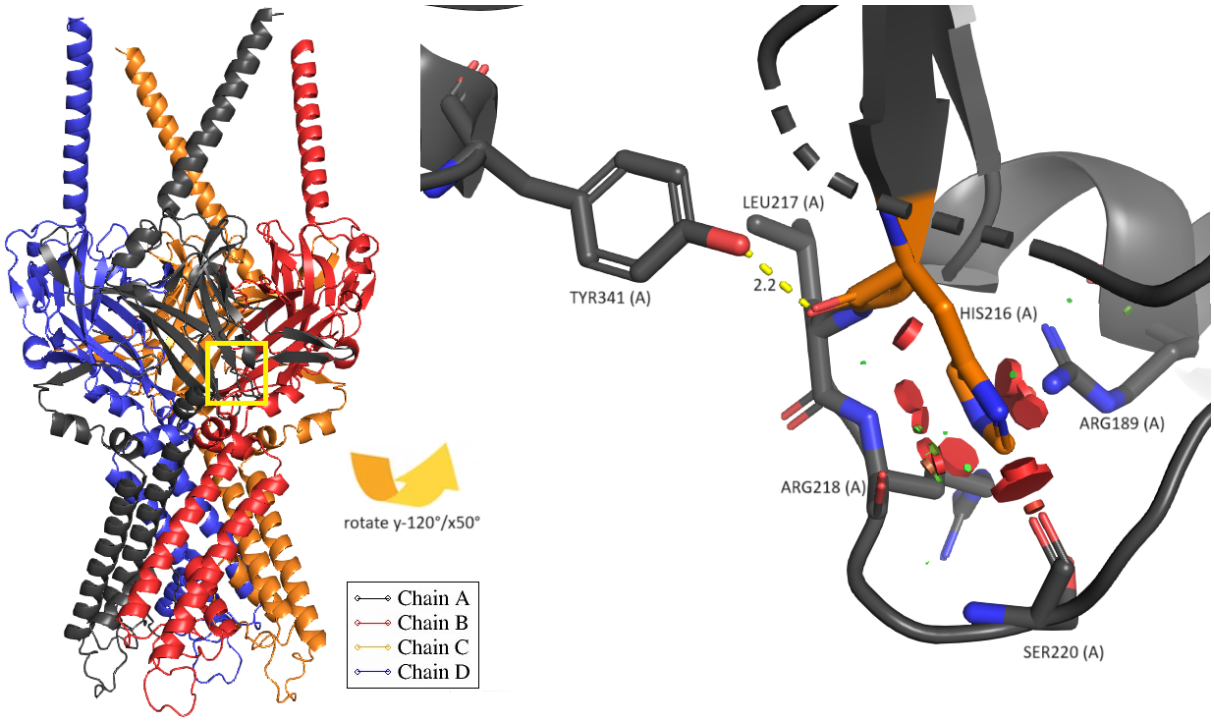

Figure 39: Left: Overview of Kir2.1 with 4 subunits. Right: N216H (orange) in chain A (black) and surrounding residues in a radius of ~5Å. Yellow lines indicate measurement in Å. Circles show clashes caused by the mutation: Size and color changes from green to red indicate the severity of the clash.

4.3.19 R218L, R218P, R218Q and R218W

Arginine 218 is a crucial amino acid located in the binding pocket for PIP_2 in the CTD and carries a positively charged side chain. It is directly involved in PIP_2 binding and interacts with G-loop gating. For interaction with the phosphate groups of PIP_2 the positive charge plays a crucial role[4] [75].

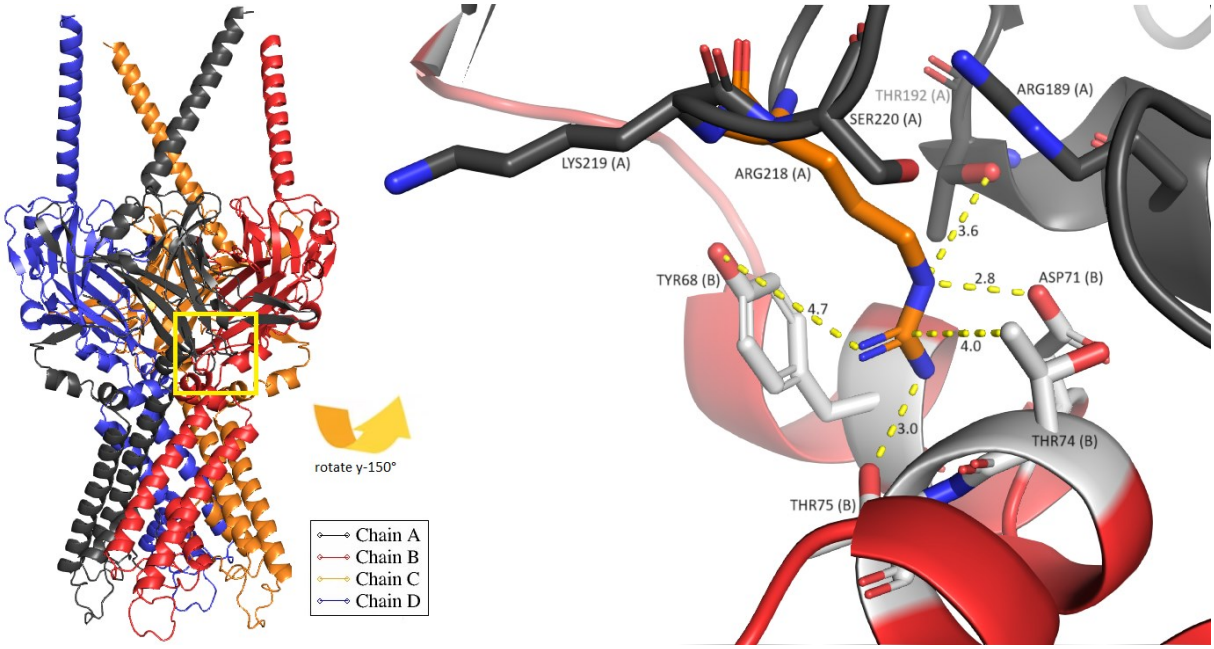

Figure 40: Left: Overview of Kir2.1 with 4 subunits. Right: Arginine 218 (orange) in chain A (black) and chain B (red) surrounding residues black (chain A) and white (chain B) in a radius of ~5Å. Yellow lines indicate measurement in Å.

Mutations of arginine 218 are missense mutations with a loss of function and cause ATS. All R218 mutations (R218L, R218P, R218Q and R218W) exchange the positively charged sidechain with a neutral one, which directly effects the ionic interactions with PIP_2. This results in non-functional channels with no measurable K^+ ion currents.[46] [53] [76] Furthermore, R218W shows a lot of clashes with tyrosine 68 (chain B) and threonine 192 (chain A). This mutation not only removes the ionic charge but also forces the backbone to change position due to the bulky aromatic ring in the side chain. The change to an aromatic ring in the side chain opens the possibility for π-stacking between R218W of chain A and Y68 of chain B, which will also have an impact on the interaction with PIP_2 and the structure of the binding pocket.

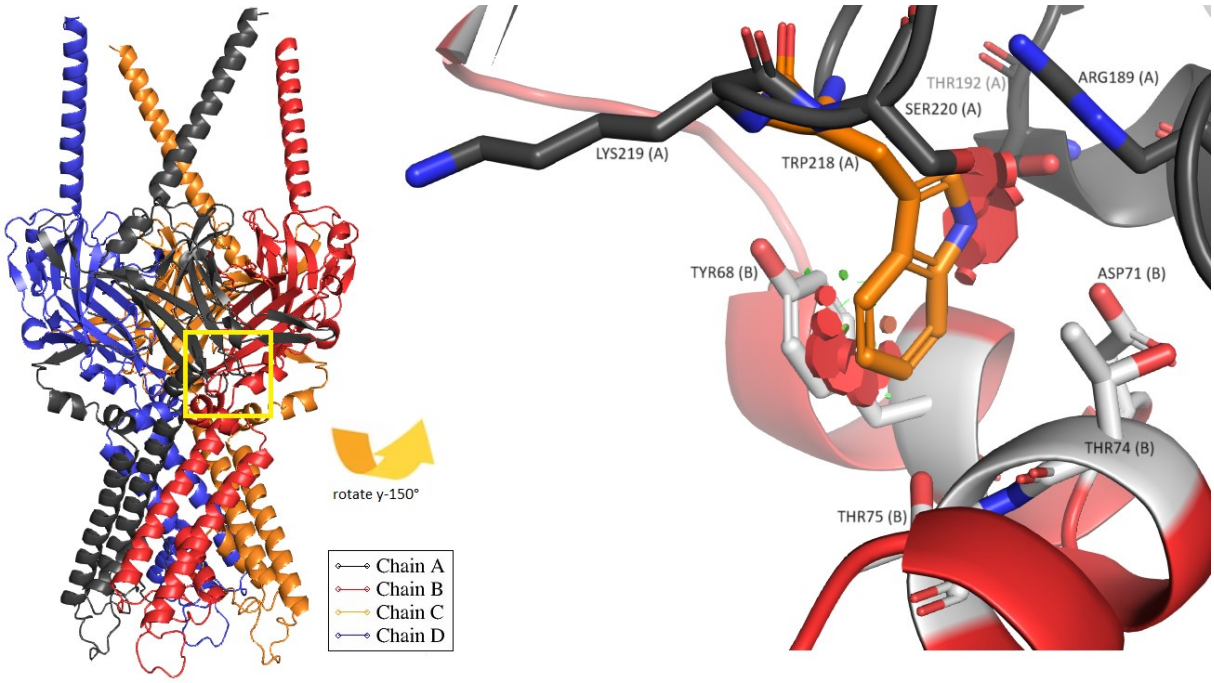

Figure 41: Left: Overview of Kir2.1 with 4 subunits. Right: R218W (orange) in chain A (black) and chain B (red) surrounding residues black (chain A) and white (chain B) in a radius of ~5Å. Circles show clashes caused by the mutation: Size and color changes from green to red indicate the severity of the clash.

4.3.20 R228Q

Arginine 228 is a positively charged amino acid facing the inside of the pore in the CTD. It forms a charged ring in the pore and influences blocking of the channel with Mg^{2+} or polyamines. It is one part of a set of charged rings inside the pore together with negatively charged residues (E224, D259, E299), which regulate gating.[77] [78]

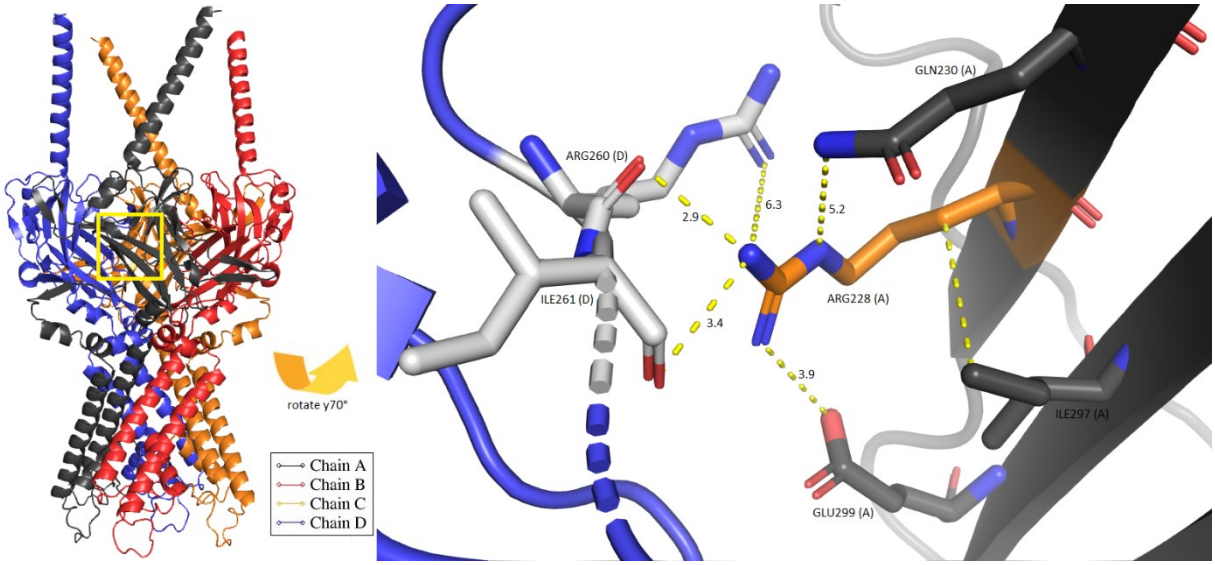

Figure 42: Left: Overview of Kir2.1 with 4 subunits. Right: Arginine 228 (orange) in chain A (black) and surrounding residues chain A (black) and chain D (blue/white) in a radius of ~7Å. Yellow lines indicate measurement in Å.

In case of R228Q the loss of the positive charge is an important factor for the normal function of the channel. If the side chain is replaced by a neutral amino acid or, like in this case, with a negatively charged side chain, the surroundings for the cationic blockers are changed and therefore the K^+ ion currents are altered. There is also the possibility of ionic interactions between glutamine 228 (chain A) and arginine 260 (chain D). They can form a salt bridge instead of repulsive interactions between chain A and D, which affects the inside of the pore and the stabilization of cationic blockers like Mg^{2+}. Arginine 260 is an important residue, which, like arginine 228, creates a positively charged ring inside the pore. R228Q therefore not only removes the positive charged ring it creates itself, but also has the possibility to interact with a second stabilizing feature of the pore.[78]

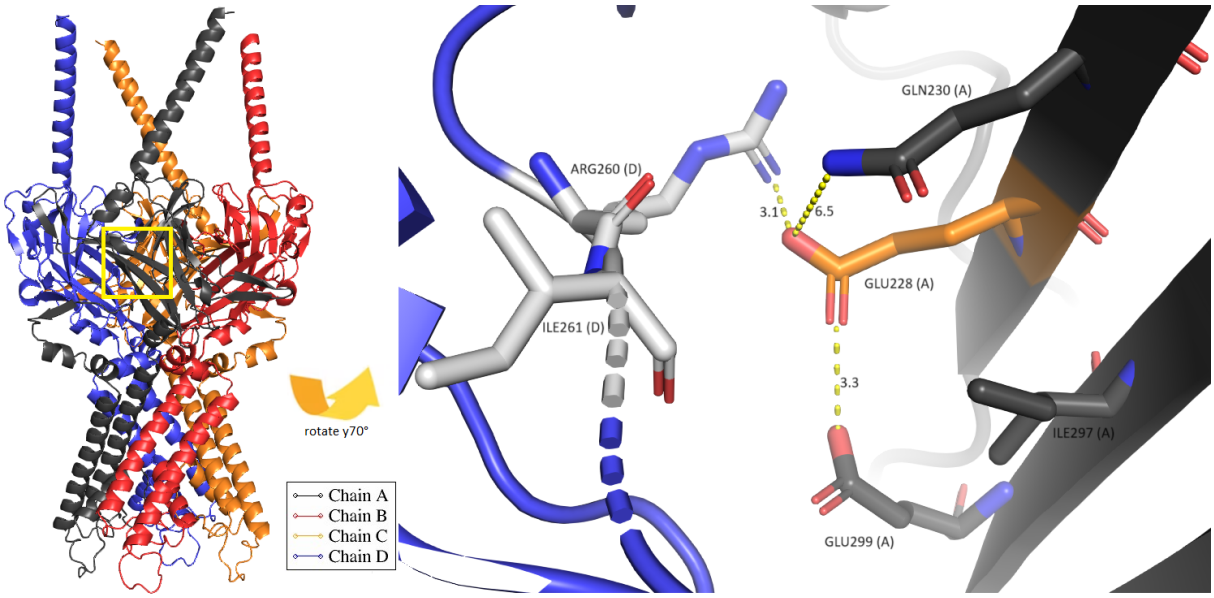

Figure 43: Left: Overview of Kir2.1 with 4 subunits. Right: R228Q (orange) in chain A (black) and surrounding residues chain A (black) and chain D (blue/white) in a radius of ~7Å. Yellow lines indicate measurement in Å.

4.3.21 R260P

Arginine 260 is located in a highly preserved region of the CTD facing the inside of the pore[63]. It carries a positive charge, and, like R228, it creates a ring within the pore which influences the cationic block of the channel. Inside the channel are several differently charged residues (E224, R228, E259, R260) located in circles to stabilize Mg^{2+} or polyamines.[78]

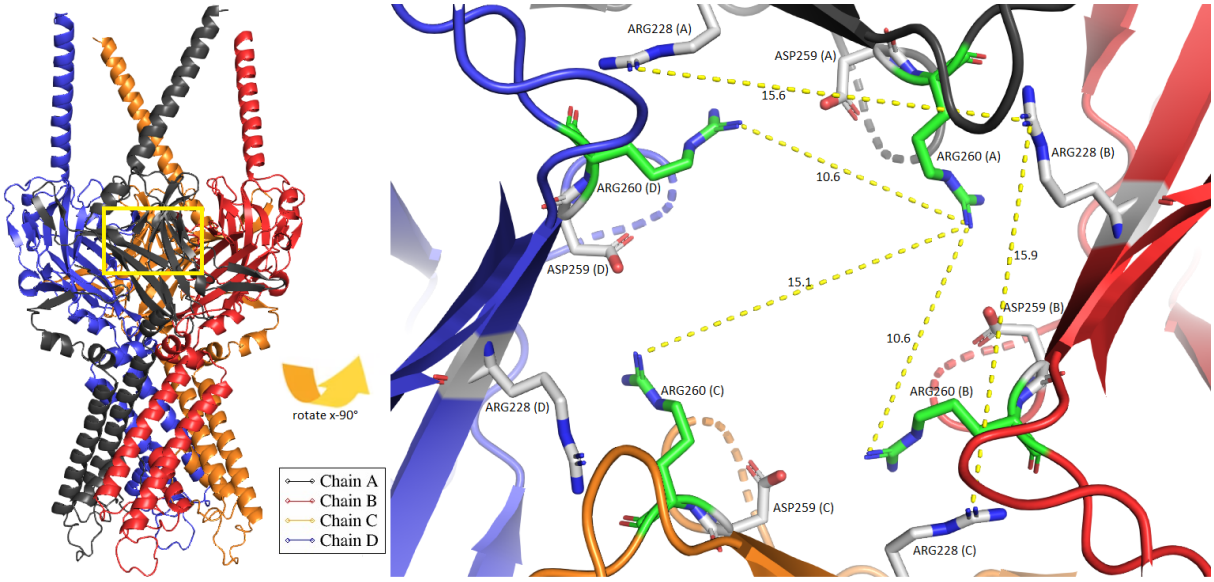

Figure 44: Left: Overview of Kir2.1 with 4 subunits. Right: Arginine 260 (green) in all chains (A black, B red, C orange, D blue) and arginine 228/glutamic acid 259 (white). Yellow lines indicate measurement in Å. Asparagine 260 and asparagine 228 form positive charged and glutamic acid negative charged rings inside the channel for interaction with Mg^{2+} or polyamines[78].

R260P is a loss of function mutation, because the positively charged arginine is exchanged with a neutral, non-polar proline[43]. This results in the loss of one charged ring to interact with cations. R260P shows no measurable current when homomeric, has a strong dominant negative effect on wild type channel and interferes with channel trafficking.[63] As proline is a very rigid amino acid[67] there are some clashes with the surrounding residues (Asp259 in the same chain) that would require a shift in the backbone to avoid. Furthermore, due to the reduction in the size of the side chain the diameter of the pore increases from 10.6 to 11.7 Å between neighboring subunits and 15.1 to 16.6 Å between the opposite subunits.

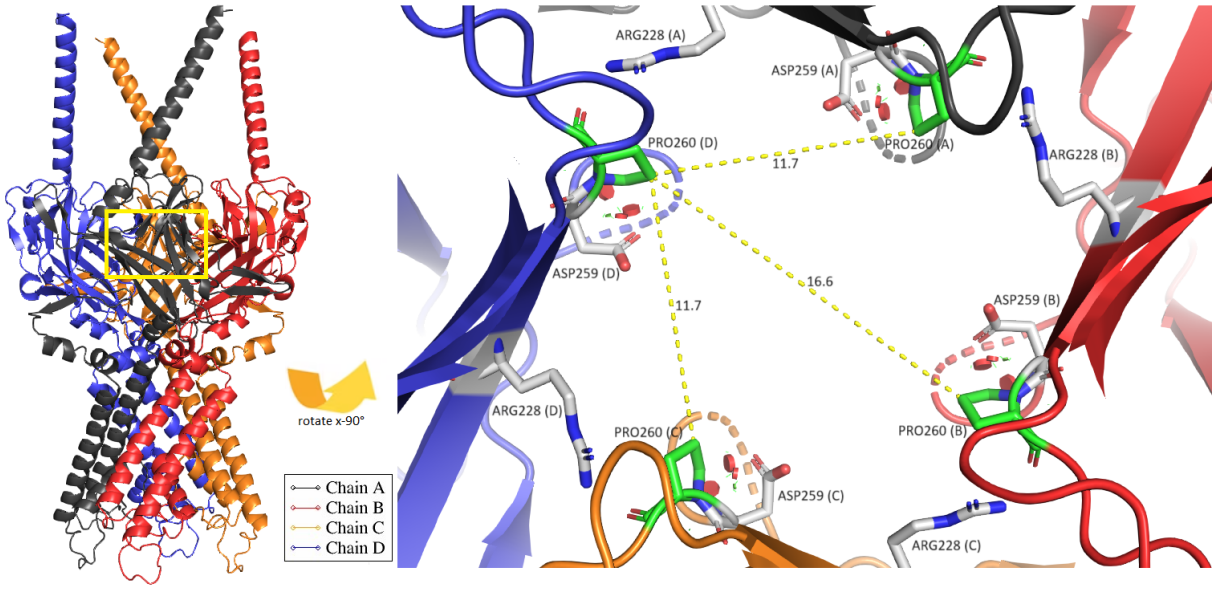

Figure 45: Left: Overview of Kir2.1 with 4 subunits. Right: R260P (green) in all chains (A black, B red, C orange, D blue) and arginine 228/glutamic acid 259 (white). Yellow lines indicate measurement in Å. Circles show clashes caused by the mutation: Size and color changes from green to red indicate the severity of the clash.

4.3.22 G300A, G300D and G300V

Glycine 300 is the first residue of the G-loop, a conserved region reaching from G300-Y315. It can restrict the pore diameter and is involved in channel gating.[4] As glycine has the smallest possible side chain, every mutation is likely to cause steric problems with neighboring residues.

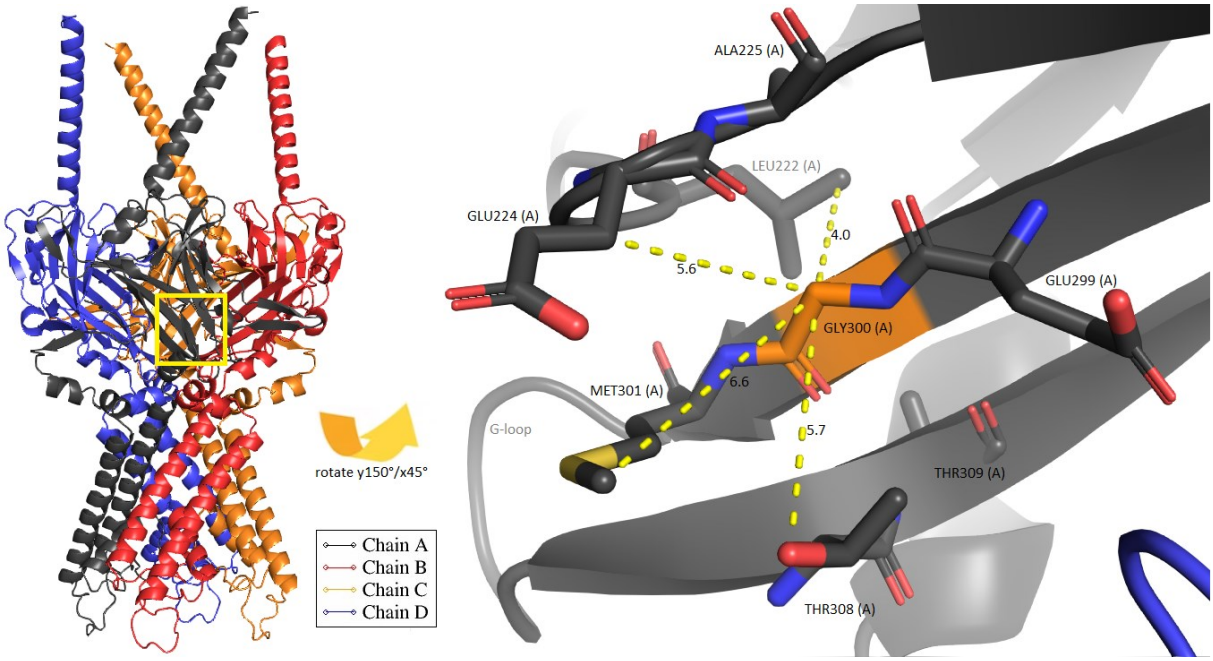

Figure 46: Left: Overview of Kir2.1 with 4 subunits. Right: Glycine 300 (orange) in chain A (black) and surrounding residues of chain A (black) in a radius of ~7Å. Yellow lines indicate measurement in Å.

The substitution of alanine in position G300 decreases PIP_2 binding, which is likely to be an allosteric effect on the PIP_2 binding site, because of the change in size. This indicates a connection between PIP_2 binding and the G-loop gating mechanism.[10] In our model no steric clashes are shown for this mutation, but the mutation might cause problems in different conformations.

G300D is a missense mutation, which leads to a loss of function due to structural changes as it is involved in g-loop gating.[79] The introduction of an aspartic acid with a positively charged side chain instead of the neutral glycine[43] can affect the gating mechanism after interaction with PIP_2[80]. As a result of the change in size this mutation causes several clashes with the surrounding residues. The backbone needs to shift quite a lot to create the space needed. Especially residues leucine 222 to alanine 225 show crucial clashes with aspartic acid 300.

G300V is able to form multimers with wild type subunits and traffic to the cell membrane, but shows no currents of K^+ ions[48]. Like G300D it shows a lot of clashes with residues leucine 222 to alanine 225, forcing the backbone to change in structure.

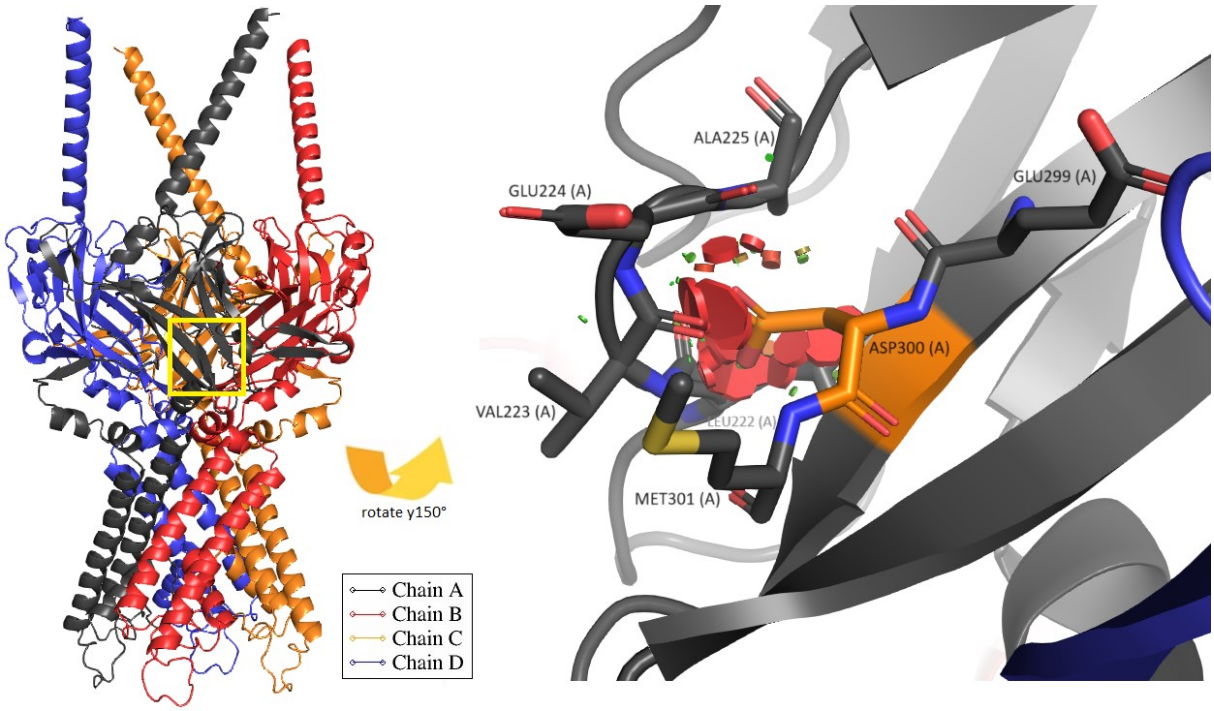

Figure 47: Left: Overview of Kir2.1 with 4 subunits. Right: G300D (orange) in chain A (black) and surrounding residues of chain A (black) in a radius of ~7Å. Circles show clashes caused by the mutation: Size and color changes from green to red indicate the severity of the clash.

4.3.23 V302M

Valine 302 is part of the G-loop, which is a conserved region in the CTD of Kir21, facing to the inside of the channel. It acts as a flexible barrier for K^+ ions in combination with PIP_2 binding.[81]

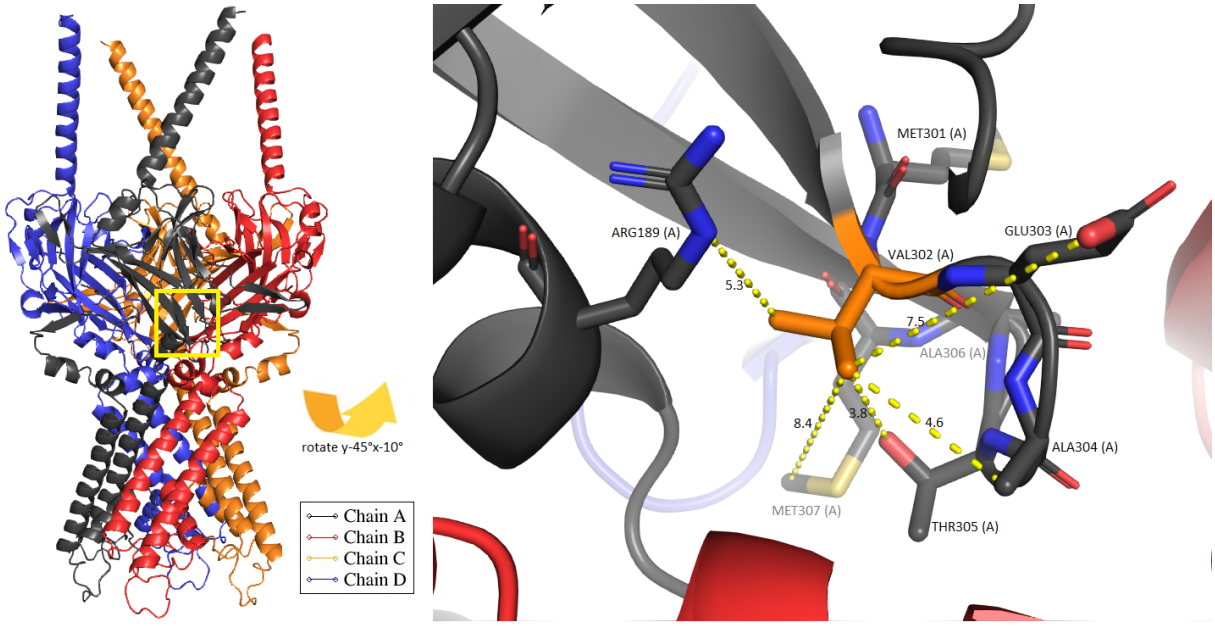

Figure 48: Left: Overview of Kir2.1 with 4 subunits. Right: Valine 302 (orange) in chain A (black) and surrounding residues of chain A (black). Yellow lines indicate measurement in Å.

V302M is a nonsense mutation exchanging a valine for a methionine, introducing a larger side chain, with a thioether group. This mutation alters the K^+ ion currents, but not the trafficking of homomeric or heteromeric multimerization, by interfering with PIP_2 sensitivity. This suggests that hydrophobic interactions play a crucial role in this area.[81] Even though the side chain of methionine is larger than the side chain of valine, it only causes a steric problem with arginine 189. But as arginine 189 is directly involved in PIP_2 binding, this will affect the interaction.

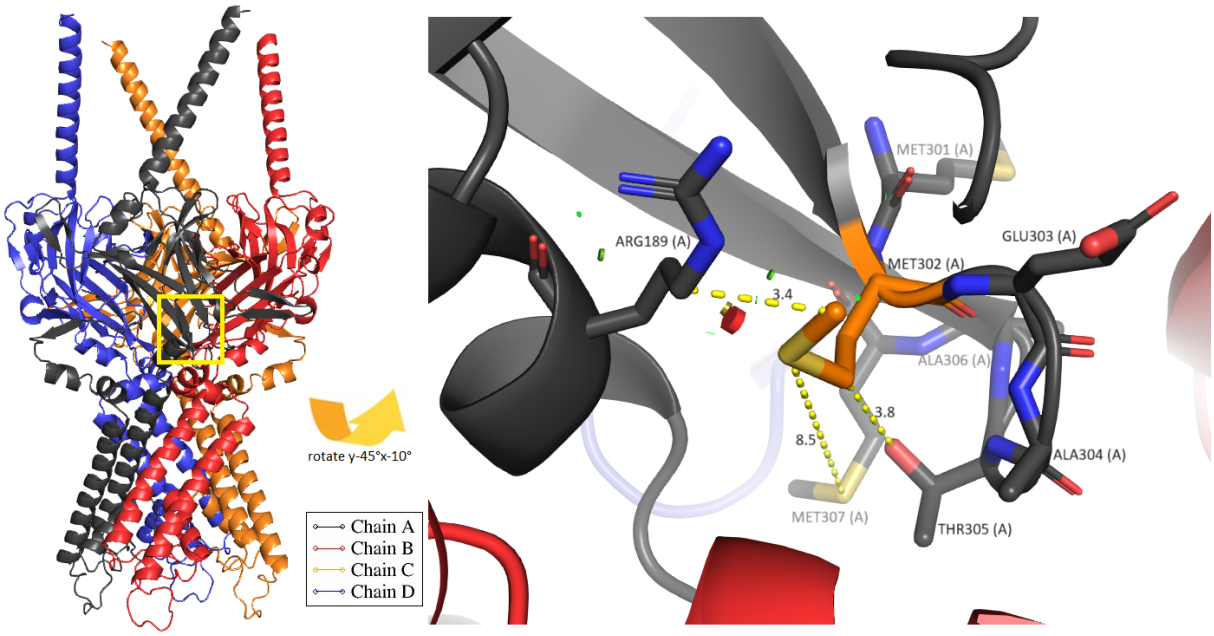

Figure 49: Left: Overview of Kir2.1 with 4 subunits. Right: V302M (orange) in chain A (black) and surrounding residues of chain A (black). Yellow lines indicate measurement in Å. Circles show clashes caused by the mutation: Size and color changes from green to red indicate the severity of the clash.

4.3.24 E303K

Like G300 and V302 glutamic acid is located in the G-loop, but other than glycine 300 or valine 302, glutamic acid is a negatively charged amino acid. This enables E303 to interact with R312 (B) or with H221 (A) via salt bridge or hydrogen bonds creating an intersubunit network. These characteristics make E303 a very important residue for the coordination of PIP_2 binding and channel gating of the G-loop.[4]

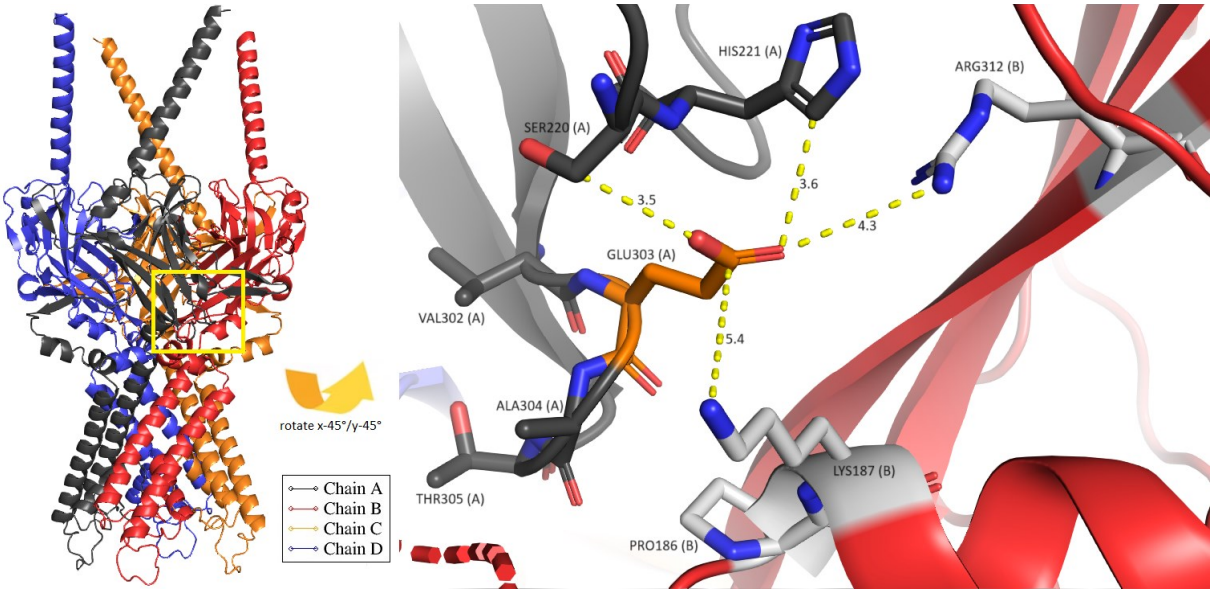

Figure 50: Left: Overview of Kir2.1 with 4 subunits. Right: Glutamic acid 303 (orange) in chain A (black) and surrounding residues of chain A (black) and of chain B (white) in a radius of ~6Å. Yellow lines indicate measurement in Å. Glu303 (A) can establish salt bridges or hydrogen bonds with His221 (A) or Arg312 (B)[4].

E303K is a missense mutation, which results in a loss of function, due to the exchange of the negatively charged side chain of glutamic acid with a positively charged lysine[43]. Thereby the residue loses its ability to create a salt bridge with arginine 312. This leads to a non-conductive channel, which causes ATS.[48] As the surrounding residues (histidine 221 (A), lysine 187 (B) and arginine 312 (B)) all carry a positive charge, the introduction of lysine in position 303 (A) leads to a repulsive effect in this area. Due to the similar size of the side chains of glutamic acid and lysine there are no steric problems.

4.3.25 T305P

Threonine 305 is a polar amino acid, located in the apex of the G-loop in the C-terminus of Kir2.1. This is a flexible region and plays an important role in channel gating in combination with PIP_2 binding. Furthermore A306, the neighboring residue, is one of the 4 constriction points of the channel.[4] [42]

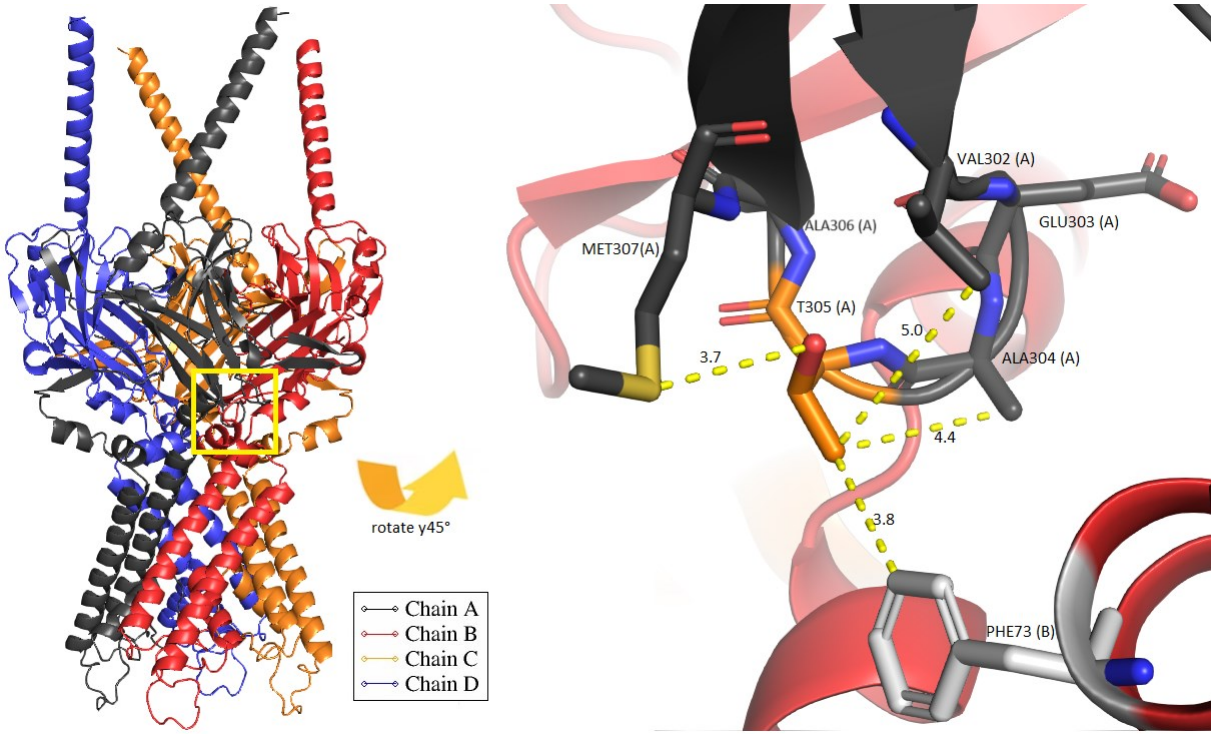

Figure 51: Left: Overview of Kir2.1 with 4 subunits. Right: Threonine 305 (orange) in chain A (black) and surrounding residues of chain A (black) and chain B (red/white) in a radius of ~5Å. Yellow lines indicate measurement in Å.

Having a crucial role in channel gating, a mutation in this position, that prevents the backbone from moving freely, has a big impact on the function of the channel. Proline is the only proteinogenic amino acid that forms a ring with its side chain and the backbone. Therefore, it is more rigid and cannot move as much as all other residues.[67] Furthermore, T305P eliminates the polar -OH group in the side chain and exchanges it with a non-polar residue. Even though there are no strong hydrogen bonds in this conformation of the protein, the -OH group can still have an important role during conformational changes during gating. This mutation causes a loss of function and a dominant negative effect when co expressed with wild type channel.[42]

4.3.26 M307V

Like the other residues in the G-loop, methionine 307 is crucial for channel gating and PIP_2 interaction. The residue is highly conserved in the Kir2.1 family and part of a complex region involving several hydrogen bonds and salt bridges in close proximity. A306 is one of the four constriction points of the pore and, as it is the neighbor to M307, structural changes will directly impact this region.[4]

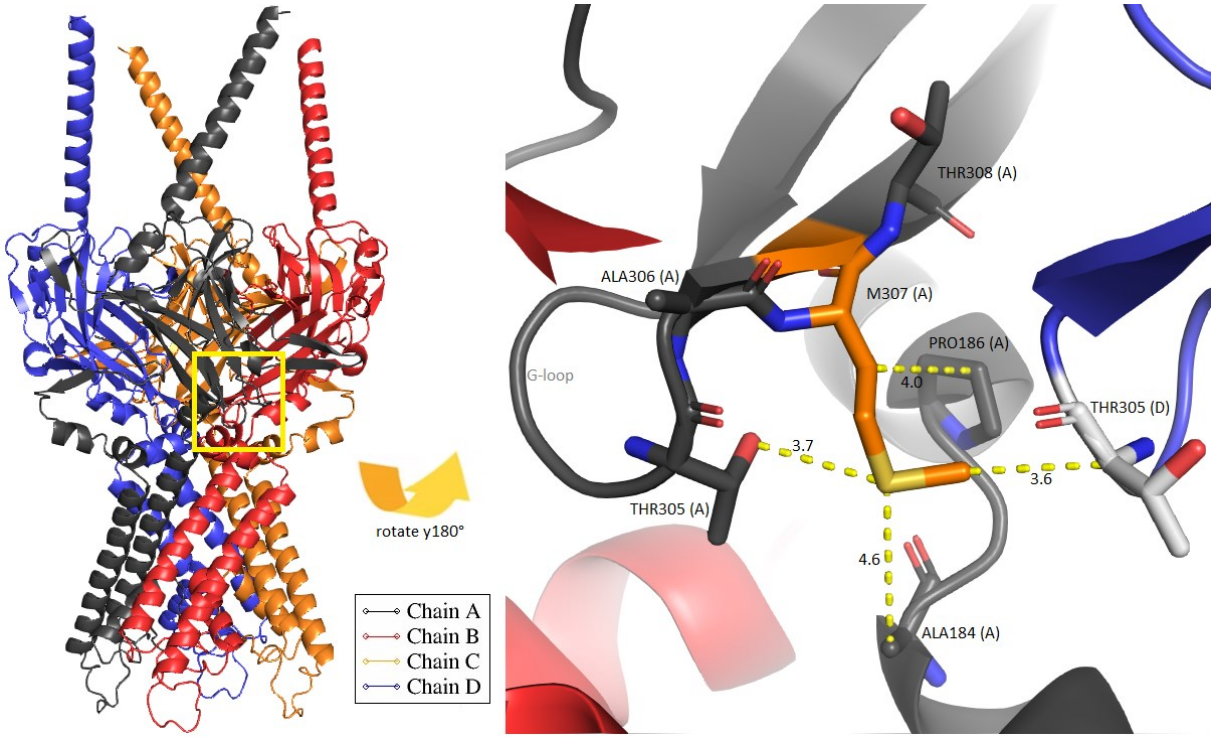

Figure 52: Left: Overview of Kir2.1 with 4 subunits. Right: Methionine 307 (orange) in chain A (black) and surrounding residues of chain A (black) and chain D (blue/white) in a radius of ~5Å. Yellow lines indicate measurement in Å.

Methionine 307 is located directly beside the constriction point of alanine 306 and, if it is exchanged with valine, the side chain causes steric problems with threonine 305 and proline 186 of the same chain. This is a result of the side chain in valine being branched not linear. M307V mutation is a loss of function mutation with a dominant negative effect on wild type. It is known to cause ATS. Even though there is no effect on channel expression or trafficking to cell membrane, it shows reduced currents for K^+ ions.[82]

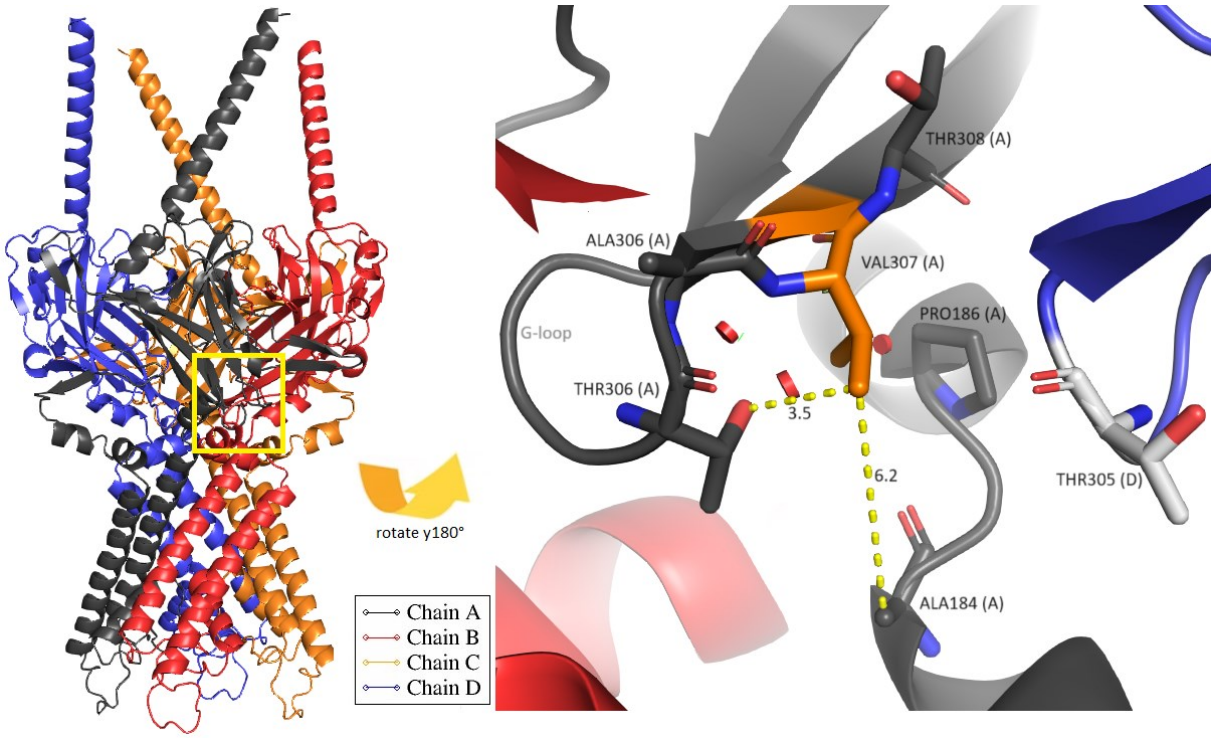

Figure 53: Left: Overview of Kir2.1 with 4 subunits. Right: M307V (orange) in chain A (black) and surrounding residues of chain A (black) and chain D (blue/white). Yellow lines indicate measurement in Å. Circles show clashes caused by the mutation: Size and color changes from green to red indicate the severity of the clash.

4.3.27 T309I

Threonine 309 is part of the G-loop and close to the PIP_2 binding pocket. Pegan et al.[83] [84] suggested a salt bridge between R218 (A) and T309 (A), but in our structure the two residues are 10.8Å apart. This might be due to a different state the channel is in. In our model it is more likely there is a hydrogen bond with asparagine 190 (A). However, T309 (A) is in a crucial region involved in gating and can influence PIP_2 sensitivity if mutated.[4]

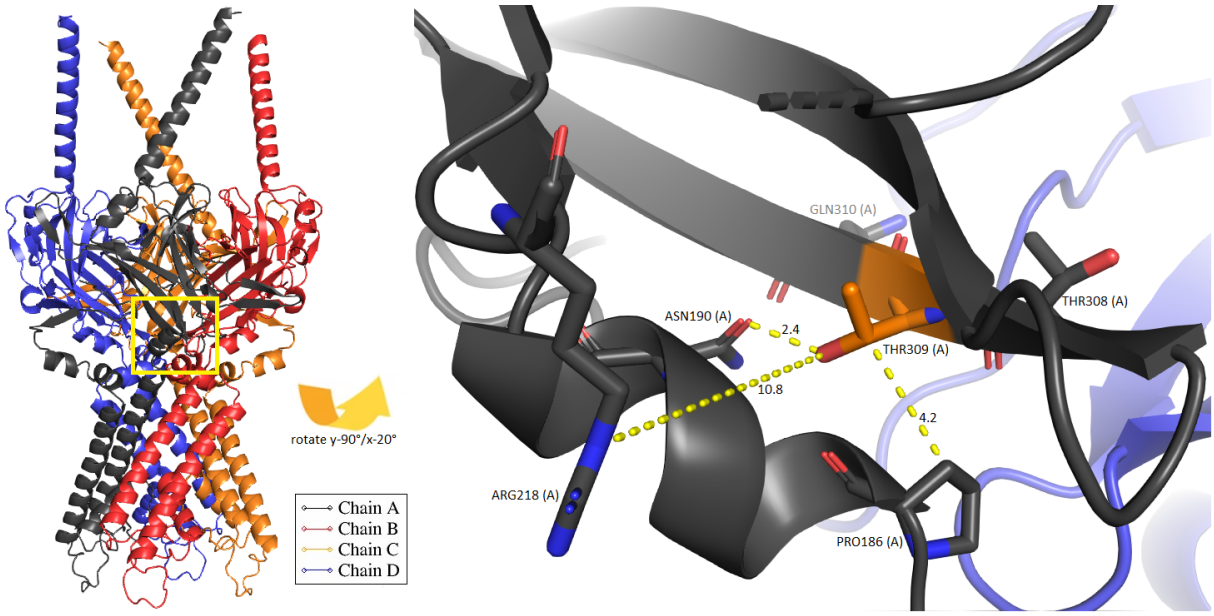

Figure 54: Left: Overview of Kir2.1 with 4 subunits. Right: Threonine 309 (orange) in chain A (black) and surrounding residues of chain A (black) in a radius of ~5Å. Additionally R218 (A) is shown to measure the distance. Yellow lines indicate measurement in Å.

T309I is a nonsense mutation within the G-loop of the CTD. The loss of the polar side chain influences the surrounding residues, as there are no hydrogen bonds possible with the non-polar isoleucine[43]. Structural changes in this region, leading to clashes with proline 186, asparagine 190 and leucine 193, affect the sensitivity of PIP_2 binding or the gating mechanism, as it is the case in other mutations in the G-loop. This leads to a loss of function with no K^+ ion inward currents and a dominant negative effect, causing ATS.[64]

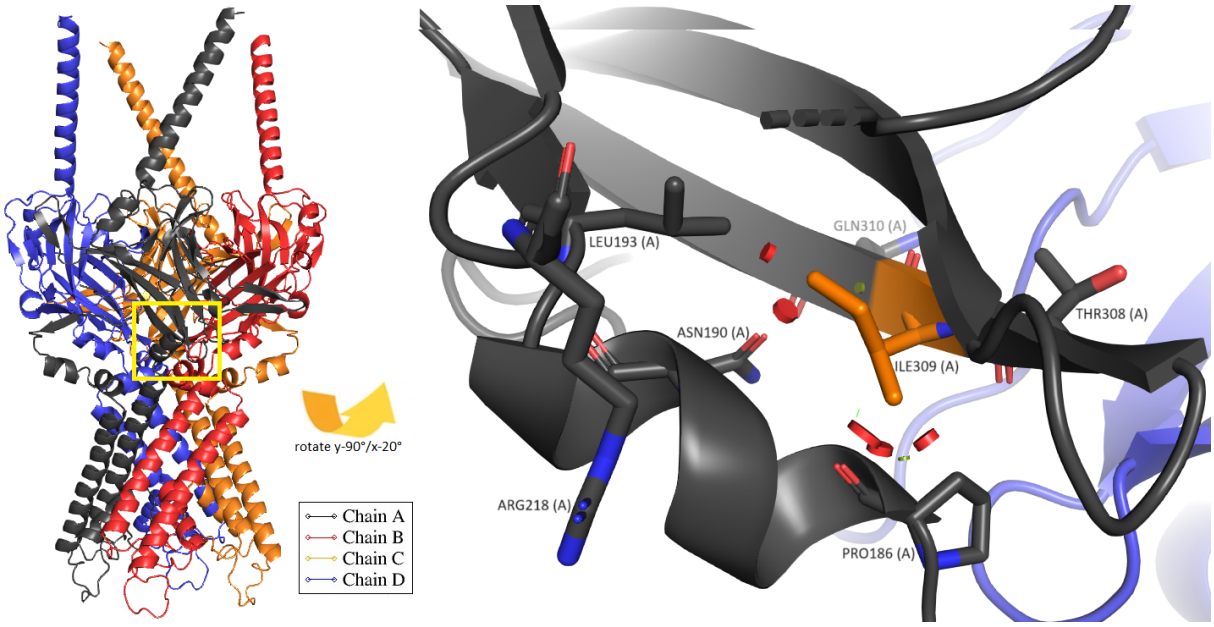

Figure 55: Left: Overview of Kir2.1 with 4 subunits. Right: T309I (orange) in chain A (black) and surrounding residues of chain A (black). R218 is shown but is not close enough for interaction. Circles show clashes caused by the mutation: Size and color changes from green to red indicate the severity of the clash.

4.3.28 R312C and R312H

Arginine 312 is one of the last residues of the G-loop (G300-Y315) in the C-terminus, located in the CTD. It carries a positive charge[43] in its side chain and is involved in a network of hydrogen bonds or salt bridges with surrounding amino acids histidine 221 (D) and glutamic acid 303 (D) or glutamine (A). This complex interaction between subunits plays an important role in PIP_2 sensitivity. Mutants of arginine 312 are known to cause ATS.[4]

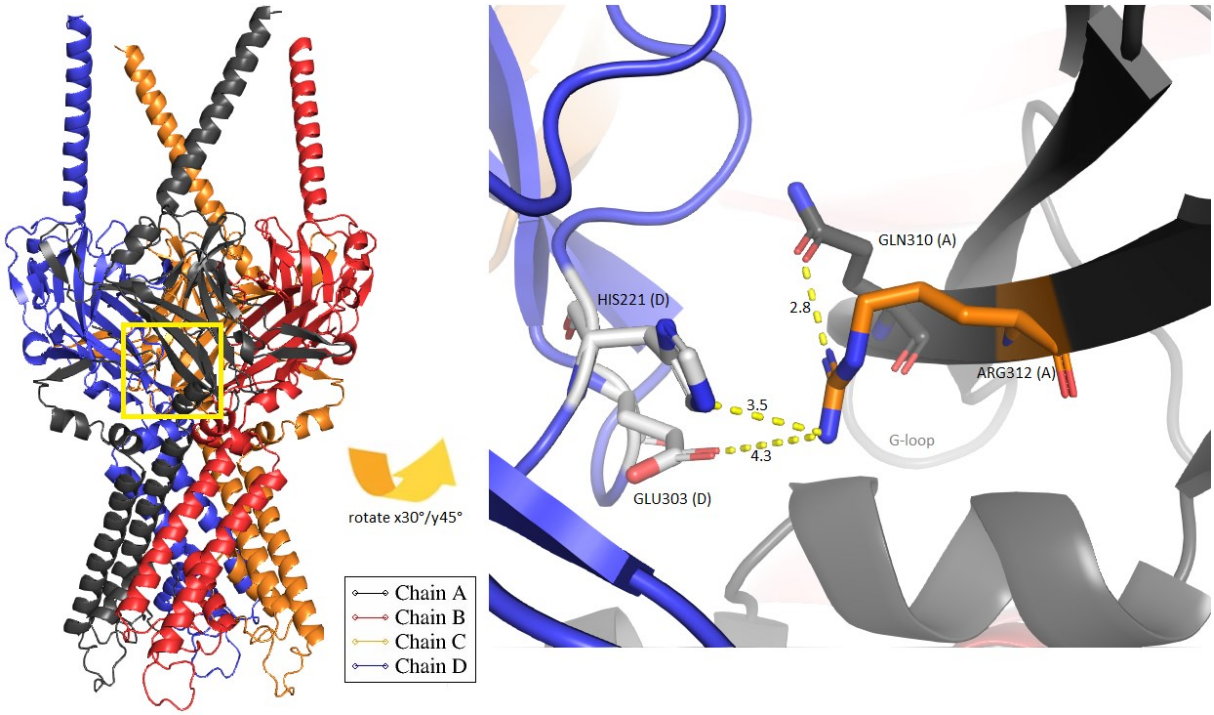

Figure 56: Left: Overview of Kir2.1 with 4 subunits. Right: Arginine 312 (orange) in chain A (black) and surrounding residues of chain A (black) and chain D (blue/white) in a radius of ~5Å. Yellow lines indicate measurement in Å.

R312C is a loss of function mutation, due to the exchange of the positively charged side chain in arginine with a neutral cysteine[43]. This prevents a formation of a salt bridge with E303 or hydrogen bonds with glutamine 310 which destabilizes the region, weakening the binding strength of different PIPs[45]. Sterically this mutation causes no problems, since the side chain is shorter and not branched.

In case of R312H the side chain is altered to histidine, which is a weak basic amino acid compared to the strong basic arginine. Furthermore, the distance between the neighboring chains increases which results in a weakening of the salt bridge leading to a lowered binding affinity for PIP_2 and a loss of function. The aromatic ring of

R312H also causes clashes with amino acids isoleucine 297 and glutamine 310 of the same chain the mutation is in.[4]

Despite the structural change, PIP_2 is still able to bind, but the channel is unable to open, suggesting that the network of interactions around R312 has a crucial role in G-loop gating.[4]

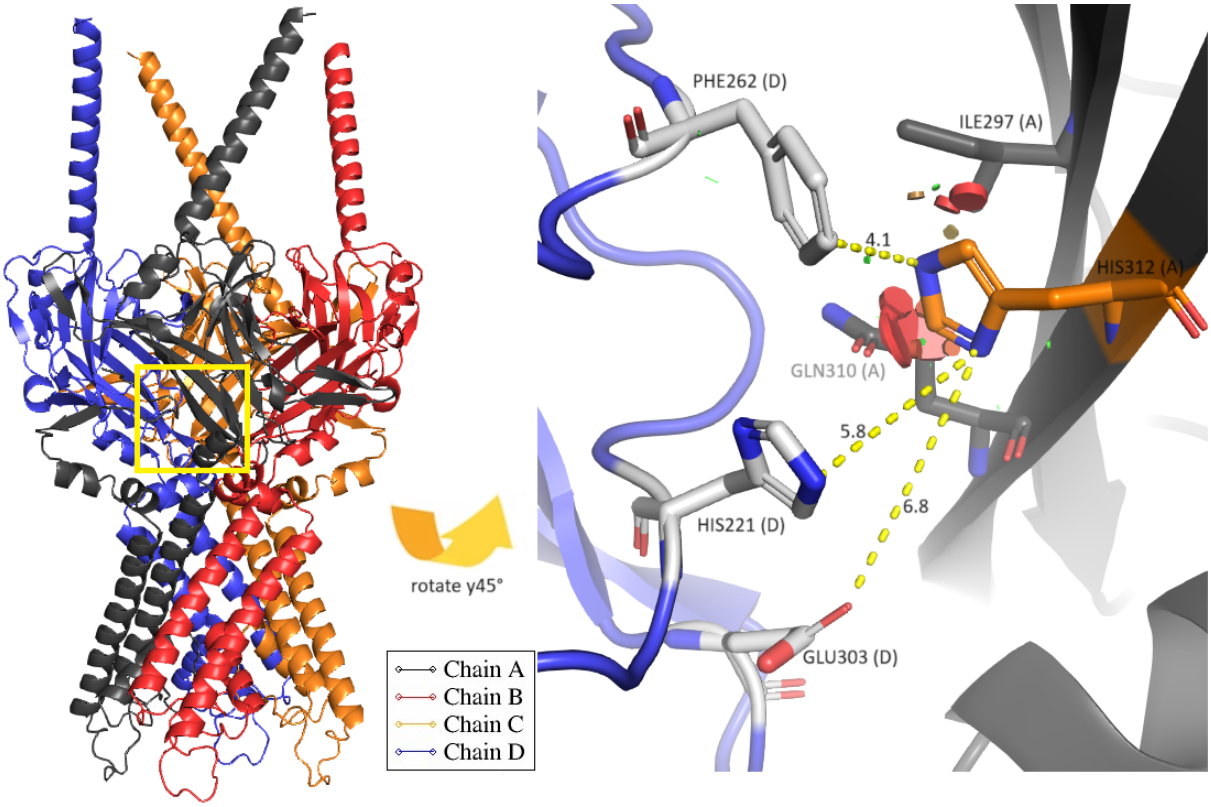

Figure 57: Left: Overview of Kir2.1 with 4 subunits. Right: R312H (orange) in chain A (black) and surrounding residues of chain A (black) and chain D (blue/white). Yellow lines indicate measurement in Å. Circles show clashes caused by the mutation: Size and color changes from green to red indicate the severity of the clash.

4.3.29 SY314-315

The amino acids serine 314 and tyrosine 315, located in the C-terminus of the protein, are the final residues of the G-loop region. Therefore they are involved in gating and are close to the PIP_2 binding site.[4] [42] Both residues carry a -OH group and are therefore able to form a hydrogen bond to stabilize the region. In our model serine 314 is close to the side chain of glutamic acid 293. Tyrosine 315 is near the backbone of serine 196 to create hydrogen bonds and thereby stabilizing this region.

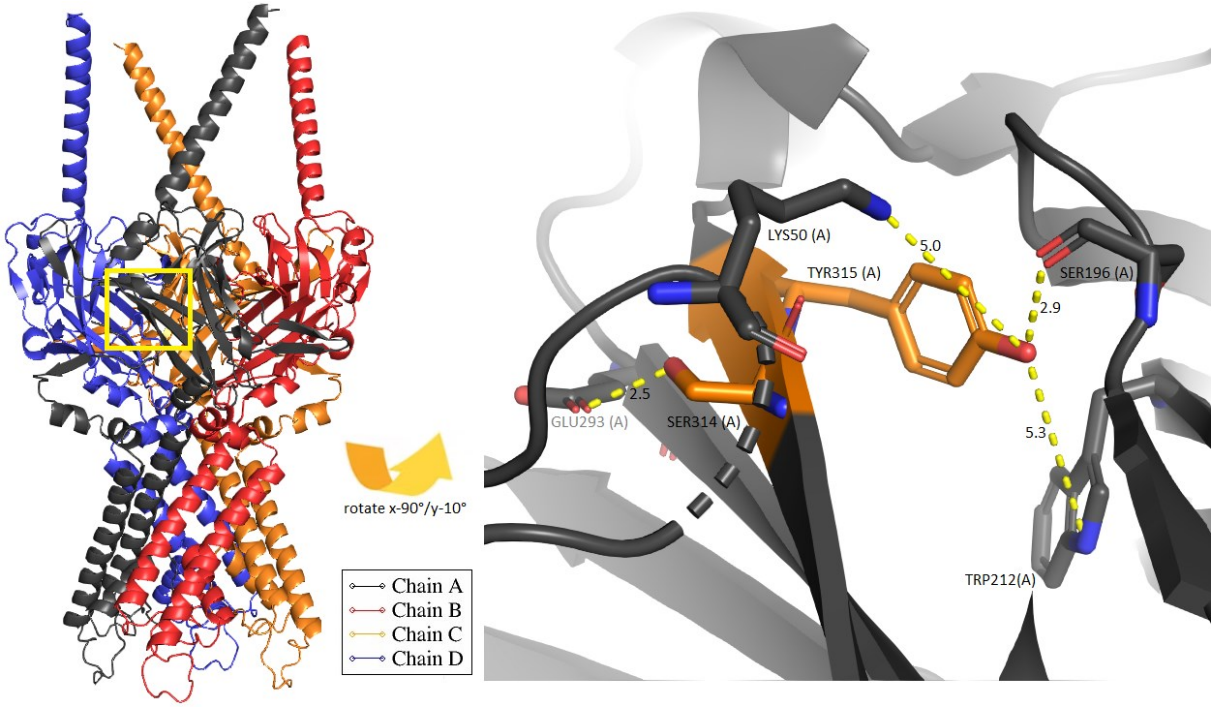

Figure 58: Left: Overview of Kir2.1 with 4 subunits. Right: Serine 314 and Tyrosine 315 (orange) in chain A (black) and surrounding residues of chain A (black) in a radius of ~5Å. Yellow lines indicate measurement in Å.

SY314-315Δ is an in-frame deletion and the loss of two possible hydrogen bonds stabilizing the area leads to a misfolding of the channel. Therefore the channel is unable to traffic correctly to the cell membrane, resulting in a loss of function and causing ATS.[66]

4.3.30 W322C

Other than most of the known mutations in Kir2.1 tryptophane 322 is located at the outside of the channel rather than inside the pore.

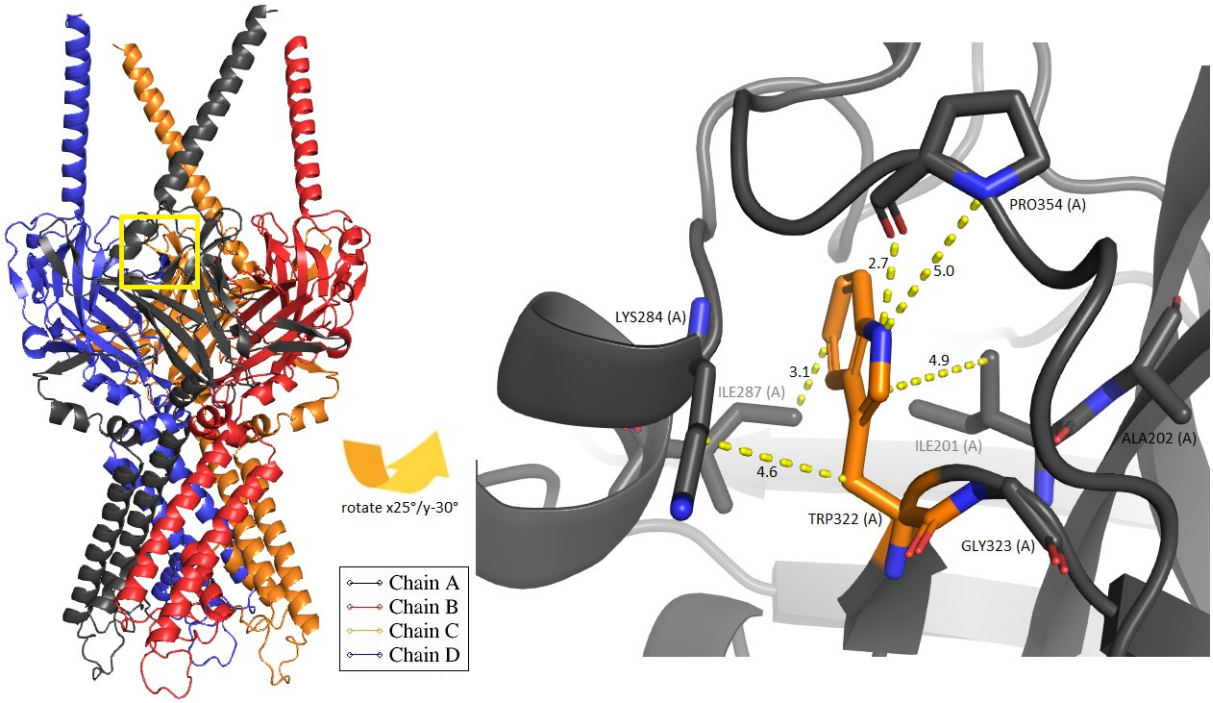

Figure 59: Left: Overview of Kir2.1 with 4 subunits. Right: Tryptophan 322 (orange) in chain A (black) and surrounding residues of chain A (black) in a radius of ~5Å. Yellow lines indicate measurement in Å.

W322C is a missense mutation leading to a change in size of the side chain and the newly introduced cysteine is more hydrophilic, as there is no aromatic ring[43]. Even though the mutation is on the outside of the channel, this still causes a problem in trafficking to the membrane and degradation, which results in a loss of function with reduced K^+ ion currents. W322C is a mutation causing ATS with only cardiac phenotype.[85]

5. Discussion

In summary we showed that mutations of the Kir 2.1 channel can influence the structure of the backbone and therefore alter the normal function or trafficking to the membrane.

Initially we planned to perform MD-simulations for selected mutations such as position G144 or G146, inside the selectivity filter. In order to assess the quality and stability of the WT cryo- EM structure[4], we started a MD-simulation. Unfortunately, the cryo-EM structure[4] was not stable enough to compare the outcome of mutated and wild type channel. We came to this conclusion after calculating the root mean square fluctuation for our channel and got results that indicated deformations of the backbone especially in the selectivity filter. Reasonable results as typically seen in many MD simulations on K^+ channels would have shown RMSF values <0,1nm in the selectivity filter. As our RSMF scores have a range up to 0,33nm this suggests a loss of selectivity for K^+ ions as shown in other studies like T. Friesacher *et al*[40] and S. Jekhmane *et al*[41]. It would be very interesting to see the effect of any mutation in MD-simulation, but this will be a future project as soon as a stable experimental structure of Kir2.1 will become available.

Therefore, we decided to have a look at a wider range of mutations in different crucial regions of the channel. We compared the properties of each mutated residue with the wild type, considering potential hydrogen bonds, disulfide bridges, ionic interactions or steric clashes. We built a model of Kir2.1 using AlphaFold2[7] [8], including the templates available in the protein data bank (RCSB.org)[86]. The advantage of our model is that there are several high-resolution models in the protein data bank (RCSB.org)[86] of related Kir2 channels. We did not perform more MD simulations but focused on a static model to insert mutations. All mutations were added without adapting the backbone and this is why it is not the actual structure of the mutated channel, but only a visual to indicate problems that might occur. In future it might be important to check all mutations using separate models for each mutated residue to better understand the changes of the protein structure and even perform MD simulations with them, as a static model can only provide certain information.

Most of the mutations we studied in our model, were clustered in crucial regions of the channel or nearby so that they might have allosteric influences. Especially in the

G-loop there are at least 10 out of 15 amino acids known to be able to carry a mutation, which directly impact the gating mechanism.[4] Furthermore, in our structure 16 mutated residues are involved in intersubunit connections either via hydrogen bonds, salt bridges, hydrophobic interactions or disulfide bridges. In the selectivity filter as well as in constriction points of the pore, mutations change the diameter and thereby influence normal ion flux or destabilize ionic blockers during closed states due to the loss of charged sidechains[77] [78]. It can be easily imagined that mutations in these regions disrupt normal channel function. The work represented in this thesis provides an important starting point towards a better understanding of ATS mutations. In future it will be important to see the effect of these mutations in different gating states. MD simulations will be helpful to get more information about the conformational changes induced by the various mutations.

6. References

[1] L. Reilly and L. L. Eckhardt, “Cardiac potassium inward rectifier Kir2: Review of structure, regulation, pharmacology, and arrhythmogenesis,” *Heart Rhythm*, vol. 18, no. 8, Art. no. 8, Aug. 2021, doi: 10.1016/j.hrthm.2021.04.008.

[2] K. Chen, D. Zuo, Z. Liu, and H. Chen, “Kir2.1 channels set two levels of resting membrane potential with inward rectification,” *Pflugers Arch - Eur J Physiol*, vol. 470, no. 4, pp. 599–611, Apr. 2018, doi: 10.1007/s00424-017-2099-3.

[3] H. Hibino, A. Inanobe, K. Furutani, S. Murakami, I. Findlay, and Y. Kurachi, “Inwardly Rectifying Potassium Channels: Their Structure, Function, and Physiological Roles,” *Physiological Reviews*, vol. 90, no. 1, Art. no. 1, Jan. 2010, doi: 10.1152/physrev.00021.2009.

[4] C. A. H. Fernandes *et al.*, “Cryo–electron microscopy unveils unique structural features of the human Kir2.1 channel,” *Sci Adv*, vol. 8, no. 38, Art. no. 38, Aug. 2023, doi: 10.1126/sciadv.abq8489.

[5] “KCNJ2 - Inward rectifier potassium channel 2 - Homo sapiens (Human) | Variants viewer | UniProtKB | UniProt.” Accessed: Aug. 24, 2023. [Online]. Available: https://www.uniprot.org/uniprotkb/P63252/variant-viewer

[6] S. Stefl, H. Nishi, M. Petukh, A. R. Panchenko, and E. Alexov, “Molecular Mechanisms of Disease-Causing Missense Mutations,” *Journal of Molecular Biology*, vol. 425, no. 21, pp. 3919–3936, Nov. 2013, doi: 10.1016/j.jmb.2013.07.014.

[7] M. Varadi *et al.*, “AlphaFold Protein Structure Database: massively expanding the structural coverage of protein-sequence space with high-accuracy models,” *Nucleic Acids Research*, vol. 50, no. D1, pp. D439–D444, Jan. 2022, doi: 10.1093/nar/gkab1061.

[8] J. Jumper *et al.*, “Highly accurate protein structure prediction with AlphaFold,” *Nature*, vol. 596, no. 7873, Art. no. 7873, Aug. 2021, doi: 10.1038/s41586-021-03819-2.

[9] D.-K. Song and F. M. Ashcroft, “ATP Modulation of ATP-sensitive Potassium Channel ATP Sensitivity Varies with the Type of SUR Subunit *,” *Journal of Biological Chemistry*, vol. 276, no. 10, pp. 7143–7149, Mar. 2001, doi: 10.1074/jbc.M009959200.

[10] S. Pegan *et al.*, “Cytoplasmic domain structures of Kir2.1 and Kir3.1 show sites for modulating gating and rectification,” *Nat Neurosci*, vol. 8, no. 3, Art. no. 3, Mar. 2005, doi: 10.1038/nn1411.

[11] C.-L. Huang, S. Feng, and D. W. Hilgemann, “Direct activation of inward rectifier potassium channels by PIP2 and its stabilization by Gβγ,” *Nature*, vol. 391, no. 6669, Art. no. 6669, Feb. 1998, doi: 10.1038/35882.

[12] B. KATZ, “The Efferent Regulation of the Muscle Spindle in the Frog,” *Journal of Experimental Biology*, vol. 26, no. 2, pp. 201–217, Aug. 1949, doi: 10.1242/jeb.26.2.201.

[13] K. S. Cole and H. J. Curtis, “MEMBRANE POTENTIAL OF THE SQUID GIANT AXON DURING CURRENT FLOW,” *Journal of General Physiology*, vol. 24, no. 4, pp. 551–563, Mar. 1941, doi: 10.1085/jgp.24.4.551.

[14] E.-M. Zangerl-Plessl, M. Qile, M. Bloothooft, A. Stary-Weinzinger, and M. A. G. van der Heyden, “Disease Associated Mutations in KIR Proteins Linked to Aberrant Inward Rectifier Channel Trafficking,” *Biomolecules*, vol. 9, no. 11, Art. no. 11, Nov. 2019, doi: 10.3390/biom9110650.

[15] A. N. Lopatin, E. N. Makhina, and C. G. Nichols, “Potassium channel block by cytoplasmic polyamines as the mechanism of intrinsic rectification,” *Nature*, vol. 372, no. 6504, pp. 366–369, Nov. 1994, doi: 10.1038/372366a0.

[16] N. D’Avanzo, W. W. L. Cheng, D. A. Doyle, and C. G. Nichols, “Direct and Specific Activation of Human Inward Rectifier K+ Channels by Membrane Phosphatidylinositol 4,5-Bisphosphate,” *J Biol Chem*, vol. 285, no. 48, pp. 37129–37132, Nov. 2010, doi: 10.1074/jbc.C110.186692.

[17] R. P. D. Bank, “RCSB PDB - 7ZDZ: Cryo-EM structure of the human inward-rectifier potassium 2.1 channel (Kir2.1).” Accessed: Aug. 23, 2023. [Online]. Available: https://www.rcsb.org/structure/7ZDZ

[18] O. Fürst, B. Mondou, and N. D’Avanzo, “Phosphoinositide regulation of inward rectifier potassium (Kir) channels,” *Front Physiol*, vol. 4, p. 404, Jan. 2014, doi: 10.3389/fphys.2013.00404.

[19] M. Donaldson, G. Yoon, Y. Fu, and L. Ptacek, “Andersen-Tawil syndrome: a model of clinical variability, pleiotropy, and genetic heterogeneity,” *Annals of Medicine*, vol. 36, no. sup1, pp. 92–97, Jan. 2004, doi: 10.1080/17431380410032490.
[20] N. M. Plaster *et al.*, “Mutations in Kir2.1 Cause the Developmental and Episodic Electrical Phenotypes of Andersen’s Syndrome,” *Cell*, vol. 105, no. 4, pp. 511–519, May 2001, doi: 10.1016/S0092-8674(01)00342-7.
[21] H. Kimura *et al.*, “Phenotype Variability in Patients Carrying KCNJ2 Mutations,” *Circulation: Cardiovascular Genetics*, vol. 5, no. 3, pp. 344–353, Jun. 2012, doi: 10.1161/CIRCGENETICS.111.962316.
[22] A. R. Pérez-Riera *et al.*, “Andersen–Tawil Syndrome: A Comprehensive Review,” *Cardiology in Review*, vol. 29, no. 4, p. 165, Aug. 2021, doi: 10.1097/CRD.0000000000000326.
[23] J. Lee *et al.*, “CHARMM-GUI Membrane Builder for Complex Biological Membrane Simulations with Glycolipids and Lipoglycans,” *J. Chem. Theory Comput.*, vol. 15, no. 1, pp. 775–786, Jan. 2019, doi: 10.1021/acs.jctc.8b01066.
[24] S. Jo, J. B. Lim, J. B. Klauda, and W. Im, “CHARMM-GUI Membrane Builder for Mixed Bilayers and Its Application to Yeast Membranes,” *Biophysical Journal*, vol. 97, no. 1, pp. 50–58, Jul. 2009, doi: 10.1016/j.bpj.2009.04.013.
[25] E. L. Wu *et al.*, “CHARMM-GUI Membrane Builder toward realistic biological membrane simulations,” *Journal of Computational Chemistry*, vol. 35, no. 27, pp. 1997–2004, 2014, doi: 10.1002/jcc.23702.
[26] E. Jurrus *et al.*, “Improvements to the APBS biomolecular solvation software suite,” *Protein Science*, vol. 27, no. 1, pp. 112–128, 2018, doi: 10.1002/pro.3280.
[27] J. Lee *et al.*, “CHARMM-GUI Input Generator for NAMD, GROMACS, AMBER, OpenMM, and CHARMM/OpenMM Simulations Using the CHARMM36 Additive Force Field,” *J. Chem. Theory Comput.*, vol. 12, no. 1, pp. 405–413, Jan. 2016, doi: 10.1021/acs.jctc.5b00935.
[28] B. R. Brooks *et al.*, “CHARMM: The biomolecular simulation program,” *Journal of Computational Chemistry*, vol. 30, no. 10, pp. 1545–1614, 2009, doi: 10.1002/jcc.21287.
[29] M. J. Abraham *et al.*, “GROMACS: High performance molecular simulations through multi-level parallelism from laptops to supercomputers,” *SoftwareX*, vol. 1–2, pp. 19–25, Sep. 2015, doi: 10.1016/j.softx.2015.06.001.
[30] M. Abraham *et al.*, “GROMACS 2023.2 Manual,” Jul. 2023, doi: 10.5281/zenodo.8134388.
[31] “VSC: Home.” Accessed: Nov. 15, 2023. [Online]. Available: https://vsc.ac.at//home/
[32] R. J. Gowers *et al.*, “MDAnalysis: A Python Package for the Rapid Analysis of Molecular Dynamics Simulations,” *Proceedings of the 15th Python in Science Conference*, pp. 98–105, 2016, doi: 10.25080/Majora-629e541a-00e.
[33] “Neurosnap Inc. Accelerate your research with the latest in computational biology.” Wilmington, DE, 2022. [Online]. Available: neuronsnap.ai
[34] M. Mirdita, K. Schütze, Y. Moriwaki, L. Heo, S. Ovchinnikov, and M. Steinegger, “ColabFold: making protein folding accessible to all,” *Nat Methods*, vol. 19, no. 6, Art. no. 6, Jun. 2022, doi: 10.1038/s41592-022-01488-1.
[35] R. Evans *et al.*, “Protein complex prediction with AlphaFold-Multimer.” bioRxiv, p. 2021.10.04.463034, Mar. 10, 2022. doi: 10.1101/2021.10.04.463034.
[36] V. Mariani, M. Biasini, A. Barbato, and T. Schwede, “lDDT: a local superposition-free score for comparing protein structures and models using distance difference tests,” *Bioinformatics*, vol. 29, no. 21, pp. 2722–2728, Nov. 2013, doi: 10.1093/bioinformatics/btt473.
[37] R. P. D. Bank, “Assessing the Quality of 3D Structures.” Accessed: Aug. 31, 2023. [Online]. Available: https://www.rcsb.org/docs/general-help/assessing-the-quality-of-3d-structures
[38] Schrödinger, LLC, “The PyMOL Molecular Graphics System, Version 1.8,” Nov. 2015.
[39] O. Fürst, B. Mondou, and N. D’Avanzo, “Phosphoinositide regulation of inward rectifier potassium (Kir) channels,” *Front Physiol*, vol. 4, p. 404, Jan. 2014, doi: 10.3389/fphys.2013.00404.
[40] T. Friesacher *et al.*, “A selectivity filter mutation provides insights into gating regulation of a K+ channel,” *Commun Biol*, vol. 5, no. 1, Art. no. 1, Apr. 2022, doi: 10.1038/s42003-022-03303-1.

[41] S. Jekhmane *et al.*, “Shifts in the selectivity filter dynamics cause modal gating in K+ channels,” *Nat Commun*, vol. 10, no. 1, Art. no. 1, Jan. 2019, doi: 10.1038/s41467-018-07973-6.
[42] S. Bendahhou, E. Fournier, S. Gallet, D. Ménard, M.-M. Larroque, and J. Barhanin, “Corticosteroid-exacerbated symptoms in an Andersen’s syndrome kindred,” *Human Molecular Genetics*, vol. 16, no. 8, pp. 900–906, Apr. 2007, doi: 10.1093/hmg/ddm034.
[43] M. Aftabuddin and S. Kundu, “Hydrophobic, Hydrophilic, and Charged Amino Acid Networks within Protein,” *Biophysical Journal*, vol. 93, no. 1, pp. 225–231, Jul. 2007, doi: 10.1529/biophysj.106.098004.
[44] M. M. Kalscheur *et al.*, “KCNJ2 mutation causes an adrenergic-dependent rectification abnormality with calcium sensitivity and ventricular arrhythmia,” *Heart Rhythm*, vol. 11, no. 5, pp. 885–894, May 2014, doi: 10.1016/j.hrthm.2014.02.015.
[45] M. R. Donaldson *et al.*, “PIP2 binding residues of Kir2.1 are common targets of mutations causing Andersen syndrome,” *Neurology*, vol. 60, no. 11, pp. 1811–1816, Jun. 2003, doi: 10.1212/01.WNL.0000072261.14060.47.
[46] N. M. Plaster *et al.*, “Mutations in Kir2.1 Cause the Developmental and Episodic Electrical Phenotypes of Andersen’s Syndrome,” *Cell*, vol. 105, no. 4, Art. no. 4, May 2001, doi: 10.1016/S0092-8674(01)00342-7.
[47] H. Fodstad *et al.*, “Loss-of-function mutations of the K+ channel gene KCNJ2 constitute a rare cause of long QT syndrome,” *Journal of Molecular and Cellular Cardiology*, vol. 37, no. 2, pp. 593–602, Aug. 2004, doi: 10.1016/j.yjmcc.2004.05.011.
[48] S. Bendahhou, M. R. Donaldson, N. M. Plaster, M. Tristani-Firouzi, Y.-H. Fu, and L. J. Ptácek, “Defective Potassium Channel Kir2.1 Trafficking Underlies Andersen-Tawil Syndrome *,” *Journal of Biological Chemistry*, vol. 278, no. 51, pp. 51779–51785, Dec. 2003, doi: 10.1074/jbc.M310278200.
[49] Y. Tani *et al.*, “T75M-KCNJ2 mutation causing Andersen–Tawil syndrome enhances inward rectification by changing Mg2+ sensitivity,” *Journal of Molecular and Cellular Cardiology*, vol. 43, no. 2, pp. 187–196, Aug. 2007, doi: 10.1016/j.yjmcc.2007.05.005.
[50] C.-W. Lu *et al.*, “Functional and clinical characterization of a mutation in KCNJ2 associated with Andersen-Tawil syndrome,” *Journal of Medical Genetics*, vol. 43, no. 8, pp. 653–659, Aug. 2006, doi: 10.1136/jmg.2006.040816.
[51] N. Decher *et al.*, “Impaired interaction between the slide helix and the C-terminus of Kir2.1: A novel mechanism of Andersen syndrome,” *Cardiovascular Research*, vol. 75, no. 4, pp. 748–757, Sep. 2007, doi: 10.1016/j.cardiores.2007.05.010.
[52] N. P. Davies *et al.*, “Andersen–Tawil syndrome: New potassium channel mutations and possible phenotypic variation,” *Neurology*, vol. 65, no. 7, pp. 1083–1089, Oct. 2005, doi: 10.1212/01.wnl.0000178888.03767.74.
[53] C. M. B. Lopes, H. Zhang, T. Rohacs, T. Jin, J. Yang, and D. E. Logothetis, “Alterations in Conserved Kir Channel-PIP2 Interactions Underlie Channelopathies,” *Neuron*, vol. 34, no. 6, pp. 933–944, Jun. 2002, doi: 10.1016/S0896-6273(02)00725-0.
[54] L. L. Eckhardt *et al.*, “KCNJ2 mutations in arrhythmia patients referred for LQT testing: a mutation T305A with novel effect on rectification properties,” *Heart Rhythm*, vol. 4, no. 3, Art. no. 3, Mar. 2007, doi: 10.1016/j.hrthm.2006.10.025.
[55] M. Xia *et al.*, “A Kir2.1 gain-of-function mutation underlies familial atrial fibrillation,” *Biochemical and Biophysical Research Communications*, vol. 332, no. 4, pp. 1012–1019, Jul. 2005, doi: 10.1016/j.bbrc.2005.05.054.
[56] S. Kharche *et al.*, “Atrial proarrhythmia due to increased inward rectifier current (IK1) arising from KCNJ2 mutation – A simulation study,” *Progress in Biophysics and Molecular Biology*, vol. 98, no. 2, pp. 186–197, Oct. 2008, doi: 10.1016/j.pbiomolbio.2008.10.010.
[57] Y. Ji *et al.*, “PA-6 inhibits inward rectifier currents carried by V93I and D172N gain-of-function KIR2.1 channels, but increases channel protein expression,” *Journal of Biomedical Science*, vol. 24, no. 1, p. 44, Jul. 2017, doi: 10.1186/s12929-017-0352-x.

[58] P. S. Lange, F. Er, N. Gassanov, and U. C. Hoppe, “Andersen mutations of KCNJ2 suppress the native inward rectifier current IK1 in a dominant-negative fashion,” *Cardiovascular Research*, vol. 59, no. 2, pp. 321–327, Aug. 2003, doi: 10.1016/S0008-6363(03)00434-6.
[59] T.-A. Liu, H.-K. Chang, and R.-C. Shieh, “Extracellular K+ elevates outward currents through Kir2.1 channels by increasing single-channel conductance,” *Biochimica et Biophysica Acta (BBA) - Biomembranes*, vol. 1808, no. 6, pp. 1772–1778, Jun. 2011, doi: 10.1016/j.bbamem.2011.02.016.
[60] S. Fukumura *et al.*, “Functional analysis of a double-point mutation in the KCNJ2 gene identified in a family with Andersen-Tawil syndrome,” *Journal of the Neurological Sciences*, vol. 407, p. 116521, Dec. 2019, doi: 10.1016/j.jns.2019.116521.
[61] H. Kimura *et al.*, “Phenotype Variability in Patients Carrying KCNJ2 Mutations,” *Circulation: Cardiovascular Genetics*, vol. 5, no. 3, Art. no. 3, Jun. 2012, doi: 10.1161/CIRCGENETICS.111.962316.
[62] Y. Haruna *et al.*, “Genotype-phenotype correlations of KCNJ2 mutations in Japanese patients with Andersen-Tawil syndrome,” *Human Mutation*, vol. 28, no. 2, pp. 208–208, 2007, doi: 10.1002/humu.9483.
[63] H. Barajas-Martinez *et al.*, “Biophysical and Molecular Characterization of a Novel De Novo KCNJ2 Mutation Associated With Andersen-Tawil Syndrome and Catecholaminergic Polymorphic Ventricular Tachycardia Mimicry,” *Circulation: Cardiovascular Genetics*, vol. 4, no. 1, pp. 51–57, Feb. 2011, doi: 10.1161/CIRCGENETICS.110.957696.
[64] S. Bendahhou *et al.*, “In vivo and in vitro functional characterization of Andersen’s syndrome mutations,” *The Journal of Physiology*, vol. 565, no. 3, pp. 731–741, 2005, doi: 10.1113/jphysiol.2004.081620.
[65] S. Sacconi *et al.*, “Mechanisms underlying Andersen’s syndrome pathology in skeletal muscle are revealed in human myotubes,” *American Journal of Physiology-Cell Physiology*, vol. 297, no. 4, pp. C876–C885, Oct. 2009, doi: 10.1152/ajpcell.00519.2008.
[66] A. I. Moreno-Manuel *et al.*, “Molecular stratification of arrhythmogenic mechanisms in the Andersen Tawil syndrome.,” *Cardiovasc Res*, vol. 119, no. 4, pp. 919–932, May 2023, doi: 10.1093/cvr/cvac118.
[67] M. P. Williamson, “The structure and function of proline-rich regions in proteins,” *Biochemical Journal*, vol. 297, no. 2, pp. 249–260, Jan. 1994, doi: 10.1042/bj2970249.
[68] M. Soom, R. Schönherr, Y. Kubo, C. Kirsch, R. Klinger, and S. H. Heinemann, “Multiple PIP2 binding sites in Kir2.1 inwardly rectifying potassium channels,” *FEBS Letters*, vol. 490, no. 1–2, pp. 49–53, 2001, doi: 10.1016/S0014-5793(01)02136-6.
[69] F. M. Cruz *et al.*, “Extracellular cysteine disulfide bond break at Cys122 disrupts PIP2-dependent Kir2.1 channel function and leads to arrhythmias in Andersen-Tawil Syndrome.” bioRxiv, p. 2023.06.07.544151, Jun. 09, 2023. doi: 10.1101/2023.06.07.544151.
[70] P. Le Tanno *et al.*, “Characterization of Loss-Of-Function KCNJ2 Mutations in Atypical Andersen Tawil Syndrome,” *Frontiers in Genetics*, vol. 12, 2021, Accessed: Sep. 04, 2023. [Online]. Available: https://www.frontiersin.org/articles/10.3389/fgene.2021.773177
[71] J. Li *et al.*, “Three pairs of weak interactions precisely regulate the G-loop gate of Kir2.1 channel,” *Proteins: Structure, Function, and Bioinformatics*, vol. 84, no. 12, pp. 1929–1937, 2016, doi: 10.1002/prot.25176.
[72] T. Ai *et al.*, “Novel KCNJ2 Mutation in Familial Periodic Paralysis With Ventricular Dysrhythmia,” *Circulation*, vol. 105, no. 22, Art. no. 22, Jun. 2002, doi: 10.1161/01.CIR.0000019906.35135.A3.
[73] H.-F. Chan, M.-L. Chen, J.-J. Su, L.-C. Ko, C.-H. Lin, and R.-M. Wu, “A novel neuropsychiatric phenotype of KCNJ2 mutation in one Taiwanese family with Andersen–Tawil syndrome,” *J Hum Genet*, vol. 55, no. 3, Art. no. 3, Mar. 2010, doi: 10.1038/jhg.2010.2.
[74] Y. Hosaka *et al.*, “Function, subcellular localization and assembly of a novel mutation of KCNJ2 in Andersen’s syndrome,” *Journal of Molecular and Cellular Cardiology*, vol. 35, no. 4, pp. 409–415, Apr. 2003, doi: 10.1016/S0022-2828(03)00046-4.
[75] G. Teodorescu, “Functional characterization of KCNJ2 mutations associated with Andersen-Tawil syndrome and atrial tachycardia,” Dissertation, Universität Ulm, 2007. doi: 10.18725/OPARU-851.

[76] S. Munawar, C. Wang, M. Melnick, L. Reilly, C. Anderson, and L. L. Eckhardt, “Structural-functional characterization of KCNJ2 variants associated with ventricular arrhythmic syndrome phenotypes,” *Biophysical Journal*, vol. 122, no. 3, p. 250a, Feb. 2023, doi: 10.1016/j.bpj.2022.11.1452.
[77] N. D’Avanzo, S.-J. Lee, W. W. L. Cheng, and C. G. Nichols, “Energetics and Location of Phosphoinositide Binding in Human Kir2.1 Channels *,” *Journal of Biological Chemistry*, vol. 288, no. 23, pp. 16726–16737, Jun. 2013, doi: 10.1074/jbc.M113.452540.
[78] Y. Fujiwara and Y. Kubo, “Functional Roles of Charged Amino Acid Residues on the Wall of the Cytoplasmic Pore of Kir2.1,” *Journal of General Physiology*, vol. 127, no. 4, pp. 401–419, Mar. 2006, doi: 10.1085/jgp.200509434.
[79] S. Munawar, R. Woltz, L. Reilly, C. Anderson, N. Chiamvimonvat, and L. L. Eckhardt, “PO-01-206 MOLECULAR MODELING OF CLINICAL KCNJ2 MUTATIONS REVEALS STRUCTURE-FUNCTION IMPACT ON PIP2 BINDING SITE,” *Heart Rhythm*, vol. 20, no. 5, pp. S159–S160, May 2023, doi: 10.1016/j.hrthm.2023.03.524.
[80] M. Donaldson, G. Yoon, Y. Fu, and L. Ptacek, “Andersen-Tawil syndrome: a model of clinical variability, pleiotropy, and genetic heterogeneity,” *Annals of Medicine*, vol. 36, no. sup1, Art. no. sup1, Jan. 2004, doi: 10.1080/17431380410032490.
[81] D. Ma, X. D. Tang, T. B. Rogers, and P. A. Welling, “An Andersen-Tawil Syndrome Mutation in Kir2.1 (V302M) Alters the G-loop Cytoplasmic K+ Conduction Pathway *,” *Journal of Biological Chemistry*, vol. 282, no. 8, pp. 5781–5789, Feb. 2007, doi: 10.1074/jbc.M608776200.
[82] R. Handklo-Jamal *et al.*, “Andersen–Tawil Syndrome Is Associated With Impaired PIP2 Regulation of the Potassium Channel Kir2.1,” *Frontiers in Pharmacology*, vol. 11, 2020, Accessed: Sep. 06, 2023. [Online]. Available: https://www.frontiersin.org/articles/10.3389/fphar.2020.00672
[83] S. Pegan, C. Arrabit, P. A. Slesinger, and S. Choe, “Andersen’s Syndrome Mutation Effects on the Structure and Assembly of the Cytoplasmic Domains of Kir2.1,” *Biochemistry*, vol. 45, no. 28, pp. 8599–8606, Jul. 2006, doi: 10.1021/bi060653d.
[84] “Phosphatidylinositol-4,5-bisphosphate (PIP2) regulation of strong inward rectifier Kir2.1 channels: multilevel positive cooperativity”, doi: 10.1113/jphysiol.2007.147868.
[85] M. Limberg, “Genetische Ursachen des Langen-QT-Syndroms.”
[86] H. M. Berman *et al.*, “The Protein Data Bank,” *Nucleic Acids Research*, vol. 28, no. 1, pp. 235–242, Jan. 2000, doi: 10.1093/nar/28.1.235.